ASSESSING THE VALUE OF IMPROVED SNOW INFORMATION IN OPERATIONAL HYDROLOGIC MODELS

by

Alison Christine Burnop

A thesis

submitted in partial fulfillment

of the requirements for the degree of

Master of Science in Hydrologic Sciences

Boise State University

May 2012

BOISE STATE UNIVERSITY GRADUATE COLLEGE

DEFENSE COMMITTEE AND FINAL READING APPROVALS

of the thesis submitted by

Alison Christine Burnop

Thesis Title: Assessing the Value of Improved Snow Information in Operational Hydrologic Models

Date of Final Oral Examination: 09 March 2012

The following individuals read and discussed the thesis submitted by student Alison Christine Burnop, and they evaluated her presentation and response to questions during the final oral examination. They found that the student passed the final oral examination.

James P. McNamara, Ph.D.	Co-Chair, Supervisory Committee
Venkataramana Sridhar, Ph.D.	Co-Chair, Supervisory Committee
Alejandro N. Flores, Ph.D.	Member, Supervisory Committee

The final reading approval of the thesis was granted by James McNamara, Ph.D., Chair of the Supervisory Committee. The thesis was approved for the Graduate College by John R. Pelton, Ph.D., Dean of the Graduate College.

ACKNOWLEDGEMENTS

I would like to thank all those who contributed to the success of my thesis completion. Many thanks go to my adviser Dr. Jim McNamara, for his intellectual help along the way as well as for his moral support and many signatures. I would also like to sincerely thank the other members of my committee, Dr. Venkataramana Sridhar, and Dr. Lejo Flores for their support and assistance throughout this process. Without their expert modeling knowledge and experience, I would not have been able to get through the data and computer code challenges I faced along the way. A special thanks is due to Pam Aishlin for her constant support and providing me up to date data as I requested. Without her support and data, this thesis would not have been possible. I would also like to thank Kevin Knuss for his continued computer support and helping me to learn LINUX and many tricks of working in this computing environment.

Many thanks go to the folks at the National Weather Service for their expert advice and knowledge on the SACSMA/SNOW-17 model, specifically Michael Smith, Zhengtao Cui, Jay Breidenbach, Ray Fukunaga, Sean Reed, and Pedro Restrepo.

Funding for this research was provided by the National Weather Service, Award# NA08NWS4620047, and partially by the National Science Foundation, Award# CBET-0854522. Funding was also provided by a Teaching Assistantship at Boise State University. Funding for my tuition, fees, books, and other incidentals was provided by

the Trade Adjustment Assistance program and the Workforce Investment Act, through the federal government.

Special thanks to all those who have collected data in the field that I have used for model calibration and verification. I would also like to thank my friends and colleagues in the Department of Geosciences for their constant support and assistance, specifically Patrick Kormos, Dave Eiriksson, Erik Boe, Daniel Stanaway, and Kerry Riley.

I am also thankful for my extremely supportive family who have been there since my decision to come back to school and have been there to listen to my frustrations and successes, thanks Mom, Dad, Bobby, Kim, Vimon, and my extended family.

ABSTRACT

The National Weather Service's (NWS) operational hydrologic model, the Sacramento Soil Moisture Accounting Model (SACSMA), coupled with their temperature index snowmelt model, SNOW-17, were implemented in the Dry Creek Experimental Watershed (DCEW), located in the semi-arid region of southwestern Idaho, just north of the city of Boise, Idaho. The model was downscaled from the standard 1 HRAP to ¼ HRAP spatial resolution then calibrated using a modified manual calibration procedure from the NWS. The main modification was to decouple the SNOW-17 and SACSMA models during the calibration stage in order to accurately simulate the snow distribution without the interference of SACSMA parameter variations. The value of a site derived empirical areal depletion curve (ADC) in SNOW-17 was tested by comparing the calibrated model run using an empirical ADC to a model run using a calibrated ADC from the regional NWS office. The empirical ADC model run more accurately predicted the snow depth at internal watershed locations throughout the model simulation time period, 2000-2011. During these times, the streamflow leaving the outlet of the watershed was also more accurately simulated. The empirical ADC model run statistically performed better than the NWS calibrated ADC model run with lower RMSE, higher NSE, and more often had lower percent bias. Several of the dominant SNOW-17 parameters including the snowmelt temperature (MBASE), rain/snow temperature (PXTMP), and snow correction factor (SCF) produced more accurate snow accumulation and melt patterns as well as improved model output when they were

allowed to vary spatially across the watershed. This spatial variance allowed the model to produce the correct distribution of observed snow depth in the higher elevation pixels.

Several rain on snow (ROS) events occurred during the model simulation and the model responded differently depending on the severity of the ROS event and timing of temperature increase above freezing. This phenomena is simulated accurately during small events, 2-5 mm of rainfall, and during times when the temperature changes to above freezing in the middle of the precipitation event. When there are large rainfall events onto a snowpack during short periods of time, such as in the January 2011 ROS event, the model framework does not have the capability to handle these large events and underpredicts discharge. SNOW-17, by design, is very sensitive to large changes in air temperature, typically melting much more snow than is observed because of the models' linear relationship between snowmelt and temperature on any given day. Model simulations compared to observed snow depth records in DCEW indicate that snowmelt does not increase linearly with increases in temperature.

SACSMA/SNOW-17 was also run at the standard 1 HRAP spatial resolution, for 2000-2011, to determine the effect of incorporating a finer spatial resolution. Overall the ¼ HRAP resolution model run provided more accurate discharge simulation results after the peak discharge was observed, with smaller percent bias, higher NSE, and lower RMSE in May and June all but one year and in March and April some years. The average elevation of the model pixels between 1 HRAP and ¼ HRAP spatial resolution was the primary cause of this improvement because less snow accumulated and therefore less snow was left on the ground to melt later in the spring season using the coarser 1 HRAP resolution.

TABLE OF CONTENTS

LIST OF TABLES

LIST OF FIGURES

LIST OF ABBREVIATIONS

ADC	Areal Depletion Curve
BG	Bogus Gage stream site
BOG	Bogus Basin SNOTEL site
C1E	Confluence 1 East stream site
C1W	Confluence 1 West stream site
C2E	Confluence 2 East stream site
C2M	Confluence 2 Main stream site
DCEW	Dry Creek Experimental Watershed
ET	Evapotranspiration
fSCA	Fractional Snow Covered Area
HRAP	Hydrologic Rainfall Analysis Program
LDP	Lower Deer Point weather station
LG	Lower Gage stream site
LW	Lower Weather weather station
NDSI	Normalized Difference Snow Index
NSE	Nash-Sutcliffe Efficiency
NWS	National Weather Service
Pbias	Percent Bias
RMSE	Root Mean Squared Error
RFC	River Forecast Center

SACSMA	SACramento Soil Moisture Accounting model
SWE	Snow Water Equivalence
TL	Treeline weather station
WY	Water Year

INTRODUCTION

Hydrologic models are used to understand and predict watershed processes such as streamflow, soil moisture, and groundwater recharge using meteorological forcings, including precipitation and temperature. Hydrologic models can be broadly classified as conceptually based or physically based depending on how they represent hydrologic processes. Physically based models use physics-based equations to quantify the movement and storage of water (Dingman, 2002), typically in grid cells distributed over a watershed. Although they are often considered to be intellectually superior (Downer and Ogden, 2004; Downer et al., 2002; Ivanov et al., 2004; Kumar et al., 2009; Qu and Duffy, 2007), physically-based models require large amounts of input data and high computation time to solve. Conceptually based models use transfer functions or other systems type approaches that lump processes into fewer equations, therefore increasing computational efficiency, and have much smaller data requirements. Calibrating these models, however, can be problematic because they require historical data that is not necessarily representative of current and future hydrologic conditions.

A key difference between these modeling approaches is that the parameters in a physically based model are measureable properties while those in a conceptually based model are generally not measureable and must be calibrated. The National Weather Service (NWS) is interested in moving from their historical use of conceptual models to physically based approaches in order to accommodate their expanding mission (personal

communication, Restrepo). However, the computational expense of physically based models and the extensive suite of parameters that are related to physical properties, some of which can be measured, are prohibitive. One approach is to take small steps from conceptual to physically based by determining which processes should be represented physically to improve model performance, and which can remain conceptual. Understanding that certain watershed processes have more of an effect than others on how a hydrologic basin will respond to a particular precipitation event is key to understanding the complexity at which to represent each watershed process in a hydrologic model. This complexity also depends on the application of interest and where the model is being implemented. The success of a hydrologic model is also dependent on the number of parameters that are necessary to calibrate for any given basin. This number contributes to the overall accuracy of a model simulation because of the fact that the right answer can be easily obtained for the wrong reasons. The study presented here will test the effect of replacing a calibrated parameter in the NWS's operational conceptually based hydrologic model with a measured value for this parameter.

Important hydrologic processes vary by region and application. For this study, in semi-arid southwestern Idaho, snow accumulation and ablation is extremely important hydrologically because it is the major source of regional water for the entire year and determines the magnitude and timing of peak streamflow each spring (Bales et al., 2008; Daly et al., 2000; Fritze et al., 2011; Nayak et al., 2010; Reba et al., 2011; Rice et al., 2011; Stewart et al., 2004). One of the difficulties in using a conceptually based model in complex mountainous terrain is the representation of snow, which is known to be highly variable over small scales in such terrain. Mountainous terrain causes fractional snow

cover throughout the winter season and especially during snowmelt as hillslope characteristics such as aspect, slope, and vegetation affect where snow exists as it begins to melt. Hydrological models must take this fractional snow cover into account when determining the amount of water leaving each model pixel because snow cannot melt where it does not exist. The concept of an areal depletion curve (ADC) is commonly used, which relates fractional snow covered area (fSCA) to basin averaged snow water equivalence (SWE), to correct for overprediction of melt due to fractional snow cover. Hydrologic models such as SNOW-17 (Anderson, 1973) and the Snowmelt-Runoff Model (Martinec et al., 2008) utilize the ADC concept to account for fractional snow cover whereas models like the areally averaged snowmelt model (Horne and Kavvas, 1997), the Common Land Model (Dai et al., 2003), and the Gridded Surface Subsurface Hydrologic Analysis model (Downer and Ogden, 2004) use energy balance equations to melt snow. This ADC, like all the other parameters in a conceptually based model, is typically a calibrated parameter. This study evaluates the effect of replacing this calibrated parameter with an ADC based on field observations.

The hydrologic model used in this study and operationally by the NWS in river forecast centers (RFC's) is the Sacramento Soil Moisture Accounting (SACSMA) model (Burnash, 1995). This model is a conceptually based, spatially lumped, rainfall-runoff model that uses precipitation inputs, monthly potential evaporation, 17 parameters, and multiple model states to produce streamflow. Snow accumulation and ablation modeling is accomplished by coupling the NWS's temperature index snowmelt model, SNOW-17 (Anderson, 1973), with the SACSMA rainfall-runoff model. SNOW-17 uses precipitation and air temperature inputs, 12 parameters, and several model states to

accumulate and melt the snowpack. The concept of an ADC is utilized in SNOW-17, as a parameter, to melt snow only where snow exists. The model calculates the amount of meltwater leaving the snowpack, then uses the relationship between fSCA and the amount of SWE present, as determined by the shape of the ADC, to account for the areal fraction of snow on the ground, at each model time step.

On the 1000s of square kilometers RFC scale, this conceptually based, spatially lumped model generally works satisfactorily, once calibrated, but it has difficulty handling events such as small scale variations in the form of precipitation. It is also less accurate in snow-dominated regions, especially ones with complex mountainous topography, because of the spatial heterogeneity that is observed in mountain snowpacks combined with the coarse resolution of the model (16 km^2 pixels). Calibration of the model parameters is dependent on historical watershed conditions. It is difficult to ensure that the calibrated parameter values are accurate because most of the parameters are not measurable quantities and the historical conditions their calibration is based on are not necessarily representative of the current and future watershed conditions.

The SNOW-17 ADC is a calibrated parameter in most applications and at the RFC scale, but can be measured using remote sensing tools and a time series of SWE distribution throughout the watershed. We hypothesize that replacing the calibrated ADC with a measured ADC will improve the model accuracy in snow-dominated watersheds.

This work is part of a larger NWS project aimed at comparing conceptually based and physically based models in a semi-arid, snow dominated watershed and determining which hydrological processes are the most significant in these models. My research focuses on utilizing detailed snow information that has been collected in the Dry Creek

Experimental Watershed (DCEW) to determine the effect of a site derived/empirical ADC on the output of the SACSMA model (stream discharge) when it is coupled with SNOW-17. Model performance will be determined by comparing hydrograph components and statistics between calibrated model runs, holding all parameters the same except the ADC. The ADC will either be a site derived ADC or a calibrated ADC that was provided by the NWS for the local region. The snow accumulation and ablation trends will also be analyzed between model runs and compared to observed snow data from the watershed.

In addition to this main objective, a secondary goal of this research is to determine which hydrological processes, mainly snow, the model does poorly at representing and offer solutions to improve these aspects of the modeling framework when it is used to model streamflow in a topographically complex snow-dominated watershed. Another secondary objective of this research is to determine the value of spatial resolution on model results. The model will be run at two spatial resolutions, one with ~1 km^2 pixels and the standard coarser resolution of ~16 km^2 pixels. These spatial resolution comparisons will be performed using the empirical, site derived ADC.

The key questions we will be answering with this work are 1) what affect does an empirical, site derived ADC have on the streamflow prediction capability of SACSMA/SNOW-17 versus a calibrated ADC in a snow-dominated watershed, 2) what hydrologic processes are poorly simulated by SACSMA/SNOW-17 in a snow-dominated watershed and what solutions can we offer to improve the representation of these processes in the model framework, and 3) does a finer spatial resolution of the model pixels add value to the model output for a topographically complex watershed?

Background

Watersheds with complex mountainous topography in the intermountain United States typically receive a significant portion of their precipitation in the form of snow. Determining how explicitly to simulate snow accumulation and ablation in a hydrologic model is directly related to the success of that model producing accurate streamflow leaving the watershed. The model resolution also has a significant effect on how accurately the model can reproduce accurate snowmelt events, and ultimately streamflow, because of the complex patterns in which snowmelt is known to occur (Anderson, 2011; Liston, 1999; Luce and Tarboton, 2004; Shallcross, 2011).

Snow-dominated regions typically receive most of their annual precipitation in the winter, which is stored in the snowpack for several months, before melting over a 1-2 month period, making its way to the stream channel. These regions depend on the water stored in the snowpack as their water source throughout the drier season. The potential warming climate will greatly affect the amount of snow present at the end of the winter season as well as the timing of the peak snow water equivalent, peak snowmelt, and snow disappearance. More frequent rain on snow events will occur as the average winter temperature rises, which will further diminish the snowpack. With a warming climate, all of these factors can have detrimental consequences leading to drought and wildfire, especially in a semi-arid, snow dominated climate.

Most of the testing and experimentation with SACSMA/SNOW-17 has been completed in non-snow-dominated regions that generally have flat topography such as the American Midwest (Anderson et al., 2006; Bae and Georgakakos, 1994; Boyle et al., 2001; Khakbaz et al., in press; Kling and Gupta, 2009; Reed et al., 2004; Shamir et al.,

2005; Vrugt et al., 2006; Zhang et al., 2004). These relatively simple watersheds do not represent the complexities that are present in much of the western United States and throughout the world. Some research has been performed in more complex watersheds, such as Franz et al. (2008) in Reynolds Creek Experiemental Watershed, and two basins in the Sierra Nevadas as part of the Distributed Model Intercomparison Project – Phase 2 (DMIP2), in the North Fork of the American River and East Fork of the Carson River.

Franz et al. (2008) evaluated the differences in snowpack dynamics (melt and accumulation) and discharge between running a simpler temperature index snowmelt model (SNOW-17) and a more complex energy balance snowmelt model, the Snow Atmosphere Soil Transfer (SAST) model, both coupled with SACSMA. The results indicated similar trends by both snow models but with larger discharge errors from the SAST model because of rapid spring snowmelt and no mid-winter snowmelt. Yatheendradas et al. (in review) assimilated MODIS fractional snow extents into SAC/SNOW-17 in the topographically complex western DMIP2 basins, seeing improvements, but suggest that further improvement would be seen in less complex basins. The results of the DMIP2 in the western basins have not been released.

Shamir et al. (2006) evaluated the performance of SACSMA in several subbasins of the American River Basin and found reasonable streamflow predictions for streams without upstream regulation. They also found that high discharge events caused by rain and snow precipitation mixtures over the watershed were not modeled accurately. Determining the best calibration strategy of SACSMA has been adequately documented in the recent past (Chu et al., 2010; Khakbaz et al., in press; Martin, 2002; Vrugt et al., 2006), as well as parameter estimation techniques (Anderson et al., 2006; Hogue et al.,

2006; Shamir et al., 2005; Zhang et al., 2011), with many approaches found to be efficient and provide accurate results.

Model Representation

There are two major categories that differentiate hydrologic models, how they are spatially represented and how the watershed processes are represented. The spatial representation varies from spatially lumped to spatially semi-distributed to fully distributed. The two basic classifications of how watershed processes are represented are conceptually based and physically based with some models utilizing both characterizations.

Spatially lumped models use one value, either a parameter or state variable, for an entire basin or for very large pixels within a basin. This method requires much less data input and is therefore easier to implement. These spatially lumped inputs are not representative of the spatial variability that is known to exist at very small scales and therefore introduces many assumptions into the model. A model that is spatially distributed breaks the watershed into many small pixels and requires basin information for each pixel. This inherently requires a large amount of data that is not typically available at such small scales and even if the high resolution data exists, it substantially increases the computational time of the model simulation runs. There is still some level of homogeneity that is assumed in a spatially distributed model, only on a smaller scale. The major benefit of spatially distributed models is that they are much more representative of the actual watershed being modeled and its heterogeneity (Abbott et al., 1986; Brath and Montanari, 2000).

The representation of watershed processes in a hydrologic model always requires the use of some assumptions. A conceptually based model inherently includes more underlying assumptions than a physically based model. A conceptually based model uses transfer functions or simplifying equations to represent the processes occurring in the watershed. This is usually accomplished by creating parameters for individual processes and representing the soil column or atmospheric conditions in a reservoir-like fashion. These methods are used in order to simplify the model and create faster simulation runs. However the parameters of a conceptually based model do not typically represent real hydrologic variables, ones that have physically measurable values. This creates difficulty in diagnosing model failures and makes the model less flexible for large scale future changes such as climate change and/or land use changes. Conceptually based models usually work well and often better than physically based models, but only when well calibrated. Calibration of these models is typically based on historical hydrometeorological data, which is not necessarily representative of how the watershed will respond to similar hydrologic events in the future.

On the other hand, physically based models use physics-based equations to represent each watershed process. These equations are more representative of what is occurring in the basin but require many meteorologic and hydrologic variables in order to be solved. Another disadvantage is that these physics-based equations are usually for point scale values of that process and a model is trying to represent processes over a larger spatial scale.

SACSMA – Rainfall-Runoff Model

SACSMA is a conceptually based, spatially lumped soil moisture accounting model (Burnash, 1995); it breaks down the soil column into a combination of linear reservoirs to simulate the nonlinear behavior of water flow in the subsurface. The processes of the hydrologic cycle are modeled with equations that simulate the movement of water through the subsurface but they are not based on the physics occurring in that process like they are in a physically based model. The SACSMA model uses multiple states and 17 parameters to force the water movement through the soil column in the transfer function equations. The model states and parameters have physical meaning but few can actually be measured. The parameters and states used in SACSMA are listed in Table 1 with descriptions and the acronyms used by the NWS. A schematic of how the SACSMA model represents the watershed processes conceptually is shown in Figure 1.

Table 1. SACSMA Model Parameters

NWS parameter	Parameter	units
UZTWM	upper zone tension water capacity	mm
UZFWM	upper zone free water capacity	mm
LZTWM	lower zone tension water capacity	mm
LZFPM	lower zone primary free water capacity	mm
LZFSM	lower zone supplementary free water capacity	mm
UZK	upper zone free water storage depletion coefficient	day^{-1}
LZPK	lower zone primary free water storage depletion coefficient	day^{-1}
LZSK	lower zone supplementary free water storage depletion coefficient	day^{-1}
ZPERC	maximum percolation rate under dry conditions	dimensionless
REXP	exponent in the percolation equation	dimensionless
PFREE	% of water percolating directly to lower zone free water storage	fraction
SIDE	ratio of deep recharge to channel baseflow	fraction
ADIMP	additional impervious area	fraction
PCTIM	permanent impervious fraction of the watershed	fraction
RSERV	% of lower zone free water not transferable to lower zone tension water	fraction
RIVA	fraction of riparian vegetation	fraction
EFC	fraction of forest cover	dimensionless

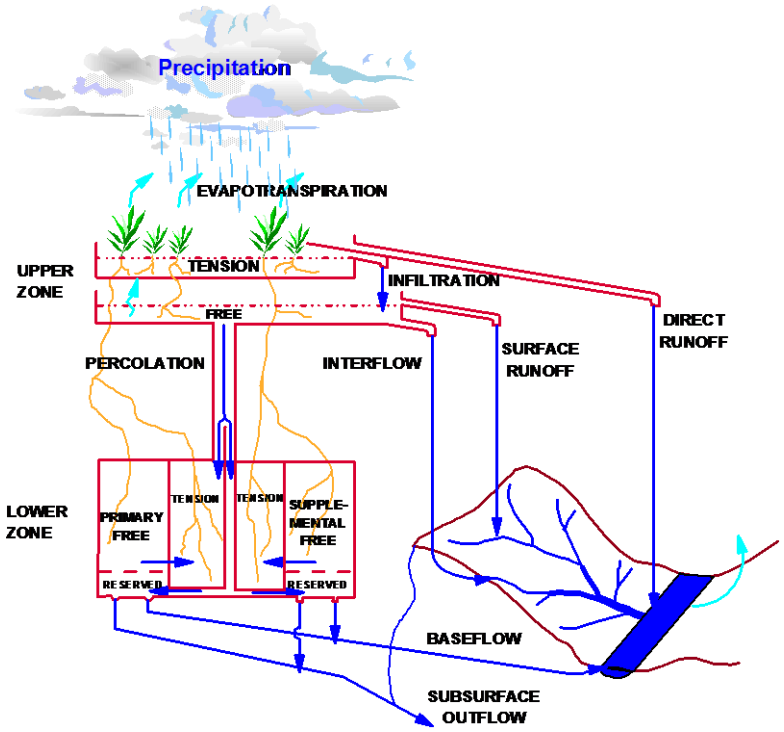

Figure 1. Conceptual Diagram of SACSMA Rainfall-Runoff Model (NWS, 2009)

SACSMA is forced with areal-averaged precipitation over each model pixel per time step (hourly in this study), and a monthly potential evapotranspiration (ET) demand curve. The discretization of the precipitation input will be discussed later and the potential ET curve was provided *apriori* from the NWS. The model calculates runoff in five forms from the different storage reservoirs (direct runoff, surface runoff, interflow, supplementary base flow, and primary base flow). Direct runoff, runoff from impervious regions of the watershed, and surface runoff, runoff from saturation excess, are routed immediately to the channel while interflow, or lateral subsurface flow, is routed to the stream channel via the upper zone depletion coefficient, UZK. There are two baseflow terms, primary baseflow, which represents the slow draining of the subsurface over long periods of time, and supplementary baseflow, which represents the fast draining of the subsurface that occurs after a rainfall. These baseflow terms drain according to Darcy's

Law and are routed to the stream channel with separate depletion coefficients (LZSK and LZPK).

The soil column is represented in SACSMA by two zones, an upper (~25cm thick) and lower zone (~125cm thick), each having multiple reservoirs, termed tension water and free water. Tension water and free water represent the two basic soil moisture uses in the subsurface. Tension water is designed to represent the water in the subsurface that is remaining after free drainage and is evapotranspired by the plants and atmosphere. Free water represents water that freely moves in the soil column through natural drainage processes. SACSMA is designed so that the tension water capacity needs are always met before other water movement processes can proceed, i.e., there is enough water present for ET demands before any water can leave the soil column and move to the stream channel.

Water moves to the lower zone through the percolation process, which is driven by the lower zone deficiency ratio and the maximum percolation rate, which is determined from the dryness and values of the REXP and ZPERC parameters. Once the water is in the lower zone, it moves to the stream channel as supplementary and primary baseflow from the free water zones and is used for ET demands from the tension water reservoir. Stream discharge is routed from model pixel to model pixel using a connectivity file that serves as a routing algorithm. The coarse resolution connectivity file was provided with SACSMA while the finer resolution connectivity file was created using GIS techniques and a 10 meter digital elevation model (Reed, 2003). The connectivity file accounts for partial pixels that occur on the watershed boundaries when a portion of the landscape inside that pixel flows to a different basin.

SNOW17 – Snowmelt Model

SNOW-17 (Anderson, 1973) is a conceptually based temperature index snowmelt model that takes precipitation and temperature as its input forcings. SNOW-17 is run in conjunction with SACSMA in regions whose water resources are dominated by a seasonal snowpack. SNOW-17 uses multiple states and 12 parameters to accumulate and melt a snowpack on the land surface. The parameters and states used in SNOW-17 are listed in Table 2 with descriptions and the acronyms used by the NWS. A flowchart of how water is stored and moved through the snowpack is shown in Figure 2. Parameters listed with a unit of per 6 hours are automatically converted in the model if the model time step is different than 6 hours.

Table 2. SNOW-17 Model Parameters

NWS Parameter	Parameter	Units
Major – must be calibrated		
SCF	snowfall correction factor (for gage catch, blowing snow, and sublimation effects)	dimensionless
MFMAX	maximum melt factor during non-rain periods – June 21st	mm/6 hr/°C
MFMIN	minimum melt factor during non-rain periods – Dec. 21st	mm/6 hr/°C
UADJ	average wind function during rain on snow events	mm/mb/6 hr
SI	mean areal water equivalent above which there is always 100% areal snow cover	mm
ADC	series of 11 values of snow covered area for an incremental normalized snow water equivalent	
Minor – assigned values based on climatological conditions		
NMF	maximum negative melt factor	mm/°C/Δt_p
TIPM	antecedent temperature index parameter (weighting of previous temperatures)	dimensionless
PXTEMP	threshold temperature for rain or snow precipitation	°C
MBASE	base temperature for snowmelt to begin	°C
PLWHC	percent liquid water holding capacity (max value is 0.4)	fraction
DAYGM	daily amount of melt that occurs on average at snow-soil interface	mm/day

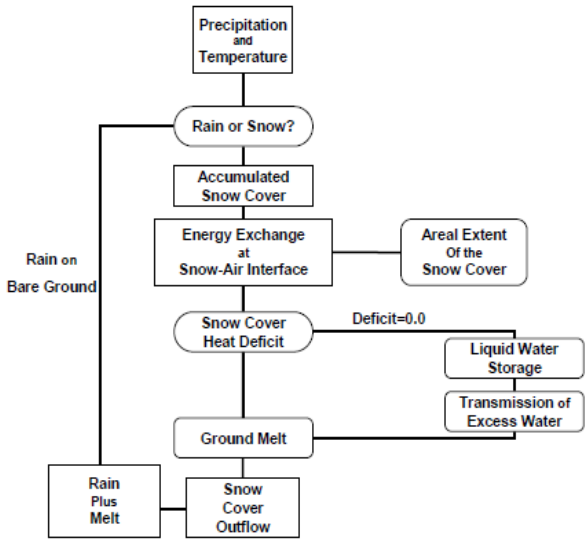

Figure 2. Schematic of SNOW-17 Snowmelt Model (NWS, 2011)

As Figure 2 indicates, when there is a precipitation event in a particular time step, the model compares the input air temperature with a rain/snow temperature (PXTMP parameter, usually 0°C) to determine if the precipitation is in the form of rain or snow. If the precipitation is rain and there is no snow on the ground, it bypasses the rest of the SNOW-17 technique and the water is routed directly to SACSMA as "Rain Plus Melt." If the precipitation input is snow, the precipitation amount is multiplied by the snow correction factor (SCF) parameter and then added to the snowpack.

The energy exchange at the snow-air interface is then determined where snowmelt is calculated two separate ways depending on whether it is raining on the snowpack or not. During rain on snow events, the snowmelt equation, a representation of the energy exchange at the snow-air interface, is solved with the UADJ parameter representing the only unknown variable, the average wind speed function. This wind speed function accounts for the turbulent heat exchange that is created when wind is present. SNOW-17's melt calculation during rain on snow time steps does not account for seasonal

variation while the non-rain snowmelt calculation is only based on a seasonal melt factor (determined by a minimum and maximum melt factor, MFMIN and MFMAX parameters) and the MBASE parameter, which defines the temperature above which snow usually melts. The seasonal melt factor that is only used for non-rain snowmelt calculations takes into account the radiation differences from the amount of sunlight that varies throughout the year. Since it is raining during rain on snow time periods, the radiation affect is not present. The amount of snowmelt computed for each time interval is multiplied by the fSCA of each pixel, which is determined from the shape of the ADC. The same ADC is used for the entire basin as it was derived as a basin depletion curve but the fSCA can vary, because the melt varies, between model pixels and is calculated at each pixel.

When the air temperature is less than 0°C, a heat deficit energy term is calculated internally in the model. This heat energy in the snowpack is calculated at each time step and is expressed in millimeters, where one millimeter of heat energy is the amount of heat required to change the state of 1 mm of ice or water at 0°C (NWS, 2011). It is equivalent to the amount of snowmelt or rain that is necessary to begin releasing water from the snowpack. This heat deficit term is also affected by the snow covered fraction in each pixel. Snow depth, SWE, fSCA, and rain plus melt are some of the available output variables for SNOW-17 (NWS, 2011).

Areal Depletion Curves

Properly predicting the amount of runoff generated from snowmelt is extremely important in correctly predicting the streamflow leaving a snow-dominated catchment.

The spatial distribution of snow accumulation and therefore snowmelt is known to be highly variable, especially in regions with complex mountainous topography (Anderson, 2011; Liston, 1999; Luce and Tarboton, 2004; Shallcross, 2011). Within these regions, the areal extent of snow cover must be taken into consideration since the entire watershed is not typically covered by snow and the model will overestimate the water leaving the watershed if this fraction is not considered. SNOW-17 achieves this by introducing the concept of an areal snow depletion curve (ADC) into the modeling framework.

The depletion curve concept has been used for decades in varying ways such as predicting melt depths based on temperature-index or degree-day methods that are then multiplied by the percent of the watershed covered in snow (Dunne and Leopold, 1978; Martinec, 1985), determining the mathematical interrelationships between the spatial distribution of SWE, snowmelt rates, and the depletion of snow covered area (Liston, 1999), to finding basin-specific relationships between SWE and fSCA (Luce and Tarboton, 2004; Luce et al., 1999; Shamir and Georgakakos, 2007), and examining the temporal evolution of fSCA over a single snowmelt season (Dery et al., 2005).

The most common method used to depict ADCs in models currently is to derive a relationship between the basin fSCA (independent variable) and basin averaged SWE (dependent variable). The shape of the ADC will vary from year to year depending on the maximum accumulation of snow that year and speed of ablation during the melt season and throughout the year. Accounting for these slight variations has been achieved by normalizing the basin average SWE by the maximum SWE during that season, providing the ability to use a single depletion curve for multiple years.

SNOW-17 normalizes the basin average SWE with an areal index, which is the smaller of the maximum SWE value over the accumulation period and the SI parameter, defined as the SWE where 100% snow cover always exists. When modeling a watershed such as DCEW, where snow only covers the entire watershed intermittently throughout the winter, it is common practice to set the SI parameter to a large value that forces the model to normalize the depletion curve by the maximum SWE value during the model time period. For watersheds with a uniform snowpack, the SI parameter usually has a low value because the watershed is 100% covered until just before the snow disappears. In these watersheds, the shape of the ADC is not important (NWS, 2011). The opposite is true in watersheds with a variable snowpack, such as DCEW, where the snowpack disappears in portions of the watershed as soon as snow begins to melt. The ADC used by SNOW-17 is defined by specifying the areal extent of snow cover at eleven normalized basin average SWE values (0 to 1 in 0.1 increments).

A DCEW basin specific ADC was developed by Procsal (2005) using MODIS reflectance values to calculate a Normalized Difference Snow Index (NDSI) in conjunction with the empirical relationship developed by Salomonson and Appel (2004) that relates the NDSI to fSCA. The SWE values used were modeled from the Utah Energy Balance model and validated by detailed snow surveys throughout the accumulation season. Procsal (2005) created 4 ADC's for DCEW, one for the lowest, middle, and highest elevations, and a basin wide ADC. The basin wide ADC (called empirical or site derived ADC hereafter) was used in this study to compare to the calibrated NWS ADC parameter. During calibration, this model parameter was held constant while the other parameters were adjusted.

The local NWS office provided the calibrated ADC parameter data that they use operationally in the Boise River Basin, which includes DCEW along the basin's northern extent (see site map, Figure 4). The Boise River Basin experiences the same weather patterns as DCEW and is also composed of weathered granite and interbedded sandstones. Three parameter sets for the Boise River Basin ADC's were provided, with the NWS upper and lower being for the region between Lucky Peak and Arrowrock Reservoirs, split into two elevation bands, above and below 5000 feet. The third NWS ADC is for the larger region between the Lucky Peak dam and Parma, Idaho with elevation ranging from 2208 feet to 6618 feet. This last NWS ADC was used in this study as the elevation range and geographic location of the basin it was calibrated for is closest in proximity to DCEW.

A range of ADC shapes are shown in Figure 3, with the outer most ADC's representing two theoretical snowpack conditions, a uniform snowpack (green line) and a highly variable snowpack (black line). The DCEW basin ADC created by Procsal (2005) is shown in orange and closely follows the shape of the more variable snowpack depletion curve (black line) for a normalized SWE of 0.4 and greater. The NWS calibrated ADC is the maroon line in Figure 3 and more closely follows the uniform snowpack theoretical ADC for normalized SWE values of 0.5 and less. Procsal's lower elevation ADC mimics the highly variable ADC for normalized SWE values of less than 0.8, which makes sense because snow at lower elevations in DCEW is shallow, highly variable, and does not last for long durations.

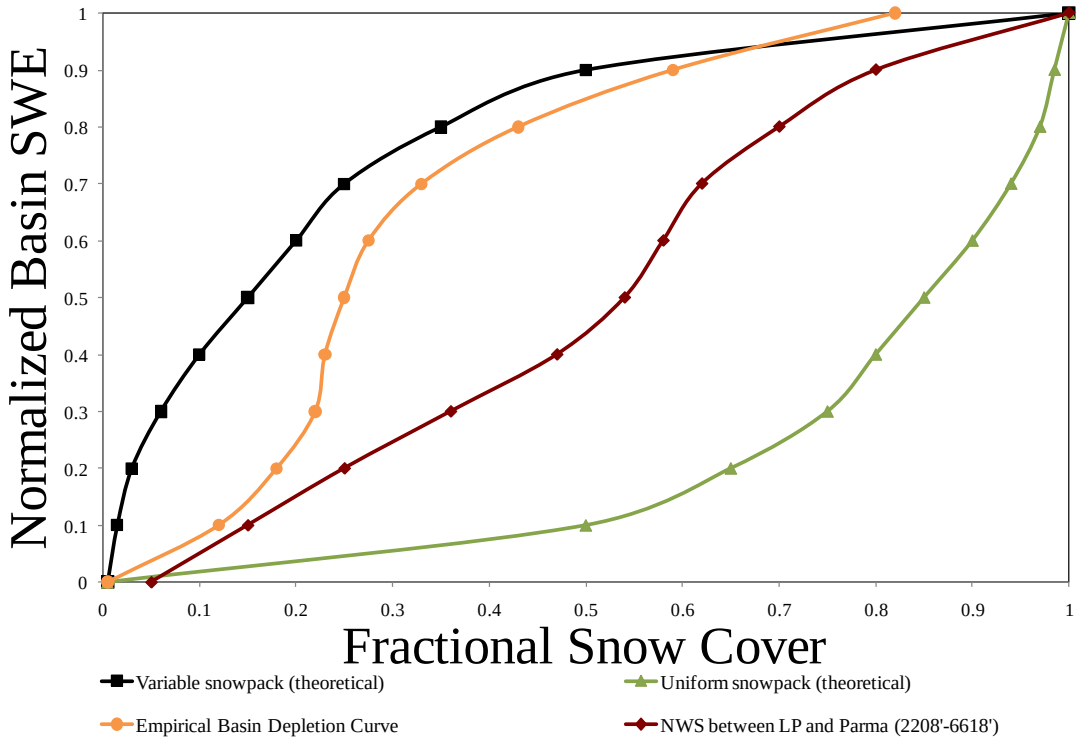

Figure 3. Variations of Areal Depletion Curves

The NWS ADC has a linear relationship between fSCA and SWE from 0-50% fSCA while the empirical ADC has a linear relationship from 0-20% fSCA. Between 20-30% fSCA, the empirical ADC has large variability in the normalized basin average SWE (25-65% SWE). The NWS ADC has the most variability (50-70% SWE) when the fSCA is 50-60%. Both ADC's assume a linear relationship between fSCA and SWE again at 70% fSCA. The NWS ADC has lower normalized SWE for any given fSCA, meaning that it will melt more snow than the empirical ADC because the calculated SWE was always multiplied by a larger fSCA.

Model Scale

SACSMA and SNOW-17 are run on the Hydrologic Rainfall Analysis Project (HRAP) grid system, which is based on a polar stereo graphic map projection with a

standard latitude of 60° North and standard longitude of 105° West. The NWS runs the RFC's river forecasts at 1 HRAP resolution, which corresponds to nominal 4km by 4km square pixels. SACSMA and SNOW-17 are capable of running at finer resolutions (½ HRAP and ¼ HRAP) and for this study were run at 1 HRAP and ¼ HRAP resolution (roughly $1km^2$ pixels, red pixels shown in Figure 4), with the majority of the analysis focusing on the ¼ HRAP model runs. The small size of DCEW (27 km^2), complex spatial heterogeneity in topography, and hillslope hydrologic controls such as aspect, soil depth, vegetation, and solar radiation provide a fair rationalization for the model scale choice. The topographic gradient in DCEW introduces complexities and large variation in snow accumulation and depletion, which are two hydrologically important watershed processes in DCEW.

SACSMA/SNOW-17 can be run with time steps of 1, 2, 3, 4, 6, 12, and 24 hours. The model was run at hourly time steps for this study because of the availability of meteorological forcings and observed data to compare model results. All results presented will be for water years (WY), starting with WY2004 (October 1 2003 – September 30, 2004). The model was run for January 2000 – June 2011 with 2000 through 2003 serving as a warm-up period. Applicability of this warm up period is evidenced by visual inspection of the modeled versus observed hydrograph and high values of the annual bias for WY2000 – WY2003.

Challenges with Complex Terrain

Complex terrain creates complex spatial heterogeneity in the field where geomorphic, geologic, meteorologic, and hydrologic data vary significantly within small

spatial scales (less than 50 m). Conceptually based, lumped parameter hydrologic models like SACSMA/SNOW-17 do not account for this complexity because they spatially lump these parameters, input and state variables, over large areas, 1 km^2 to 16 km^2 model pixels, or even assign basin wide parameter values. One problem this presents is the warm up time needed to run a model like SACSMA in a region with complex mountainous terrain. The standard warm up time needed for SACSMA is 2-6 months (NWS, 2011) but the warm up time needed for SACSMA to come to equilibrium in DCEW is on the order of 12-18 months at ¼ HRAP resolution and 18-24 months at 1 HRAP resolution. This was determined by visual inspection of the hydrograph in the early time frame of the modeling period as well as the percent bias statistic.

Determining how to discretize input forcings and/or parameter values over each model pixel is important to accurately representing the hydrologic state of the watershed at a particular point in time. It is known that spatial heterogeneity in snowpack, soil texture, and slope are known to exist at very small scales (Anderson, 2011; Liston, 1999; Luce et al., 1999; Shallcross, 2011) while model pixels overlay a watershed independent of hydrologic and land features. This inherently includes a wide topographic range in a single model pixel for complex terrain areas. Usually hydrologic data are averaged over a model pixel that likely includes a main stream channel, tributary channels, valley bottoms, steep hillsides, ridge tops, and transitioning through the treeline and potential rain/snow transition elevations.

STUDY AREA: DCEW

The headwaters of the Dry Creek Experimental Watershed (DCEW, Figure 4) are located roughly 16 km northeast of Boise, Idaho, in what is known as the Boise Front at an elevation above 2100 masl (Williams, 2005). The lower boundary of the experimental watershed is at about 1000 masl in elevation and is located where Bogus Basin Road crosses the perennial Dry Creek stream. Dry Creek is a northeast to southwest trending stream that eventually flows into the Boise River west of Eagle, Idaho. The local geology around the stream channel controls the gradient of the stream (Rothwell, 2005). The upper portion of Dry Creek is characterized by steep gradients while the lower reach has a markedly lower stream gradient. Dry Creek becomes a mainly losing stream (to groundwater recharge) downstream of the Lower Gage (LG) stream site, even drying out completely in the summer, giving rise to the name Dry Creek.

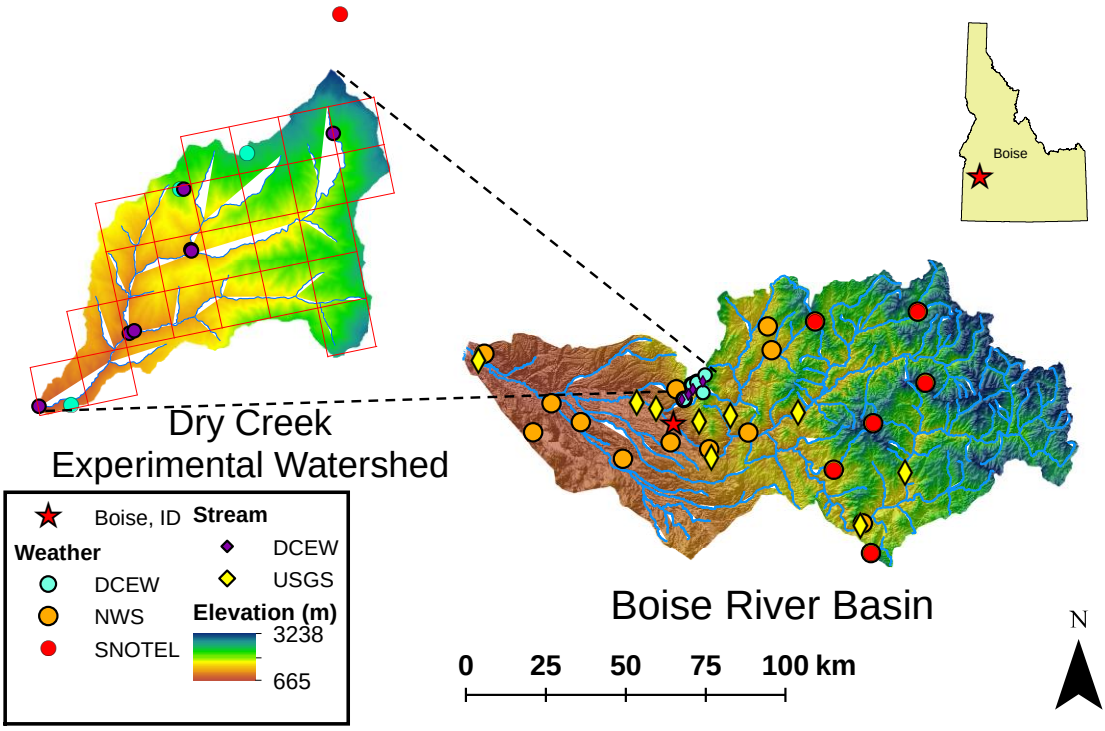

Figure 4. Boise River Basin Including Dry Creek Experimental Watershed, Discretized into 1 km^2 Pixels.

Shingle Creek is a perennial stream that flows south of and drains into Dry Creek, about 2 km upstream of the LG stream station. There are also numerous ephemeral tributaries throughout the watershed and several natural mountain springs in the eastern and northern portions of DCEW. The watershed boundary encompasses a 27 km^2 region underlain by the Atlanta lobe of the Idaho Batholith granitic intrusion that extends 275 km into north central Idaho. The mainly biotite granodiorite rocks inside the watershed and former tectonically active region have created a network of fractured, weathered bedrock and complex topography across very small scales. This easily erodible rock has formed gravelly loam to gravelly sandy loam textured soil that is shallow in nature (less than 2 meters throughout the watershed).

North facing slopes typically have deeper soils and have finer grained textures with higher silt contents where the south facing slopes are shallower and have coarser grained soil textures with higher sand contents. Clay fractions are low and similar throughout the watershed (Smith, 2010; Tesfa et al., 2009). Vegetation varies greatly throughout the watershed with the lower portions consisting of grass and shrublands and the higher elevations containing mostly coniferous forests (Ponderosa Pine and Douglas Fir). Differences in elevation, topography, slope, aspect, soil texture, and soil depth all play a factor in the vegetation type present and area covered and therefore affect the movement of water through the hillsides into the stream channels.

DCEW exists in a semi-arid climate that is driven by two main weather systems, the Pacific High system that drives the hot and dry summers with low precipitation, and the Aleutian Low system that drives the cool and moist winters when most of the precipitation falls (USDA, 1974). DCEW is situated in a temperature sensitive rain-to-snow transition region where winter precipitation falls mostly as snow in high elevations, as rain in low elevations, and as a mixture of snow and rain in middle elevations throughout the winter season. This transition elevation varies throughout the year and with each storm system. Analysis of the location of this rain-snow transition elevation in the nearby Reynolds Creek Experimental Watershed shows that the elevation has steadily increased over the last 30 years (Nayak et al., 2010).

An orographic effect is typically present in DCEW where precipitation increases and temperature decreases with increasing elevation, as shown by the annual average conditions in Figure 5 and Figure 6. While this is the normal trend, DCEW also experiences winter inversions where the temperature is higher at the high elevations and

lower, usually under cloud cover, at the lower elevations. The inversions can last for 2 days to over a month long at times.

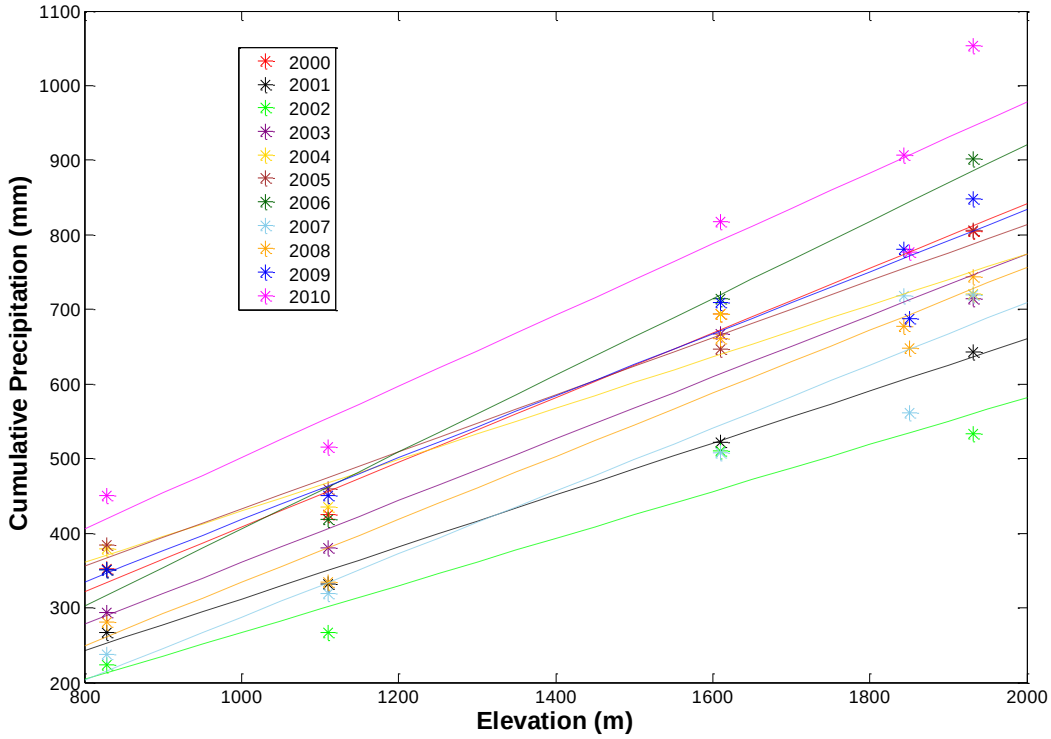

Figure 5. Cumulative Annual Precipitation Versus Elevation in DCEW

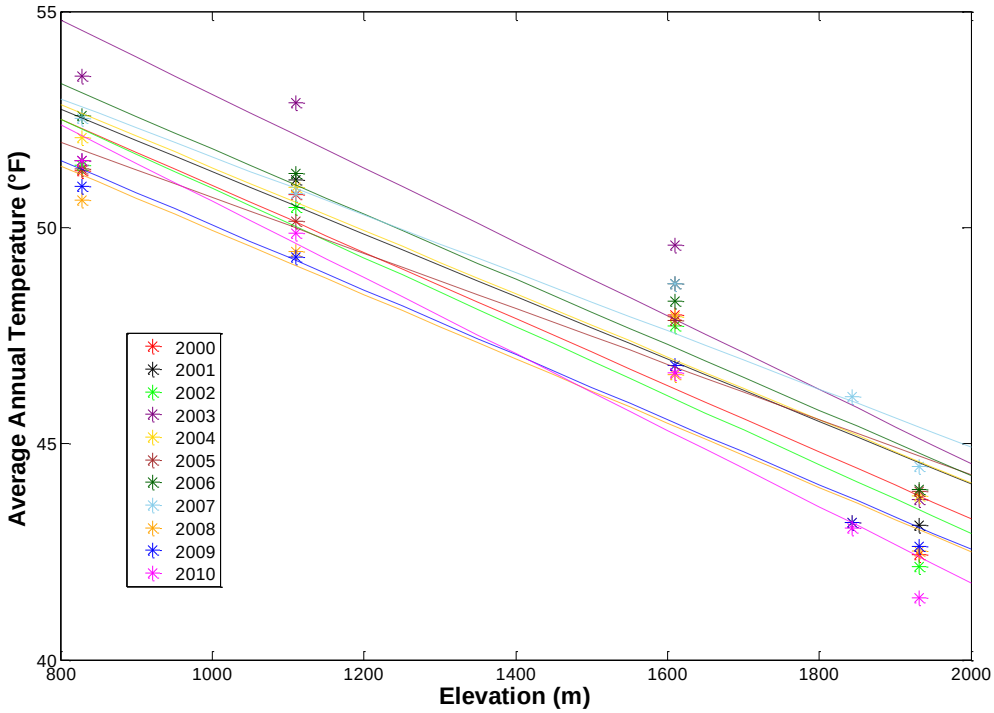

Figure 6. Average Annual Temperature Versus Elevation in DCEW

The start of each water year and fall in this region is typified by cooling average temperatures with warm days, cool evenings and occasional rains. The fall wetup period in DCEW starts in September as the ET demands slow down. The soil reaches field capacity as the snowpack covers the ground surface, in November-January, depending on elevation. Winters are characterized by cool temperatures and moist conditions. Soil moisture stays at field capacity through the winter until approximately one month after the snowpack melts (March – May), then continually decreases to the wilting point in late summer to early Fall (late August – early October) (Smith, 2010).

The spring season in DCEW has warming temperatures causing the snowpack to melt with occasional precipitation events where snow falls at the highest elevations transitioning to mostly rain in the middle and lower elevations. Summers are typically

hot and dry with little precipitation (Figure 7 and Figure 8). The summers also have low soil moisture conditions for several months when ET demands are the highest.

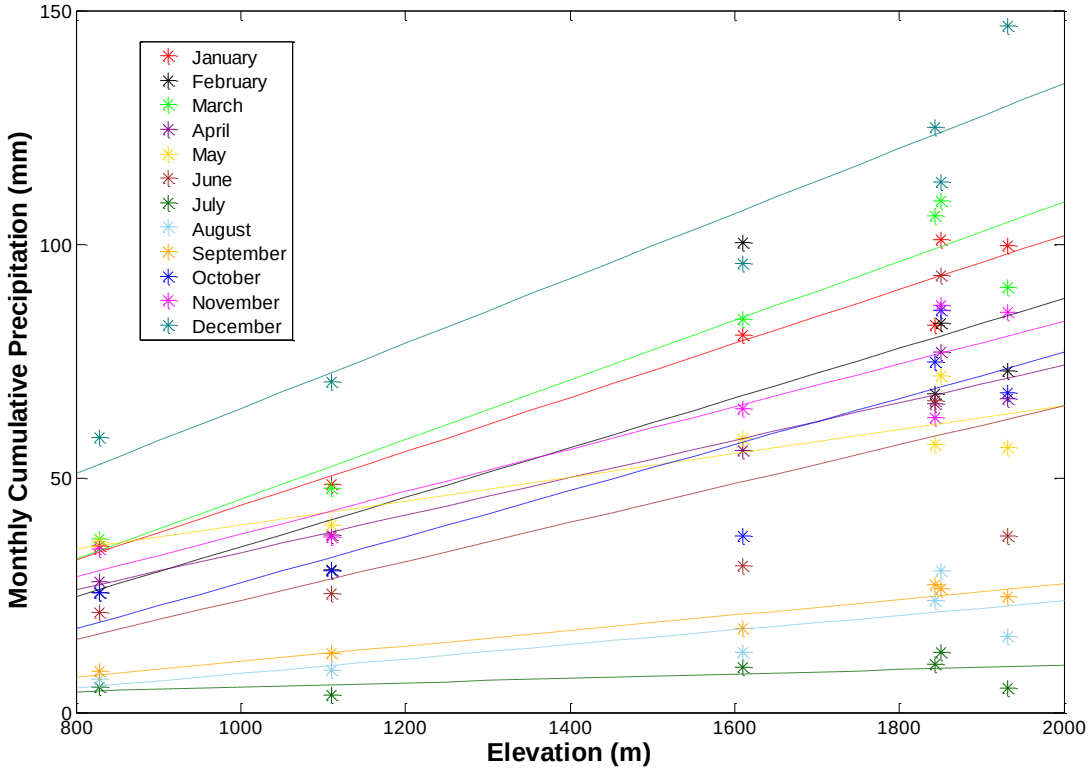

Figure 7. Average Monthly Cumulative Precipitation Trends in DCEW (2000-2010).

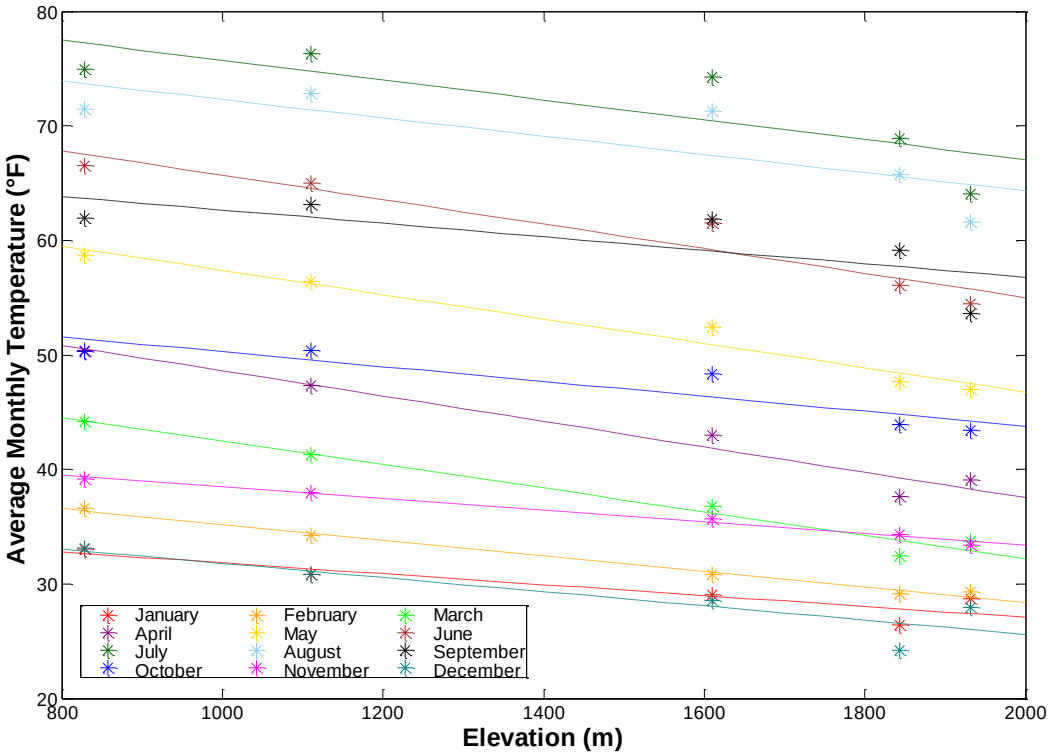

Figure 8. Monthly Average Temperature Trends in DCEW (2000-2010).

DCEW Data

There are 4 weather stations inside DCEW that measure air temperature, snow depth, incoming solar radiation, wind speed and direction, relative humidity, soil moisture, soil temperature, and precipitation. Lower Weather (LW) and Treeline (TL) weather stations, 1100 masl and 1650 masl were installed in 1998, Lower Deer Point (LDP), 1850 masl was installed in 2007, and Shingle Creek Ridge (SCR), 1710 masl was installed in 2010. There are three additional weather stations in close proximity to DCEW. The Bogus Basin SNOTEL station (BOG), ran by the National Resource Conservation Service, is located just outside of the DCEW boundary, at 1932 masl. The Bureau of Reclamation runs the Boise AgriMet weather station south of DCEW, at 829

masl and the Boise Airport has a weather station at 875 masl. There are seven stream gages in DCEW, 6 additional soil moisture pit locations (aside from the weather station soil moisture pits, 4 duplicate pits with multiple depths at each location), and numerous snow depth sensors. Other experimental hydrologic data is available for short time periods including snowmelt data from four lysimeters and subsurface flow at a hillslope scale plot at TL.

Streamflow Sites

Five of the seven gauged streams in Dry Creek are perennial with the largest flow observed at the LG stream site. As the name implies, LG serves as the outlet of the watershed and is located near the LW weather station. The streamflow record at LG is the most complete in DCEW and has been gap filled using other subwatershed streamflow records during important flow events, although gaps still exist in the LG record.

Semi-complete streamflow records are available for five interior points, at Bogus Gage (BG, high elevation site, 1700 masl), Con 2 Main (C2M, perennial and last main confluence before LG, 1143 masl), Con 2 East (C2E, perennial, also known as Shingle Creek, 1158 masl), Con 1 East (C1E, perennial and next gauge downstream of BG, 1335 masl), and Con 1 West (C1W, ephemeral, 1347 masl), for 2004 - present. These data are not gap filled but have enough data to analyze the streamflow within the watershed during most years in the period of record. Each of these measurement sites roughly correspond with a DCEW ¼ HRAP pixel outlet and were used for comparison, validation, and analysis purposes.

Snow Depth Sensors

There is a network of snow depth sensors in DCEW, with TL and LDP having the most. The TL snow depth sensor was installed in 1999 and has data with some gaps from installation until the present day. The LDP snow depth sensor was collecting accurate data starting in the fall of 2009. The other long term time series of snow depth data available is from the BOG site, which is 90 m higher in elevation than the LDP pixel and is just outside the boundary of DCEW. This SNOTEL site typically overestimates the snow depth and SWE seen in DCEW because of the nature of the site that was selected, as is standard procedure for most SNOTEL sites across the western US.

There is also a network of ultrasonic snow depth sensors that collected local variability in snow depth data during the 2010 and 2011 water years. These sensors are located on varying aspects and elevations within the TL (5 sensors) and LDP (13 sensors) pixels.

Manual Snow Data Collection

Manual snow surveys have been completed in the upper portions of DCEW (snow dominated) for many years (Anderson, 2011; Homan, 2008; Procsal, 2005; Shallcross, 2011) and this spatial representation of snow depth and SWE were used for comparison between model runs. Basin wide surveys from each year were completed during maximum accumulation. During 2010, a $1km^2$ transect snow survey was completed

several times throughout the snow accumulation period (Anderson, 2011). This transect fell entirely in one model pixel at the finer $1km^2$ resolution. There have also been a number of experiments in the TL subcatchment where snow depth and SWE measurements were routinely made. Manual snow depth and SWE measurements collected at the snowmelt lysimeters during the 2010 and 2011 snow season were also used in analysis of model runs (Eiriksson, 2012). A LiDAR flight was run over DCEW in the summer of 2008, followed by a winter flyover in March 2009 to assess the heterogeneity of the snowpack at maximum accumulation (Shallcross, 2011). Manual verification snow depth measurements were also made during the winter LiDAR flight.

METHODS

The main objective of this study is to determine the value of a site derived ADC in an operational hydrologic model in a topographically complex, snow-dominated watershed. The value of site derived parameterization of snow in the SACSMA/SNOW-17 hydrologic model was determined by comparing model output from two calibrated model runs. These model runs differ only in the ADC that is used, with one using a calibrated ADC, provided by the local NWS office, and the other using a MODIS site derived ADC (Procsal, 2005).

In snow dominated watersheds, predicting the magnitude and timing of peak discharge is typically of interest to end users. However, for water resource purposes, predicting the timing and magnitude of snowmelt throughout the melt season is ultimately more important because storing this melted water as well as managing the amount of water sent downstream during the melt season is a top priority. Therefore, examination of the different ADC model run hydrologic statistics on LG discharge and snow depth at the TL and LDP sites during the melt season as well as visual inspection of the snow accumulation and ablation trends and the hydrograph timing and magnitude differences, compared to observed values, throughout the melt season will serve as the main determination of the importance of a site derived ADC versus a calibrated ADC.

Two secondary objectives include determining which watershed processes the model poorly represents and determining the effect of finer spatial resolution on model

output. Through the analysis of storm events and differences in the ADC model runs, it was determined which hydrologic processes are not well represented in the model framework. These model simulations were initially performed on a downscaled version (¼ HRAP) of the SACSMA/SNOW-17 model and later at the standard 1 HRAP spatial resolution for comparison purposes and the third objective. The same criteria for the ADC comparisons were used to determine the effect of the finer spatial resolution. Downscaling from the standard 1HRAP resolution was necessary because of the small size of DCEW and the high spatial variability in snow distribution and melt. This required the temperature and precipitation inputs as well as the model parameter values to be downscaled appropriately.

The SACSMA and SNOW-17 models were calibrated separately, in a decoupled fashion, followed by a coupled model run that combined each parameter set from the individual calibrations. This decoupled calibration required slight modifications to the NWS's manual calibration procedure (NWS, 2009; NWS, 2011). Model performance was determined by comparing observed watershed outlet discharge and snow data within the watershed with the model output. Annual, monthly, and event percent bias (Pbias), root mean squared error (RMSE), and Nash-Sutcliffe efficiency (NSE) statistics (see Equations 1-3) were computed for the LG discharge, TL snow depth, and LDP snow depth time series, and were also used to determine the best parameter set. Statistics at LG discharge were calculated on an hourly basis while the statistics at each snow depth location were calculated on a bi-hourly basis.

$$Pbias = \frac{\sum_{t=1}^{N}(Mod_t - Obs_t)}{\sum_{t=1}^{N} Obs_t} * 100 \quad (1)$$

$$RMSE = \sqrt{\frac{1}{N} * \sum_{t=1}^{N}(Mod_t - Obs_t)^2} \quad (2)$$

$$NSE = 1 - \left(\frac{\sum_{t=1}^{N}(Mod_t - Obs_t)^2}{\sum_{t=1}^{N}(Obs_t - \overline{Obs})^2} \right) \quad (3)$$

Percent bias calculates how much error or how far the average modeled value is from the observed value the model is attempting to simulate. This is the standard statistic used by the NWS in the calibration stages but has more usefulness for modeling larger magnitude river flows. Low streamflow like that observed leaving DCEW produces irrelevant Pbias values during the low flow time periods because of the way the statistic is calculated. Negative pbias values indicate an underestimation of the observed variable while a positive pbias indicates an overestimation of the observed variable. RMSE is a measure of the standard deviation and bias of the model simulation and has units that are the same as the variable the model is estimating (m^3/s and cm in this study). RMSE ranges from zero, a perfect fit and no error, to infinity. NSE is an efficiency index that relates the sum of the squared errors to the sum of the squares of the measured values around the observed mean. NSE can range from negative infinity to 1, where a value of 1 is a perfect fit. When NSE is equal to zero, this indicates that the model simulation is just as accurate as the observed mean value and an NSE of less than zero indicates that the observed mean is a better predictor of the true value than the model simulation value.

Model Calibration

SACSMA/SNOW-17 was calibrated by iteratively adjusting the model parameters and comparing the model output to historical hydrometeorological data, including streamflow at LG, snow depth time series at TL and LDP pixels, point observations of snow depth and SWE in the highest elevation pixels, and the BOG snow depth and SWE temporal data set. The specific calibration steps follow the manual procedures outlined by the NWS (2009; 2011) with a few modifications. These modifications stem from the decision to decouple the rainfall runoff and snow accumulation and ablation models, calibrating each separately from the other. The calibration was performed over the later years (WY2010-2011) in the simulation time period because of the availability of snow depth data at LDP.

The multiple step manual calibration procedure starts by running the model using *apriori* parameters (provided by NWS) and removing large errors first, including timing of snowmelt, form of precipitation, storm runoff/baseflow ratio errors, and incorrect storm runoff volume. The next step (for SACSMA calibration) is to obtain a reasonable baseflow simulation, followed by adjusting the tension water capacities based on maximum soil moisture deficits. The storm runoff and interflow volumes are then checked to determine if they are reasonable, and finally minor adjustments were made to improve seasonal and flow interval bias.

Decouple SACSMA and SNOW-17

During normal operation, the rainfall runoff model (SACSMA) is coupled with the snowmelt model (SNOW-17). Since we believe that the snow accumulation and

ablation is extremely important in this region, we decoupled the rainfall runoff portion of the model from the snowmelt model during calibration, to be able to focus on calibrating the snow parameters by themselves. The empirical ADC was used as the site derived depletion curve during this step and therefore was not changed throughout calibration.

SNOW-17 was first run by itself and the snow parameters were calibrated following the first step of the NWS manual calibration procedure of removing large errors, including timing of snowmelt and form of precipitation. This step also includes adjusting the major SNOW-17 parameters of MFMAX, MFMIN, SCF, UADJ, and SI (see Table 2 for parameter descriptions). SNOW-17 model results were analyzed by visual comparison of observed snow depth at the TL and LDP pixels (TL only until WY2010) with the modeled snow depth in the same pixel. Snow depth and SWE point data in the upper portions of the watershed were a secondary check on the model performance because these values were not necessarily representative of the pixel average values. Timing and magnitude of snowmelt events and form of precipitation were analyzed to determine which parameters needed to be adjusted.

BOG snow depth and SWE data were also used for general accumulation and ablation trend analysis. This data could not be directly compared as it is higher in elevation and is not as sensitive to the rain-snow transition elevation as the model pixels inside DCEW, typically melting out much later than the DCEW pixels. The later years (WY2009-2011) were examined more closely in the calibration process because of the greater number of observations, both point and time series data, that were available for comparison.

Once acceptable model results were achieved from SNOW-17 only runs, the gridded rain plus melt model output was used to drive SACSMA. During this step, SACSMA was run by itself using the water input from the calibrated SNOW-17 model run instead of the precipitation forcings derived from DCEW weather stations. The SACSMA model parameters were iteratively adjusted using the NWS manual procedure until reasonable model output was achieved. Model performance between calibration parameter sets was determined by comparing the modeled stream discharge values with the observed discharge measured at the LG stream site. Visual hydrograph comparison was the main method of comparison by analyzing the timing of the rise and fall of the hydrograph as well as the timing and magnitude of the peak and low flows. Annual and monthly percent bias, NSE and RMSE statistics of LG discharge were also used to determine relative changes between parameter sets.

Couple SACSMA and SNOW-17

With a calibrated parameter set, the two models can be combined in order to test the effect of the site derived ADC on streamflow prediction. The calibrated parameter sets from the separate runs of SNOW-17 and SACSMA were combined and SACSMA/SNOW-17 was run as a coupled model for January 2000-June 2011. During these coupled model runs, the precipitation and temperature inputs created from DCEW weather data were used to force the model. Two basic model simulations were run during this final step, comparing the ADCs that are used to melt snow. These model runs include the baseline case using the empirical ADC and a scenario using the NWS's calibrated ADC from the larger Boise River Basin. Calibration and the ADC comparison

were completed at ¼ HRAP spatial resolution. For the third objective, the coupled model was run at the standard 1 HRAP spatial resolution, using the empirical ADC, to test the affect of spatial resolution on model output. The same basin average parameter values from the ¼ HRAP model run were used at the 1 HRAP resolution model run.

Validation/Verification

Validation and verification of the model output was completed by using the time series of observed hydrologic data that has been collected over the 11 year period of record for DCEW. As was the case for calibration, visual inspection of the annual hydrographs at the outlet of DCEW is the primary validation/verification criteria. Timing of the rising and receding limbs of the hydrographs as well as timing and magnitude of peak and low flows was analyzed to determine the accuracy and differences between the model runs. Inspection of the interior hydrographs, at C2M, C1E, C1W, and BG, was also examined for differences between the model runs. Annual and monthly percent bias, NSE, and RMSE statistics on LG discharge were analyzed to determine relative improvements between the model runs with different ADCs.

The time series of snow data collected at the TL and LDP pixels was used to test the accuracy of the model and investigate times when there are differences in modeled discharge between the two ADC model runs. Annual and monthly percent bias, NSE, and RMSE statistics on TL and LDP snow depth were also analyzed. The form of precipitation and timing of snowmelt events, as determined by relative changes in snow depth, compared to observed data, was also used to determine how well the snow processes were being modeled. Observed snow depth at TL and LDP were primarily used for WY 2010 and WY 2011 since this is the only time frame both observed snow

depth time series data sets are available. The TL snow depth record goes back to the beginning of the simulation period and was evaluated during other years as well. The BOG snow depth and SWE data were used to look at general snow accumulation and ablation trends. Important hydrologic events were also investigated to determine which processes SACSMA/SNOW-17 does not accurately represent.

Scaling the Model, Input Forcings, and Parameters Down to 1 km

To run the model at a finer resolution, the source code first had to be modified to run at a different spatial resolution. A new connectivity file was also created for the finer ¼ HRAP spatial resolution using GIS techniques outlined in Reed (2003). The precipitation, air temperature, and model parameters also had to be downscaled to the correct resolution. Hourly precipitation and air temperature data from the weather stations in DCEW were used to force the coupled and SNOW-17 only model runs. For the first 7.5 years, LW and TL weather data were used as these were the only weather stations in DCEW. From mid-2007 through present day, the LDP weather station data was also used to discretize the precipitation and air temperature inputs. The SCR weather station was installed in the summer of 2010 and was used to force the model starting in 2011. The hourly gap-filled precipitation data used was processed at Boise State University while the air temperature data was provided with gaps. The BOG site as well as the Agrimet station were used for reference and gap filling of the air temperature data.

Monthly and annual cumulative precipitation and average air temperature have linear relationships with elevation, as shown in Figure 5-8. Using the average elevation of each model pixel and the elevation of the meteorological data, a linear regression was applied to the hourly precipitation and air temperature data to discretize the input forcings

into each ¼ HRAP model pixel (or 1 HRAP model pixel for the coarse resolution model runs), for each hour of the model simulation time period.

Discretization of parameters was accomplished in a slightly different manner. Parameter values were provided by the NWS at 1 HRAP scale (for CONUS) so these values were used during the coarse resolution model runs. The finer ¼ HRAP scale parameter values were derived individually by using values from the surrounding 1 HRAP scale pixels and location of ¼ HRAP pixel inside the 1HRAP pixel to average the appropriate 1 HRAP pixel values.

RESULTS

The results of the SNOW-17 calibration are presented first showing the sensitivity of model parameters to snow depth at the TL and LDP model pixels. The calibration of SNOW-17 was completed using the empirical ADC as a non-calibrateable parameter. The coupled model was then run for the two different ADCs, at ¼ HRAP resolution, and is the focus of the results and discussion below. The coupled model was then run at 1 HRAP resolution for the empirical ADC. All of the results discussed are for WY2004 – 2011. This was done to ensure we were past the model warm up time and when both models had less than 25% annual bias for the remainder of the modeled time period.

SNOW-17 Calibration Results

The decision was made to calibrate SNOW-17 separately from SACSMA because we wanted to get the snow distribution correct as this was the essence of this research. Since there are so many parameters between the two models, there was a lot of room for error due to the many combinations of parameter values possible. Per the NWS manual calibration procedure (NWS, 2009; NWS, 2011), the major parameters (see Table 2) were adjusted first to remove the large errors of snowmelt timing and form of precipitation. Of these five major parameters, only three, SCF, MFMAX, and SI, were sensitive to the snow depth model output, with MFMIN needing only minor adjustments from *apriori* values. The UADJ parameter surprisingly did not have any sensitivity to the model output and was left at its *apriori* values. As mentioned above, the SI parameter

was quickly set to a high value so that the ADC normalized the SWE by the maximum SWE during each accumulation season.

Adjustments made to SCF and MFMAX only were not allowing the model to accurately predict the snow distribution at the two internal locations where we have a time series of snow depth so the minor parameters were also examined. It was found that the model output was also sensitive to PXTMP and MBASE, which along with SCF have single values across the entire watershed. Adjusting these single values provides improvement at one internal location while the other internal location model simulation became worse. A grid of values for these three parameters, PXTMP, MBASE, and SCF, was ultimately used to get the distribution of snow correct between the two internal locations. The spatial grid used was determined by elevation and topographic characteristics of each pixel as well as a trial and error process.

Figure 9 and Figure 10 compare the model run with the final calibration parameter set (spatial grids of PXTMP, MBASE, and SCF; black line) with a single low (Figure 9) and single high (Figure 10) value for these parameters. Each line in these figures is a model run with one parameters' value changed (e.g. the red line in Figure 9 is for model run with SCF=1 and all other parameter values being from the calibrated parameter set). It is evident from these comparisons that spatial grids of the PXTMP, MBASE, and SCF parameters are not only necessary in DCEW, because the *apriori* values (0°C, 0°C, and 1, respectively) do not closely follow the observed blue line, but it also requires a range of values between model pixels, based on the relative differences between single value parameter model runs and the green calibrated lines for the TL and

LDP model pixels. The spatial grids that were used for these parameters are shown in Figure 11 and Figure 12

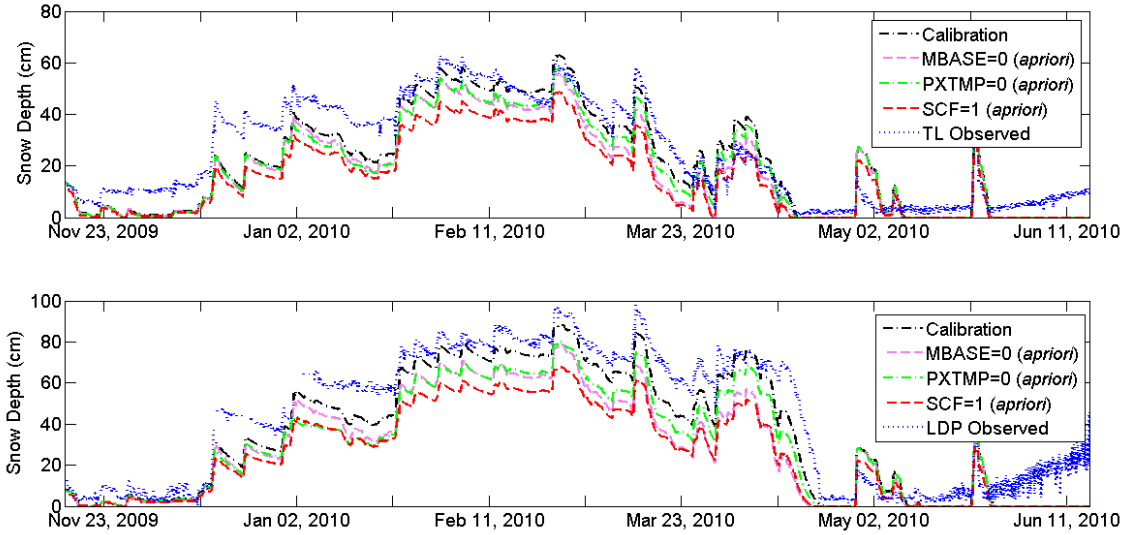

Figure 9. SNOW-17 Decoupled Calibration Gridded Parameter Comparison of Low Grid Values for WY2010. The Top Panel is TL Snow Depth and the Bottom Panel is LDP Snow Depth.

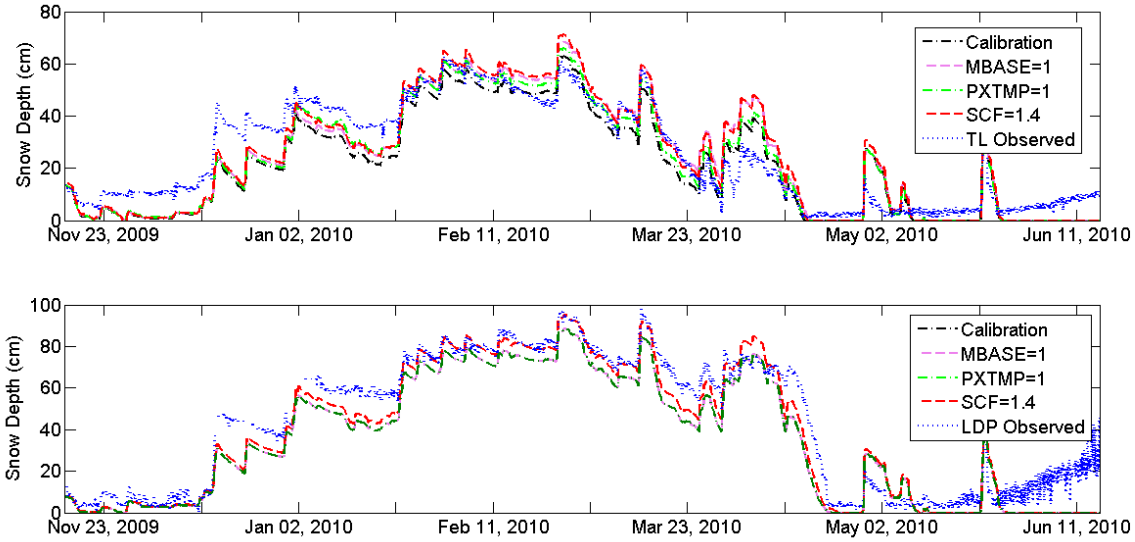

Figure 10. SNOW-17 Decoupled Calibration Gridded Parameter Comparison of High Grid Values for WY2011. The Top Panel is TL Snow Depth and the Bottom Panel is LDP Snow Depth.

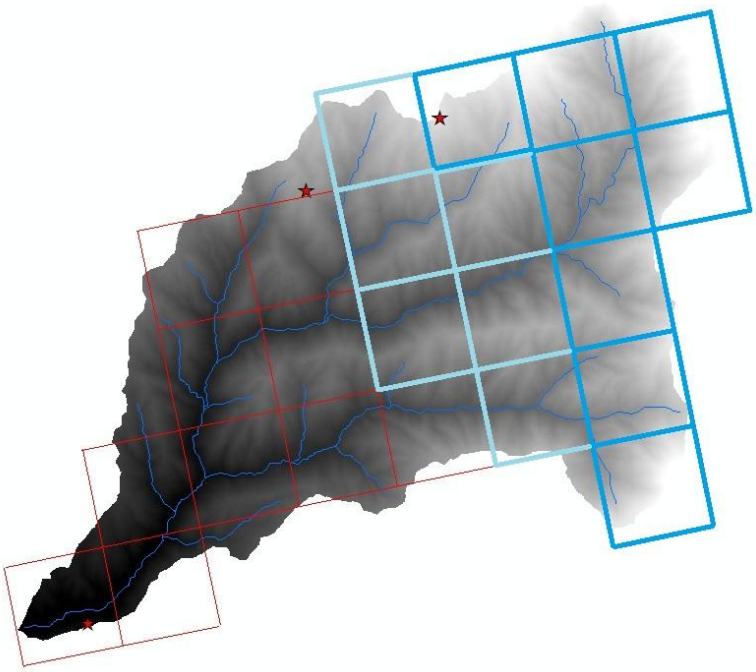

Figure 11. Calibrated Spatial Variation in PXTMP and MBASE Parameters. Dark blue is 1°C, Light Blue is 0.5°C, and All Other Pixels are 0°C.

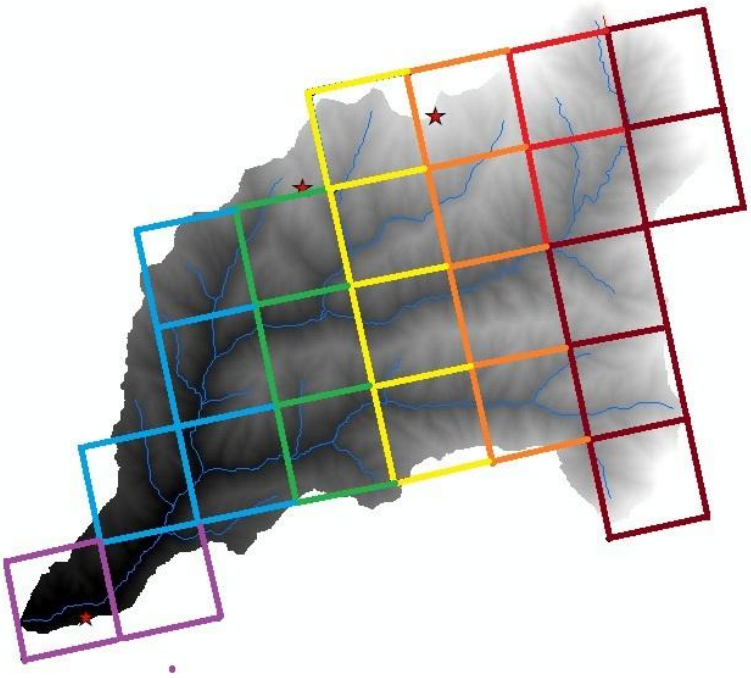

Figure 12. Calibrated Spatial Variation in SCF Parameter. Dark Red is 1.4, Red is 1.35, Orange is 1.3, Yellow is 1.25, Green is 1.2, Blue is 1.15, and Purple is 1.1.

Empirical Basin ADC versus NWS Basin ADC – Hydrograph and Snow Depth Comparison Results

Overall, both the empirical and NWS basin ADC model runs predict the observed streamflow to within 25% annual bias, had an annual RMSE of 0.062-0.2 m^3/s (NWS ADC) and 0.055-0.17m^3/s (empirical ADC), and an annual NSE of 0.40-0.84 (NWS ADC) and 0.46-0.88 (empirical ADC) (WY2004 – 2011, except for low flow WY2005 and 2007). Visually, the empirical basin ADC typically predicts the observed streamflow with higher accuracy earlier in the year (December – March), before the observed peak streamflow (March – May) and both ADCs model the receding limb more accurately than the other some years. Both the empirical and NWS model runs show a positive bias most years (empirical: 5.1% - 21.5% bias and NWS: 9.5% - 20.2% bias), where the discharge is being overestimated and a negative bias (model underestimates streamflow) in WY2006 (empirical: -4.8% bias and NWS: -3.2% bias) and WY2008 (empirical: -24.1% bias and NWS: -20.0% bias). The years with negative bias also have the highest annual NSE values meaning that the models overestimate the discharge (positive bias, lower NSE) more severely than they underestimate the discharge (negative bias, higher NSE). Overall, the empirical ADC has higher annual NSE values and lower annual RMSE values, indicating a better model fit. The annual biases between the two ADC runs are very close in value.

The only difference in the parameter set between the two model runs is the shape of the ADC as shown in Figure 3. Both model runs hit the peak streamflow some years and completely miss it others. When the peak streamflow is less than 0.5 m^3/s, both models tend to grossly overestimate peak flow (e.g. WY2005, empirical 113% higher and

NWS 99% higher, and WY2007, empirical 45% higher and NWS 73% higher). When the peak streamflow is greater than 3 m^3/s, both models tend to grossly underestimate peak flow (e.g., WY 2006, empirical 51% lower and NWS 49% lower, and ROS event in 2011, both models predicting flow of ~0.5 m^3/s when the observed flow was 3.4 m^3/s). When the peak streamflow is between 0.75 m^3/s and 2.5 m^3/s, both models do a good job of modeling the observed peak streamflow (e.g. WY 2004, 2008, 2009, 2010, main peak in 2011; see annual hydrograph comparisons in Appendix A). The mean annual flow between the ADC model runs are very similar, ranging from 0.14% to 5.8% difference.

The models produce very similar discharges during the dry summer season as indicated visually and by the July-October monthly bias, NSE, and RMSE values. During this time frame, the empirical and NWS model runs are within 5% bias of each other, with the exception of October 2007 where the empirical ADC has a 4.4% bias and NWS has a 6.3% bias. For most years, the April monthly bias values between the two model runs are the most different from one another. The observed peak discharge is typically seen in April each year, although the observed peak could come as early as March (e.g., WY2004 with an extended above freezing temperature time frame starting in March), or as late as May, as was the case for WY2005 and the second WY2008 peak. The month of February shows many years with significantly different monthly bias values between the two model runs. The average monthly flow for February between the two ADC model runs is 0.11m^3/s and the percent difference between the model runs ranges from 4.7% difference in 2005 to 20.5% difference in 2008.

Six time frames/events were selected to analyze the differences and determine causes of stream hydrograph response to the same precipitation and snowmelt events

between the empirical ADC and NWS ADC model runs. Two events from 2009, 2010, and 2011 were chosen, one before peak streamflow and one after peak streamflow. These events (shown in Table 3) were selected because the hydrograph response between the two model runs was significantly different and therefore were used in determining the importance of a site derived ADC. Several rain on snow (ROS) events were also analyzed to demonstrate model performance during these unique precipitation events that are becoming more common. Event hydrograph, snow depth, and water input comparison plots will be shown for a few events here and the others can be seen in Appendix B.

Table 3. Event Data for ADC Comparison Model Analysis

Event #	Start Date	End Date	Empricial ADC Volume (m^3)	NWS ADC Volume (m^3)	Observed Volume (m^3)
1	3/10/2009	4/16/2009	1,635,072	2,038,950	1,223,668
2	4/17/2009	5/20/2009	1,613,489	1,175,949	1,201,610
3	3/1/2010	4/15/2010	1,144,244	1,468,098	691,511
4	4/7/2010	5/5/2010	1,686,874	1,538,880	977,177
5	2/4/2011	3/30/2011	1,211,533	1,563,907	999,320
6	5/5/2011	6/18/2011	2,137,545	1,687,474	1,948,634

Early Season Events

Event #1

There was a small ROS event on 3/15/09 (2-3 mm rain, depending on elevation) that started as a snow event just after daylight hours and changed to rain as the temperature rose the following day. The modeled streamflow had already started rising from the warm temperatures on the previous two days, two days sooner than the rise in discharge was observed at LG. The early rise in the modeled discharges is because the

model runs melted more snow than was observed, the empirical ADC decreasing the snowpack depth 63% more than observed and NWS decreased the snowpack depth 45% more than was observed at TL. The extra water from the NWS ADC is because it completely melted out both the TL and LDP pixels whereas the empirical ADC decreased the snow depth but more water was retained within the snowpack.

The next minor peak was initiated from several days of above freezing temperatures, inducing melt across the watershed and continued with a ROS event right before the peak flow that sent the last slug of melt water to the stream channel. The modeled discharge initiated its rise one day earlier than the observed rise in discharge. There was a larger ROS event (5-6 mm of rain, depending on elevation) on 3/21/09 that caused the final rise in streamflow where a minor peak was observed on 3/22/09. Both model runs appear to model this rise well, with the empirical ADC being 10% lower at the peak and NWS ADC overshooting the peak by 33%, but both models underpredicted the amount of rise that was due to the slug of meltwater from the ROS event. The NWS ADC overestimated the streamflow after the minor peak by 100% or more. The higher increase in streamflow modeled by the NWS ADC at the minor observed peak is due directly to the snowmelt leaving the highest elevation pixels and the complete meltout of the TL pixel one day before the peak discharge. There is 25-65% more snowmelt occurring per pixel in the three highest elevation pixels when the NWS ADC is used during this time frame while the empirical ADC melts 14% more snow from the TL pixel (due to the complete meltout by the NWS ADC). The three highest elevation pixels have a larger fSCA in the NWS ADC model run during this higher melt timeframe while the TL pixel has a lower fSCA than the empirical ADC model run.

Following this peak discharge, both modeled hydrographs begin to recede with the NWS ADC losing streamflow more quickly at first than the empirical ADC. There is a small snowmelt event (3/29/09) affecting the rain/snow transition elevation pixels, releasing water from the snowpack at the TL pixel in both model runs and ripening the snowpack at the higher elevation pixels, from an increase in temperature. There is a notable difference in LDP snow depth during this time (steeper decline by NWS ADC) between the two model runs that can be attributed to the different melt patterns induced by the ADCs. Only the NWS ADC releases water from the snowpack (2 mm) in this pixel as the snow depth approaches zero.

After the local minimum streamflow on 4/4/09, both model runs begin to melt the snow much faster than is observed and consequently the modeled discharge begins to diverge again from the observed discharge. The hummocky nature of this discharge rise is due to the cyclic nature of the air temperature during this time frame, shutting down or slowing down snowmelt when there are lower temperatures. The last rise in discharge that reached the annual peak modeled discharge was due to a final ROS event that rained over 7 mm on the TL pixel and 5 mm of rain with 2-3 mm of snow mixed in at the highest elevation pixels. The increase in streamflow from the empirical ADC run was 40% lower and the NWS ADC was 45% lower in discharge increase than the observed flow for this ROS event.

Comparison of snow depth at the TL pixel with the modeled snow depth shows that the empirical ADC closely matched the observed TL snow depth throughout this event time period, slightly underpredicting its value and being closer to observed after the peak discharge. The NWS ADC grossly underpredicted the snow depth and melted the

snow faster, leading to the increase in modeled streamflow that was not observed. When the empirical ADC snow depth more closely matched the observed snow depth, the modeled discharge was also closer to the observed value.

For the entire event period, the empirical ADC statistically performed better with respect to the LG discharge and TL snow depth for all three statistics. The percent bias for discharge at LG was 33% compared to 66% for the NWS ADC and -20% versus -48% for the NWS ADC for the TL snow depth. The NSE was quite high at 0.84 for TL snow depth compared to 0.25 for the NWS ADC and both NSE values were negative for discharge at -0.133 and -1.63. The RMSE was also much better for the empirical ADC with 0.207 m^3/s versus 0.315 m^3/s for LG discharge and 8.72 cm versus the NWS ADC's 18.9 cm for TL snow depth.

The interior hydrographs show very similar trends to the LG hydrograph during this event. The empirical ADC matched all the interior hydrographs more closely throughout the first rise and fall of this event. Both ADCs grossly overestimated the discharge at all the interior location during the second rise on 4/9/09. The C1E discharge was the closest match for both ADC model runs but the models predicted the rise in streamflow two days earlier than what was observed.

Event #3

A similar phenomena is occurring when both ADC hydrographs take a sharp rise in streamflow and the observed only increases slightly on 3/15/10 (see Figure 13). Both models were trending well with the observed discharge prior to this rise in streamflow, with the empirical ADC discharge closely matching the magnitude while the NWS discharge was 120-130% higher than the observed discharge. The empirical ADC was

trending just above the observed snow depth at TL while the NWS ADC was consistently lower and releasing more water from the snowpack, causing the rise in modeled discharge. Both models underpredicted the snow depth at the LDP pixel with the empirical ADC being closer in magnitude and doing a better job of modeling the melt/reduction in snowpack trend (see Figure 15).

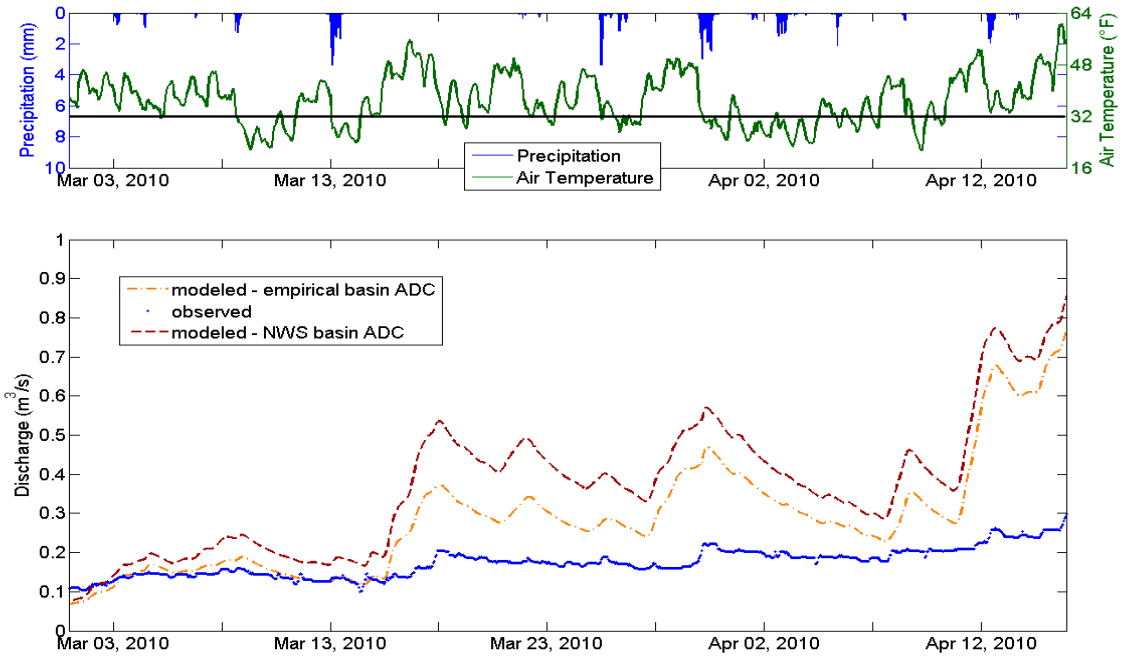

Figure 13. Event Hydrograph for Event #3

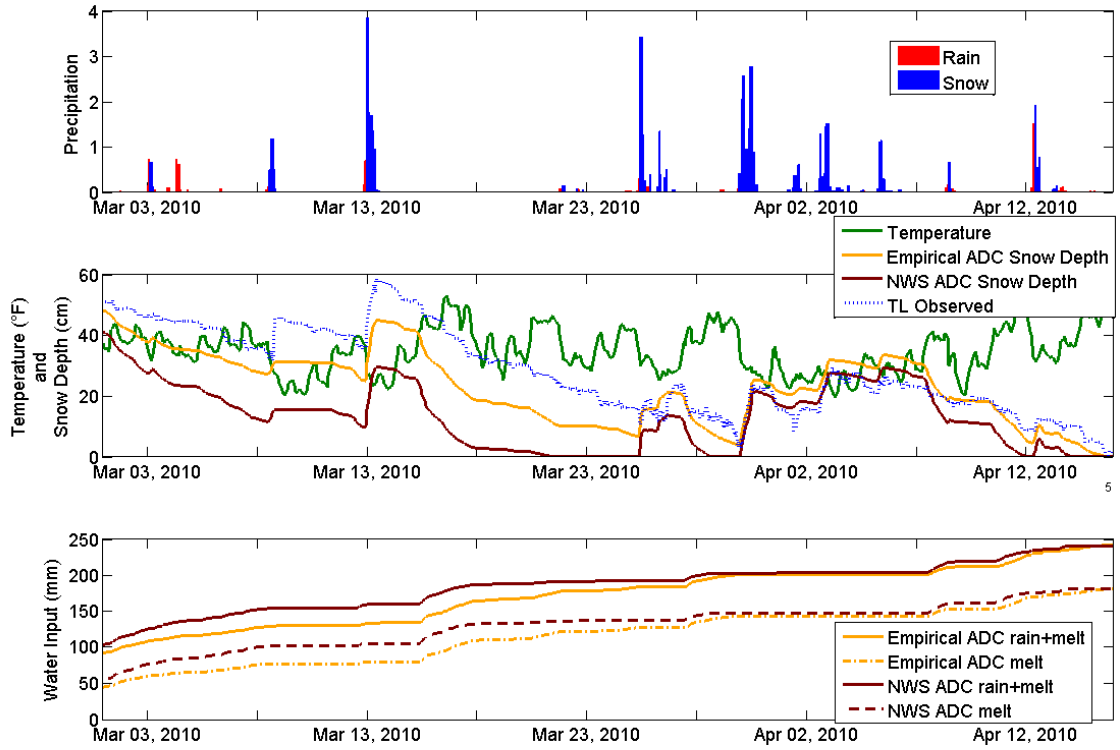

Figure 14. Snow Depth and Water Input Comparison at TL for Event #3. Top Plot is Precipitation, Middle Plot is Temperature and Snow Depth, and Bottom Plot is Cumulative Water Input to the Subsurface.

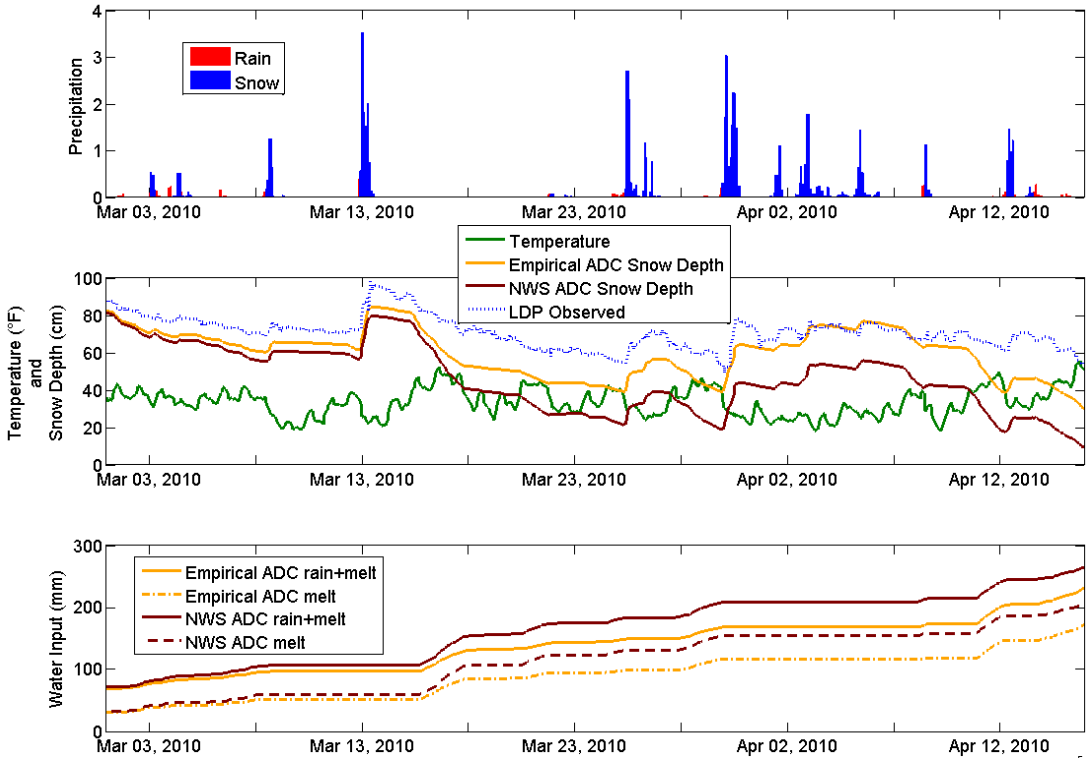

Figure 15. Snow Depth and Water Input Comparison at LDP for Event #3. Top Plot is Precipitation, Middle Plot is Temperature and Snow Depth, and Bottom Plot is Cumulative Water Input to the Subsurface.

Three days after the start of 3/15/10 divergence between modeled and observed discharge at the first peak, the NWS ADC streamflow is 162% higher and the empirical ADC streamflow is 81% higher than the observed flow. Both ADC's show the largest contribution of snowmelt during the rise in streamflow starting 3/15/10 to be from the LDP pixel with the NWS ADC sending 38% more snowmelt to the stream channel. The empirical ADC releases 13% more water from the TL pixel snowpack than the NWS, which releases 33-40% more water from the snowpack at the three higher elevation pixels during this time frame, causing the larger increase in streamflow. The observed snow depth trend was decently followed in the TL pixel, with each model predicting a 21 cm decrease in depth versus the 16 cm of observed snow depth decrease. The 17 cm observed decrease in snow depth at the LDP pixel was not well modeled, with the

empirical ADC modeling a 65% higher decrease and NWS ADC modeling a 115% higher decrease in snow depth.

This melt event was driven by a significant increase in air temperature (up to 20°F more than the assigned snowmelt temperature), which caused the immediate and steep rise in streamflow. As the temperature drops again, the snowmelt ceases or slows down and the modeled streamflow (from both ADC's) recedes until the next significant temperature increase. This cyclic pattern continues with each high temperature/high snowmelt event causing a sharp rise in the modeled streamflow, sharper than what is observed.

The empirical ADC was better than the NWS ADC in all three statistics for the LG discharge, and TL and LDP snow depths. The discharge percent bias was 65.5% compared to 112% for NWS ADC while both NSE values were below zero with the empirical ADC being -18.9 and the NWS ADC being -42.7. The RMSE for discharge was closer between the model runs than the other statistics but the empirical ADC was superior with 0.16 versus 0.24 m^3/s RMSE. There were substantial differences in the statistics between the two model runs for both the TL and LDP snow depths. The percent bias was -18% and -15%, NSE was 0.61 and -1.4, and the RMSE was 8.7 and 12.9 cm for the TL and LDP pixels, respectively, for the empirical ADC while the numbers for the NWS ADC were -52% and -35% bias, NSE was -0.78 and -9.1, and RMSE was 18.5 and 26.7 cm for the TL and LDP pixels.

The empirical ADC followed the interior hydrographs more closely during this event but both models missed the small rises in discharge at C1E in the middle of March. The small rise at BG was modeled but the modeled rise was early and much greater in

magnitude. The rise at C1E on 3/17/10 was modeled very well by the empirical ADC while the NWS ADC rise was more than observed.

Event #5

The two modeled streamflow values depart from each other on 3/1/11 and both rise above the observed streamflow with the NWS ADC being 121% higher and the empirical ADC being 61% higher than the observed streamflow as they both reach a minor peak flow on 3/3/11. Prior to the peak flow, the NWS modeled snow depth more closely followed the observed depth at the TL pixel, which was during the time when the NWS discharge more closely matched the observed flow. At the peak flow, the TL snow depth is modeled almost perfectly by the empirical ADC and continues to follow closely until a significant snowmelt event on 3/10/11 where both model runs overpredicted the amount of snowmelt in the TL and LDP pixels, causing the sharp increase in streamflow.

The NWS ADC produced 77% more snowmelt than the empirical ADC at the TL pixel during the initial rise in streamflow (3/1/11) while the other high elevation pixels are just reducing their negative heat storage values (amount of heat that must be added to the snowpack to bring it to the melting temperature), essentially ripening the snowpack. The streamflow in both model runs plateau for several days after that, with the empirical ADC streamflow closely following the observed streamflow. There is the same cyclic nature of the streamflow during this time period that mimics the air temperature trend crossing the freezing temperature.

The empirical ADC snow depth at LDP matches the observed snow depth starting on 3/6/11 and continues to closely follow it until 3/26/11 when the observed snow depth decreases slightly and the modeled snow depth increases. The NWS snow depth is

always lower than the empirical ADC snow depth during this event and does match the observed snow depth at times, which correspond to times when the NWS streamflow more closely matches the observed flow.

The modeled streamflow takes a sharp rise again 3/11/11, where the NWS ADC rises to 228% higher and the empirical ADC is 97% higher than the observed flow. This is caused by a significant increase in air temperature for a couple of days that reduces the negative heat storage in the highest elevation pixels and melts snow from the TL and LDP pixels. The melt from the TL pixel is essentially the same for both model runs but the melt from the LDP pixel is 45% higher from the NWS ADC than the empirical ADC. Both model runs produce more melt from these pixels (higher decrease in snow depth) than is seen in the observed snow depth decrease.

There is a third local peak seen in modeled and observed streamflow on 3/16/11 (highest streamflow on event plot) where the NWS ADC is 58% higher and the empirical ADC is 21% higher than the observed flow. During this final rise in modeled streamflow (3/14/11 – 3/16/11) there is a significant precipitation event that started as rain and changed over to snow around the time of peak modeled discharge. Both models melted about the same amount of snow during this event but the NWS discharge was already much higher than observed so the same increase in streamflow produced a much higher overprediction of the local peak discharge.

Immediately after the peak on 3/16/11, the empirical ADC recedes quickly back to the observed flow and then oscillates just above the observed flow until 3/27/11, during which time the observed and modeled snow depth at TL and LDP pixels closely match. The NWS ADC hydrograph is 30-42% higher than the observed flow during the

same time period and its modeled snow depth is 20-70% lower than observed depth at both TL and LDP pixels. There are several small melt events at the TL pixel where the NWS ADC models 21-88% more melt than the empirical ADC, which keep the streamflow elevated above the observed flow.

A large precipitation event from 3/24/11 – 3/28/11 produced a 16-20 mm mixture of rain and snow. Both ADC's model runs show the same trend in snow depth decrease and accumulation, with different starting depths. The amount of snow was overestimated during this large rain and snow mixture event, reducing the amount of water moving to the stream (because it is being stored in the snowpack) and underestimating the streamflow. At the beginning of this large precipitation event, the empirical ADC snow depth at LDP matched perfectly, then rain was observed at the LDP pixel while snow was modeled. There were intermittent rain and snow events observed in the TL snow depth (decrease and accumulation) while both models accumulated snow.

As with the previous two early season events, the empirical ADC outperformed the NWS ADC statistically in all categories. The percent bias was low for all three hydrologic variables with the empirical ADC with streamflow being 21% versus 56% for the NWS ADC, 5.5% (empirical) versus -32% (NWS) for TL snow depth, and 1.7% (empirical) versus -11% (NWS) for LDP snow depth. The NSE for discharge and LDP snow depth were very high for the empirical ADC with 0.63 and 0.85 compared to the NWS ADC values of -0.48 and 0.63 for discharge and LDP snow depth, respectively. The TL snow depth NSE was negative for both model runs with the empirical ADC NSE being much less negative at -1.03 versus the NWS ADC NSE of -7.5. The RMSE was good for both model runs but the empirical ADC was better overall. The RMSE was

0.088 m^3/s for discharge and 6.8 cm for both TL and LDP snow depths under the empirical ADC while the NWS ADC has values of 0.18 m^3/s for discharge, 13.9 cm for TL, and 10.5 cm for LDP snow depth.

Both model runs predicted similar trends in the interior discharge values as they did for LG with the empirical ADC being closer in magnitude throughout the duration of this event. Most interior locations had a modeled rise in discharge on 3/10/11 that was much higher than observed. This slightly receded before all interior locations had an observed rise in discharge on 3/15/11 that was modeled by both ADC model runs.

Late Season Events

Event #2

Prior to this event, the modeled streamflow from both models was essentially the same and had just receded from a fairly large overestimation of the observed discharge, but had not receded all the way to the observed flow. The previous rise (peak modeled flow but not peak observed flow) was due to a significant increase in air temperature (into the low 60's) that included a 6 mm rain on snow event (at highest elevations because snow had melted out at low elevations already) at the modeled peak flow. There is an oscillatory nature to the observed streamflow as it rises to the peak on 4/22/09 that is modeled but with a dampened affect, due to the oscillations in air temperature.

When the modeled discharges matched on 4/17/09, the empirical ADC had 40 cm of snow in the LDP pixel (NWS had none), 40% more snow in the second highest elevation pixel (pixel 23), and 10% more snow in the highest elevation pixel (pixel 24). The NWS ADC underestimated the observed peak streamflow on 4/22/09 by 14% and

the empirical ADC overestimated the observed flow by 10%. The modeled peak discharge was reached by the NWS ADC one day early and does not exhibit the bimodality that exists in the peak observed discharge. The empirical ADC reached its peak at the same time as the modeled streamflow and does exhibit the double peak in streamflow that was observed. The NWS ADC better matched the magnitude of the observed recession while the empirical ADC better matched the recession trend but was consistently 50-75% higher than the observed flow.

The amount of snowmelt that caused the peak streamflow differs between the two model runs in most pixels with the exception of pixel 23 where both model runs melted the same amount of snow. The NWS ADC melted 16% more snow in the highest elevation pixel and melted out the LDP pixel ~5 days sooner than the empirical ADC. Both models melted at similar rates but much more water (78 mm versus 14 mm from the LDP pixel) was sent to the stream channel from the empirical ADC, mainly from the LDP pixel.

The three small oscillations in early May seen in both models and observed streamflow was caused by three back-to-back precipitation events (8 mm, 10 mm, and 3 mm of precipitation) that occurred over 12-18 hour periods each with a few hours in between each event where no precipitation fell. The form of precipitation was all rain at the TL pixel, a small amount of snow at the start of the event at the LDP pixel, and intermittent rain and snow events at the two highest elevation pixels. The TL and LDP pixels were completely melted of snow before these three precipitation events as well as pixel 23 in the NWS model run, which accumulated snow in each miniature event then subsequently melted it as the temperature rose each day. The NWS ADC discharge was

close in magnitude to the oscillations in early May but each oscillation was slightly delayed and did not show as steep of a rise as the observed flow oscillations. The empirical ADC discharge matched the timing and relative increase in the observed oscillations but was higher in magnitude because of the antecedent conditions of its discharge prior to the first precipitation event.

As there was no snow present at the TL pixel during this event and the LDP snow depth was not being recorded, the only statistical measure that can be analyzed for this event is the discharge at LG. As seen visually by the hydrograph comparison, the NWS ADC was statistically better than the empirical ADC in all three statistics calculated. The percent bias was -2.1% for the NWS ADC versus 34%, NSE was 0.62 versus -0.11 for the empirical ADC, and the RMSE was 0.11 m^3/s for the NWS ADC compared to 0.18 m^3/s for the empirical ADC.

As was the case for the LG discharge, the NWS ADC more accurately predicted the discharge at all interior points compared to the empirical ADC except for BG. The discharge trend at C1W at the beginning of this event was not well captured by either model as the observed discharge was holding steady while the models were diverging in value from one another. The observed rise at BG on 4/21/09 was overpredicted by both models with the empirical ADC being closer. Both models were also several days early in their predicted streamflow rise.

Event #4

On 4/7/10, the modeled discharge values were fairly close to the observed flow then began a rise and fall cycle until the two model discharges diverge from each other on 4/18/10 (see Figure 16). The first rise in discharge that was only slightly seen in the

observed flow (4/9/10) was due to a significant overestimation of snowmelt at the TL pixel (see Figure 17) and to a lesser extent at the LDP pixel (see Figure 18).

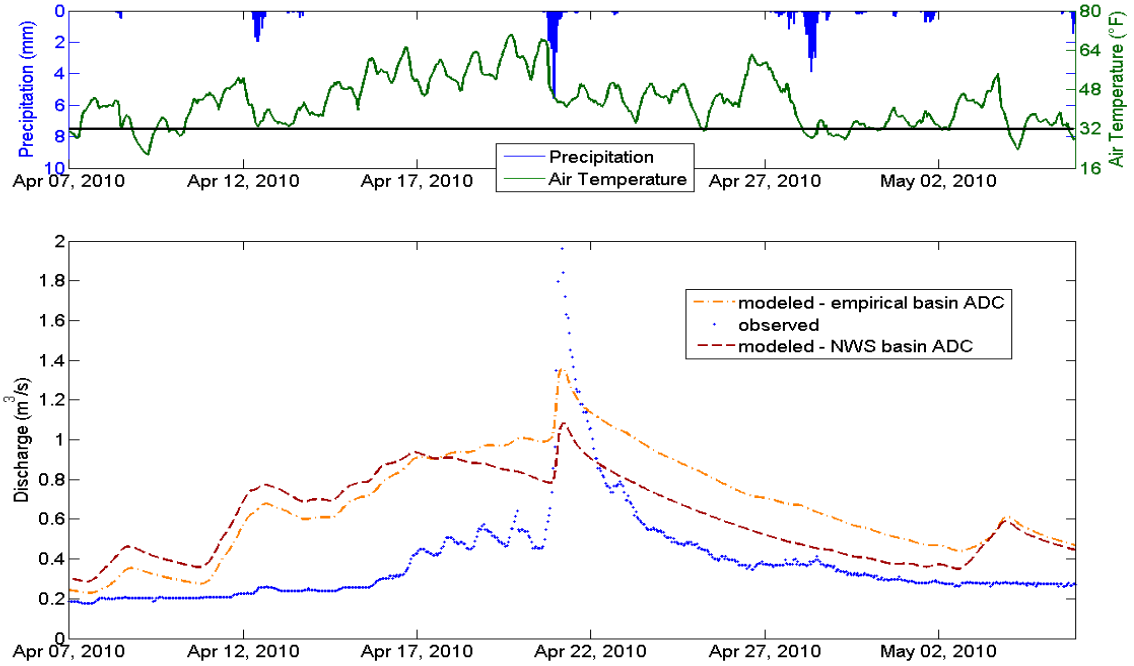

Figure 16. Event Hydrograph for Event #4.

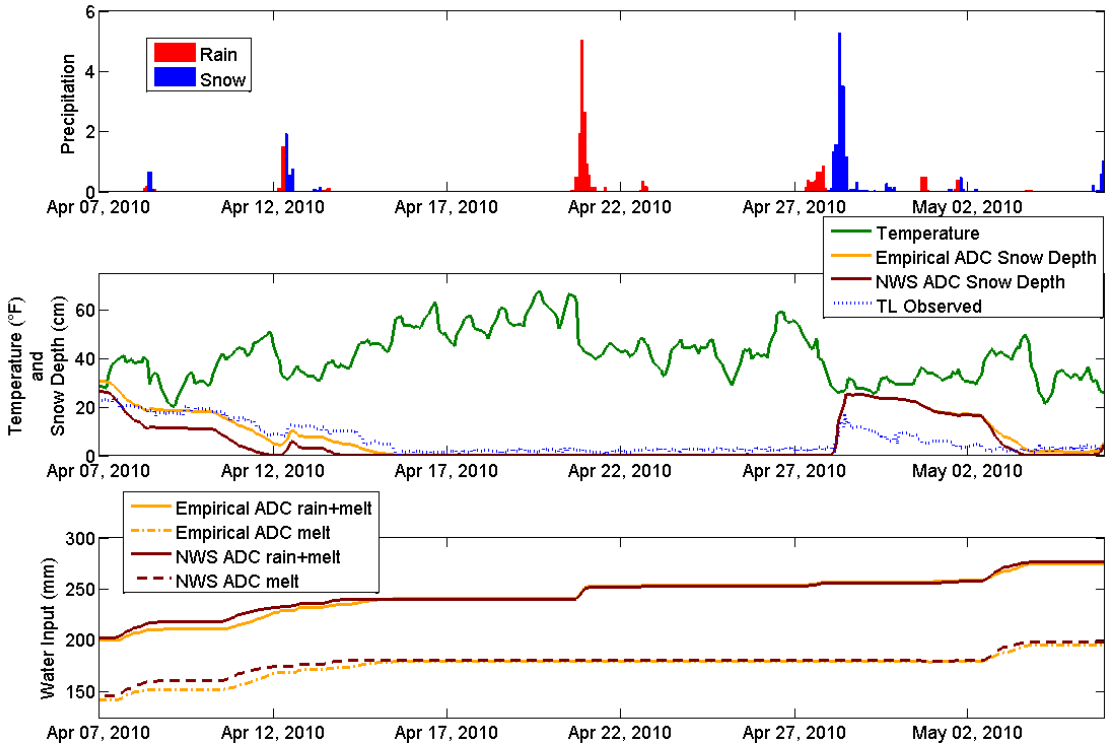

Figure 17. Snow Depth and Water Input Comparison at TL for Event #4. Top Plot is Precipitation, Middle Plot is Temperature and Snow Depth, and Bottom Plot is Cumulative Water Input to the Subsurface.

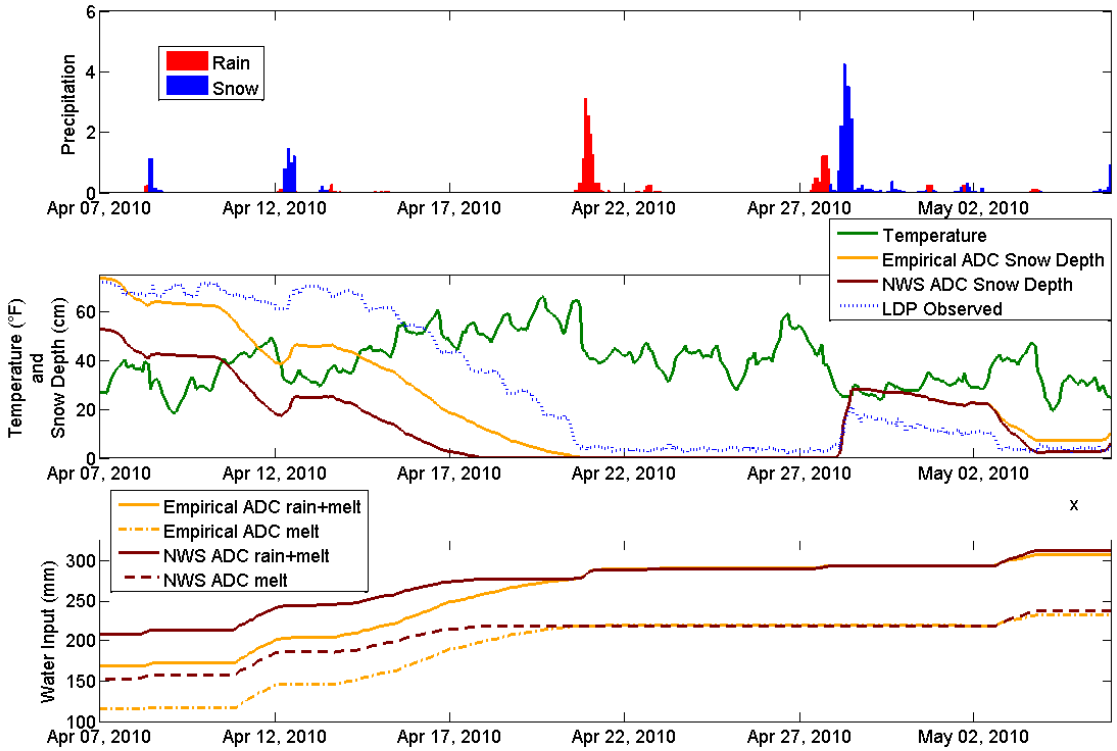

Figure 18. Snow Depth and Water Input Comparison at LDP for Event #4. Top Plot is Precipitation, Middle Plot is Temperature and Snow Depth, and Bottom Plot is Cumulative Water Input to the Subsurface.

On 4/10/10, there was another snowmelt event initiated by a significant rise in air temperature. The empirical ADC snow depth at the TL pixel closely followed the observed snow depth until 4/12/10 when the observed snow depth stopped decreasing and the model continued to melt the snowpack. With the smaller depth of snow modeled by the NWS ADC at the start of this event, the TL pixel completely melted out from this warming event. Both models did a poor job of simulating the melt dynamics at the LDP pixel as the observed snow depth decreased by 10 cm while the modeled snow depths decreased by 25 cm during the same time frame. This overestimation of melt water leaving the snowpack resulted in the overestimation of observed streamflow by 160% (empirical ADC) and 200% (NWS) on 4/17/10.

The modeled streamflow values diverge from each other on 4/18/10 as the NWS discharge continued to decrease and the empirical ADC discharge continued to increase. Both models had melted out the TL pixel by this time and the NWS ADC melted out the LDP pixel, 3 days sooner than the empirical ADC. The empirical ADC streamflow continued to rise after 4/18/10 because of the continued melt in the LDP and highest elevation pixels.

An 11 mm precipitation event occurred on 4/21/10 while the temperatures were still well above the snowmelt temperature threshold (see Figure 16), even though they dropped significantly as the precipitation event started. This caused a significant observed snowmelt event, an 11 cm change in snow depth, in the LDP pixel that was not captured at all by the NWS model because this pixel had already melted out while the empirical ADC melted the tail end of its snowpack (6 cm depth 2 days prior to the observed peak discharge) by the end of daylight on 4/21/10. The modeled peak streamflow was underestimated by both model runs, 35% lower by the empirical ADC and 60% lower by NWS. The steep rise in streamflow during this, mostly rain with rain on snow in the highest elevations, melt event was modeled but with a lower magnitude because the highest elevation pixels had snow remaining to melt. Both model runs receded with similar trends after the peak flow with the NWS ADC more closely matching the observed flow (10-42% higher) while the empirical ADC was 55-86% higher than observed until the model discharge values matched again on 5/3/10.

There were intermittent snowmelt events in the two highest elevation pixels modeled by the empirical ADC after the peak discharge that are not seen in the NWS model run because the snow had completely melted in pixel 23 at the peak discharge and

had all but melted in pixel 24 at peak discharge (less than 5 cm of snow from 4/18/10 until 4/26/10). The water inputs contribute to the empirical ADC modeled discharge, keeping it elevated above the observed and NWS discharge values.

A 17 mm snowfall event began 4/27/10 onto a snow free watershed, as modeled by the NWS ADC, and a mostly snow free watershed as modeled by the empirical ADC. The models accumulated 25 cm of snow at the TL pixel and 30 cm at the LDP pixel, both significantly higher than the observed increase in snow depth at these locations (44% higher at TL and 33% higher at LDP). It is assumed that there is a significant overestimate of snow depth at pixel 23 and 24 also, based on the occurrence at the TL and LDP pixels and the relative increase in snow depth observed at the Bogus Basin SNOTEL site (28 cm increase in snow depth at pixels 23 and 24 and 13 cm snow depth increase at Bogus). Because of this large overestimate of snow depth, the subsequent melt on 5/3/10 contributed much more water to the stream than was observed. Both modeled hydrographs overestimated the discharge during this time (empirical was 120% higher and NWS was 112% higher at the local peak discharge.

During this event, the NWS ADC does better at predicting the LG discharge while the empirical ADC does a better job at predicting the snow depth at the TL and LDP pixels. The percent bias is 57.5% for the NWS ADC discharge while the empirical ADC has a 72.6% bias. Although the discharge statistics are better for the NWS ADC, the NSE and RMSE are close between the two model runs. The NSE for discharge is negative for both model runs with the NWS ADC being -0.43 and the empirical ADC being -0.63. The discharge RMSE is 0.31 m^3/s and 0.33 m^3/s for the NWS and empirical ADC's, respectively. The TL snow depth statistics for the empirical ADC are 10.6%

bias, 0.078 NSE, and 5.89 cm while the NWS ADC values are -18.0% bias, -0.28 NSE, and 6.94 cm. The LDP snow depth statistics for the empirical ADC are -22.0% bias, 0.74 NSE, and 14.0 cm and the NWS ADC has -51.6% bias, 0.17 NSE, and an RMSE of 24.9 cm.

The modeled rise in discharge at all points in DCEW on 4/11/10 was not observed in the two interior discharge records available while there was a slight rise at LG two days later. The empirical ADC modeled the interior discharge slightly better leading up to the main rise on 4/21/10 by trending in the same direction as the observed while the NWS ADC discharge was decreasing although neither ADC was very close in magnitude. The timing of the hydrograph rise at all interior points was correct for both model runs during this event.

Event #6

The modeled discharges diverge from each other on 5/6/11 with the empirical ADC discharge more closely matching the steep rise seen in the observed discharge, but not with enough magnitude. The steep streamflow rise was a result of the observed steep decline in snow depth at the LDP pixel. This melt regime was not modeled well by either model but better by the empirical ADC (45% less versus NWS's 72% less of a snow depth decrease). There was a second pulse of melt as the daylight hit the following day where the empirical ADC underestimated the snow depth decrease by 71% and NWS by 87%. This corresponded to a local peak discharge underestimation by both models (20% lower by the empirical ADC and 28% lower by NWS) as well as a delay in the local peak discharge by 12 hours.

During the rising hydrograph (5/6/11 – 5/9/11), the TL pixel had already melted out. The empirical ADC overestimates the LDP pixel snow depth while the NWS ADC underestimates the LDP snow depth. The snowmelt event observed at the LDP pixel on 5/6/11 was not captured by either the empirical ADC (50% lower snow depth decrease) or NWS (75% lower snow depth decrease) model runs, which were melting more gradually. The difference in snow depth between the two highest elevation pixels is larger in the NWS run and almost nonexistent in the empirical ADC model run, meaning that the NWS run was melting more snow from these pixels during this time frame (15-22% more snowmelt from pixels 23 and 24). After the local peak, the empirical ADC discharge was consistently higher than observed while the NWS ADC discharge was consistently lower. The empirical ADC model run produced more snowmelt during this time frame from the LDP pixel (42 mm of snowmelt by the empirical ADC from LDP versus 5 mm by NWS) where the NWS run melted snow from the two highest pixels because the LDP pixel melted out on 5/14/11.

After a slight recession that the empirical ADC matched almost perfectly (from its peak discharge), there is an increase in streamflow that is observed and modeled by the empirical ADC while the NWS discharge increases only slightly and stays lower than observed. The continued increase in the empirical ADC discharge that was not seen in the observed flow is from it melting out the rest of the LDP pixel snowpack. The NWS ADC streamflow continues to underestimate stream discharge by 5-50%, with the exception of a 2-3 day period (5/18/11 – 5/21/11) where it increases to slightly above the observed discharge.

Between 5/11/11 and 5/17/11, the observed discharge is again cyclic in nature, with both model runs modeling this phenomenon initially. The NWS discharge starts to decline only on 5/14/11 as the highest elevation pixels melt out. The cyclic nature of the observed discharge is again from the large difference in day and night time air temperatures. After 6/1/11, both model runs underestimate the observed streamflow for the rest of the modeled time frame.

The snow depth at TL was only present for a couple of days, intermittently, throughout this event and the sensor monitoring the snow depth was beginning the capture the vegetation growth so statistics on TL snow depth were not calculated for this event. The snow depth at LDP was present for the first two weeks and then was intermittent. The statistics calculated for LDP snow depth for this event are only for the first two weeks of the event time frame. The percent bias was better for the discharge and LDP snow depth from the empirical ADC model run while the NSE and RMSE were both better from the NWS ADC model run for both the discharge and LDP snow depth. The percent bias was 9.7% and -13.4% for discharge and 52.4% and -68.5% for LDP snow depth for the empirical ADC and NWS ADC model runs, respectively. The NSE was relatively high for discharge, 0.70 and 0.55, and negative for LDP snow depth, -0.48 and -2.74, for the NWS ADC and the empirical ADC model runs, respectively.

The NWS ADC more accurately modeled the discharge at C2M and C1W during this event. Both models grossly overpredicted the streamflow rise at BG, which did not see an observed rise over the event time period. Both models also missed the rise that was observed at C1E on 5/7/11but closely followed the discharge after 5/18/11.

Rain on Snow Event Analysis

Table 4. Event Data for Rain on Snow Model Analysis

Event #	Start Date	End Date	Empricial ADC Volume (m^3)	NWS ADC Volume (m^3)	Observed Volume (m^3)
ROS1	12/20/2005	1/10/2006	643,972	702,940	306,524
ROS2	3/8/2009	3/30/2009	645,397	927,563	542,771
ROS3	12/27/2009	1/4/2010	42,709	51,428	50,237
ROS4	1/5/2010	1/20/2010	153,626	172,986	124,062
ROS5	11/28/2010	1/7/2011	429,421	501,595	314,506
ROS6	1/12/2011	1/25/2011	288,030	308,339	546,056

ROS Event #1

The first part of the ROS event in late 2005 and early 2006 did not show a significant rise in observed streamflow while both models predicted an early rise in the discharge by 5 days (see Figure 19). The overall event was characterized by mixed rain and snow throughout the event with significant amount of rain and above freezing temperatures. The early rise in discharge was caused by a 21-23 mm rain event on a 25-35 cm deep snowpack, depending on elevation, with the higher elevations receiving more rain and having a deeper initial snowpack. Both model runs began to rise in discharge within one day of the onset of above freezing temperatures. The observed discharge at LG did not rise until 12/25/05, 5 days later, and was smaller in magnitude than was modeled (empirical ADC was 64% higher and NWS was 82% higher at the first local peak discharge).

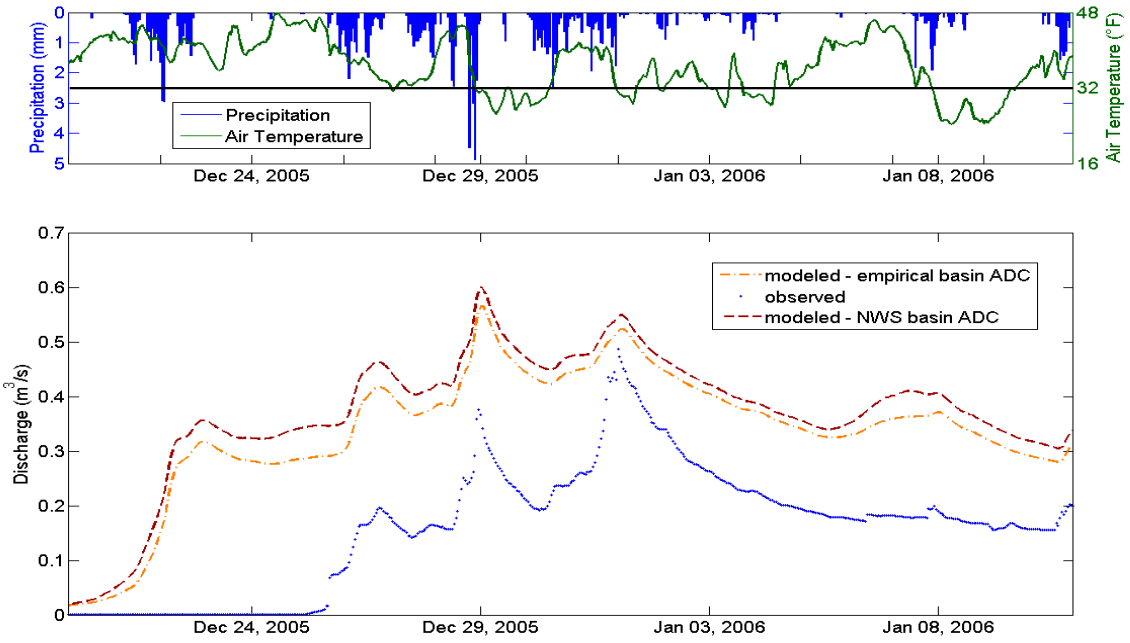

Figure 19. Hydrograph Comparison for ROS Event #1.

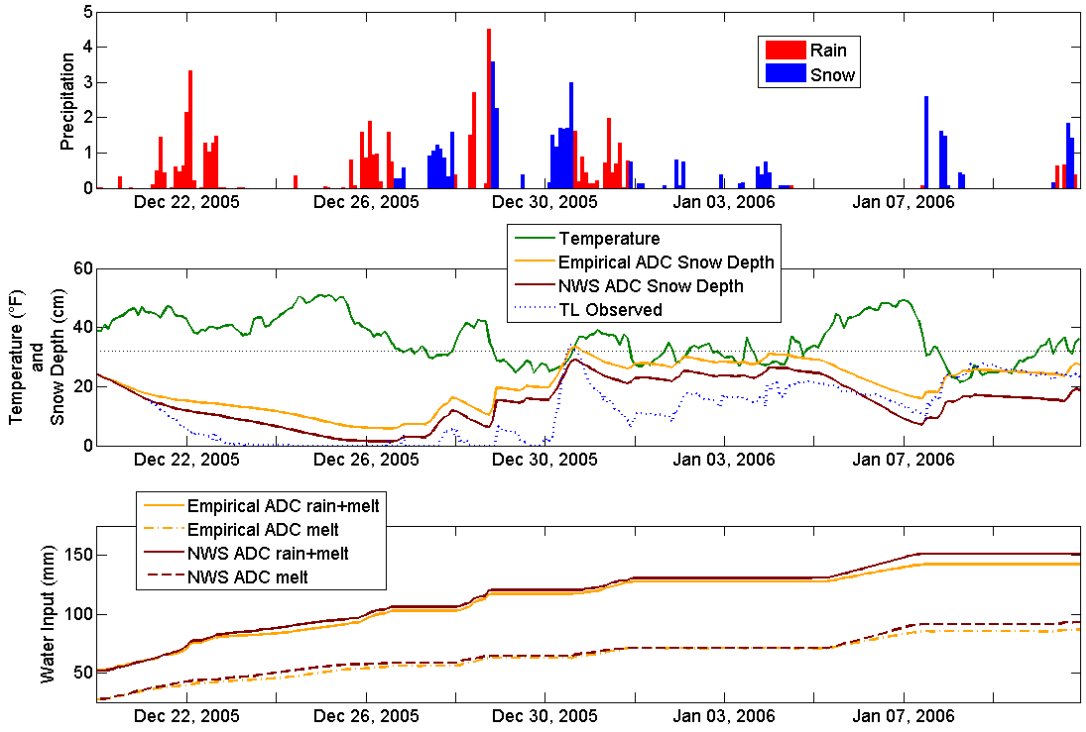

Figure 20. Snow Depth and Water Input Comparison at TL for ROS Event #1. Top Plot is Precipitation, Middle Plot is Temperature and Snow Depth, and Bottom Plot is Cumulative Water Input to the Subsurface.

The observed TL snowpack melted in 3-4 days (33 cm drop from 12/19-12/23, Figure 20) while neither model completely melted the TL pixel and did not reach the minimum value until 12/25/05, just prior to the temperature dropping below the freezing temperature for a short stint. After this initial ROS event that was modeled poorly, there were three subsequent ROS events in which the modeled and observed discharges rose together. The first of these ROS events on 12/26/05 rained 9.5-11.5 mm on the TL and upper three elevation pixels but the TL pixel had no observed snow in it at that time. The rise in streamflow was modeled well by both models with the empirical ADC rise being 3% lower and the NWS ADC rise being 8% lower. There was a cold spell before the next rise that snowed 7-12 mm, depending on elevation, in the upper elevation pixels. The next rise on 12/28/05 was initiated by a rainfall of 8-9 mm on snow in these upper elevations. This rise in discharge was not as well captured by either model with the empirical ADC modeling a rise 18% lower and the NWS ADC modeling a rise that was 16% lower than the observed rise.

On 12/30/05, with the temperature below freezing, a one day snowstorm produced an increase in the modeled snow depths of 14 cm (at TL) while the TL snow depth sensor measured a 33 cm increase in snow depth (from zero). This subsequently melted in one day as the temperature rose above freezing and 8-9 mm of rain fell in the highest elevations. The snowpack at TL decreased to 6cm (27 cm decrease in snow depth), while the models predicted a 7-8 cm decrease in snow depth at TL. This melting caused the fourth local peak on 1/1/06 and the empirical ADC discharge was only 3% higher and the NWS discharge was 8% higher than the observed. However, the rise from this last ROS event was simulated poorly by both models, each predicting a rise that was 70% less than

the observed rise. The modeled discharge also rose early at the C2M stream site but on time with the observed at the other interior stream gages.

During this ROS event, the empirical ADC discharge remains lower than the NWS ADC and closer to the observed discharge while the majority of the time the TL observed snow depth is more closely modeled by the NWS ADC. The discharge statistics are better for the empirical ADC (110% bias versus 129% bias, -1.78 versus -2.80 NSE, and 0.19 versus 0.22 m^3/s RMSE) and the TL snow depth statistics are better for the NWS ADC (23.2% versus 65.5% bias, 0.44 versus -0.027 NSE, and 7.78 cm versus 9.97 cm RMSE).

ROS Event #2

The warmer than freezing melt event on 3/14/09 caused a modeled melt (by both models) that was more significant than what was observed. Shortly after the rise in temperature, there was a 3-4 mm rain event causing additional melt and a slight rise in the observed discharge. Both models simulated a rise that was 24% more than the observed rise from this ROS. The temperature dropped below freezing briefly after this ROS event before rising back above freezing and remaining there for several days, which included a 5-6 mm rain event on 3/21/09, just prior to below freezing temperatures again.

This ROS event mentioned under event #1 above (on 3/21/09) appears to be modeled fairly well by both models with the empirical ADC model run slightly underestimating (10% lower than observed) the local peak discharge and the NWS model run overestimating the peak (33% higher than observed, peak in Figure 21). However, the modeled discharges were already higher than the observed discharge because of the warm temperature snowmelt from the previous several days. The change in streamflow

that was caused from the slug of water after the ROS event was 40% less for the NWS ADC and 55% less for the empirical ADC model run.

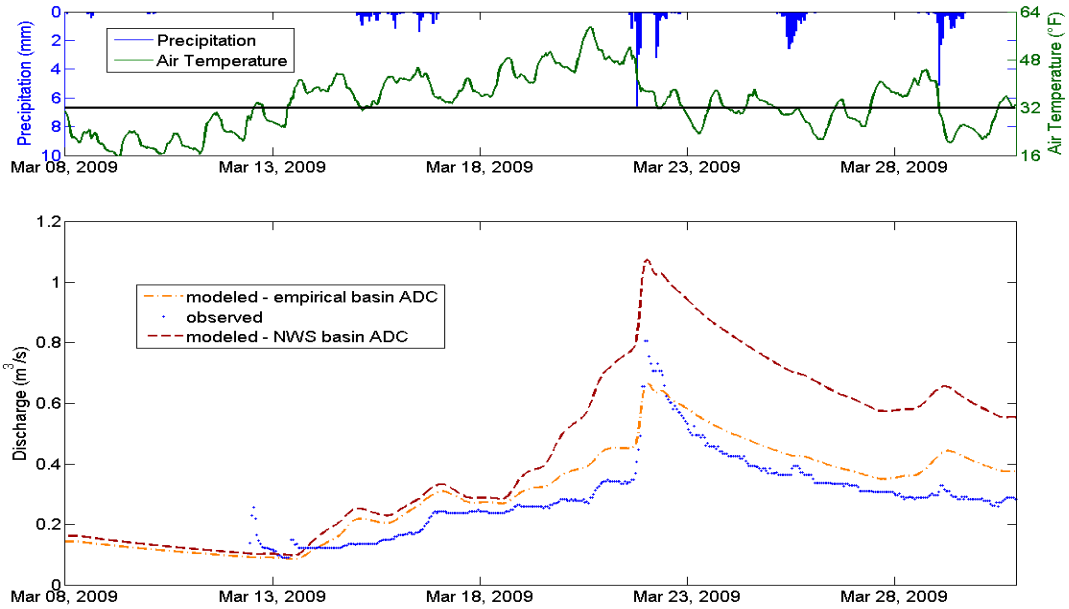

Figure 21. Hydrograph Comparison for ROS Event #2.

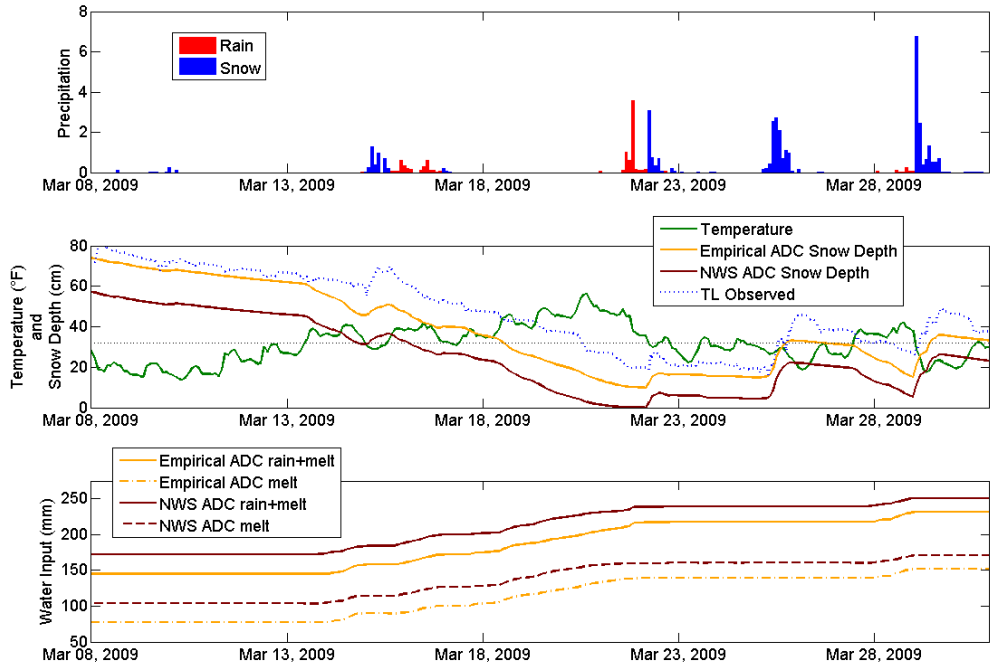

Figure 22. Snow Depth and Water Input Comparison at TL for ROS Event #2. Top Plot is Precipitation, Middle Plot is Temperature and Snow Depth, and Bottom Plot is Cumulative Water Input to the Subsurface.

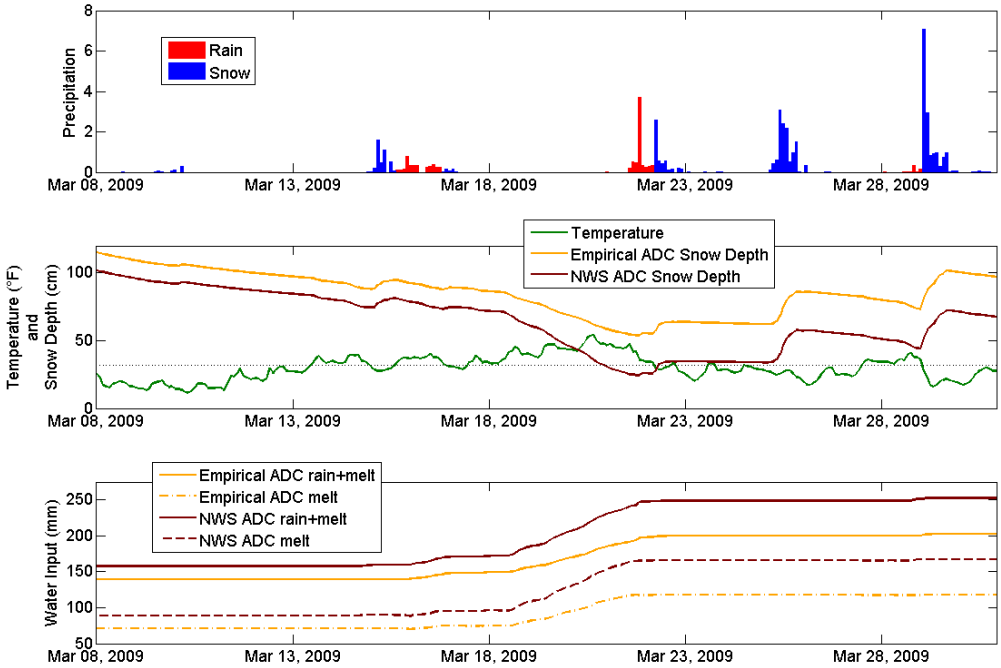

Figure 23. Snow Depth and Water Input Comparison at LDP for ROS Event #2. Top Plot is Precipitation, Middle Plot is Temperature and Snow Depth, and Bottom Plot is Cumulative Water Input to the Subsurface.

The empirical ADC did follow the observed discharge more closely throughout the event. This can be attributed to the fact the TL snow depth, as modeled by the empirical ADC, also closely followed the observed snow depth at TL during the event, as shown in Figure 22.

These results are consistent with the event statistics calculated where the empirical ADC produces low percent bias values (18.9% and -14.4%), high NSE values (0.75 and 0.81), and low RMSE values (0.067 m^3/s and 8.8 cm) for discharge and TL snow depth, respectively. The statistics from the NWS ADC model run were 70.9% and -43.1% bias, -2.1 and -0.029 NSE, and 0.24 m^3/s and 20.7 cm RMSE, for discharge and TL snow depth, respectively.

ROS Event #3

There was an ROS event at the end of 2009 into early January, 2010 that started as all snow across the watershed with well below freezing temperatures. The storm remained all snow in the highest elevations for one day, snowing 9-10 mm. There was intermittent rain and snow in the intermediate elevations 12-18 hours after the start of the event. As the temperatures rose, there was 4-5 mm of rain at the highest elevations with more at the intermediate and lower elevations (6-10 mm) depending on how long the temperature allowed the precipitation to be snow. By the end of the precipitation event, the temperature dropped again and 3 mm of snow was observed at the highest elevations while rain was still observed at the TL site and lower in elevation.

The temperature was hovering around the rain/snow transition temperature during this event and the model did not accurately predict the correct form of precipitation at several time frames during this event, based on the modeled and observed snow depth

trend comparisons. The model usually erred on the side of modeling snow when it was actually rain. Therefore, the modeled rise in streamflow at LG was approximately 12 hours late and the two peaks in streamflow were approximately 18 hours later than what was observed.

The percent bias data between the two model runs for this event are close for both snow depth locations (TL snow depth is -35.8% for the empirical ADC and -41.5% for NWS while LDP snow depth has 73.6% for the empirical ADC and 69.8% for NWS) but the NWS ADC has a much better discharge percent bias (2.37% versus -15.0%). The NSE and RMSE data for discharge and TL snow depth are close between the model runs but slightly better for the empirical ADC model run. The NSE is negative for all the hydrologic variables and model runs. The LDP snow depth data is very intermittent in this event time frame and is missing during the actual ROS event so will not be discussed.

ROS Event #4

There was a small ROS event on January 5-6, 2010, where the temperature rose slightly above freezing for a short period of time. At the TL site, 0.5 mm fell as rain and 1 mm fell as snow during the 18 hour storm, while the higher elevation pixels received 0.3 mm of rain and 1.3-1.5 mm of snow during the same storm. This caused a slight rise in the observed streamflow that was modeled well by both ADCs (20% less streamflow rise by the empirical ADC and 8% more streamflow rise by the NWS ADC). This was followed by a 4 day period of below freezing temperatures and some snowfall. Early on January 11, 2010, the temperatures rose above freezing and stayed there for two days with intermittent precipitation events falling as rain, totaling 0.9 mm and 3.6 mm of rain

at the highest and TL pixels, respectively. The temperature dropped below freezing at the highest elevation before the heaviest precipitation mid-day on January 13, 2010, but not at TL, so TL saw much more rain than the highest elevations.

As the temperatures rose above freezing on 1/11/10, melting the snowpack at the lowest elevations, the modeled LG discharge began to rise, one day earlier than was observed. One day later, the modeled discharge plateaued while the observed discharge decreased before rising significantly the following morning with the overnight ROS event mentioned above. Both model runs predicted the total rise within 13% but were both slightly lower in magnitude than was observed. Over the next several days, the modeled discharge did not recede quickly like the observed discharge and showed rises in discharge with the above freezing temperatures causing snowmelt that were not observed at all. There was a final sharp rise in observed discharge on 1/19/10 from ROS (2-3 mm of rain on a shallow snowpack) in the lowest elevations that was barely modeled by either ADC (77% lower increase in discharge by both model runs).

Both model runs remain close to each other throughout this event period with a few differences showing up during the high temperature melt episodes. The empirical ADC is closer to the observed values of LG discharge and snow depth at the two observed locations and therefore has better statistical values compared to the NWS ADC.

ROS Event #5

There was a ROS event on 12/2/10 that resulted in 2.5 mm of rain falling at the TL site after a 9 mm snowfall event the previous 18 hours. This same event resulted in more snow (10 mm snow) and less rain (0.9-1.0 mm rain) at the three highest elevation pixels. This caused a small increase in observed discharge that was not modeled by

either ADC. Neither ADC decreased the snow depth at TL or LDP as much as was observed (65% less of a decrease at TL and LDP for both models). A second small ROS event occurred on 12/5/10 that produced less than half a millimeter of rain at the TL and higher pixels and ended as snow. This produced an uptick in the observed discharge that was modeled by both ADCs. After the observed recession, that was not modeled, the temperature stayed elevated and the modeled discharge increased rapidly, which was not observed, although the final uptick of the modeled discharge was driven by a minor ROS event that was seen in the observed discharge also.

The empirical ADC more closely followed the melt regime and subsequently LG discharge around 12/13/10, which led to the better overall statistics of it during this ROS event. The percent bias shows the most significant improvement, compared to the NWS ADC with the discharge being 36.5% bias, TL snow depth -1.43% bias, and LDP snow depth -3.52% bias compared to the NWS ADC values of 59.5%, -11.6%, and -8.87% bias for the three hydrologic variables. The empirical ADC NSE showed some improvement over the NWS ADC with discharge being -2.83 versus -5.92, TL snow depth being 0.95 versus 0.88, and LDP snow depth being 0.75 versus 0.70. The RMSE values were all very close to one another during this time period.

ROS Event #6

A large ROS event in early 2011, which produced a total of 18-26 mm of rain (depending on elevation) had an extremely high observed discharge while both models grossly underpredicted the discharge (~0.5 m^3/s modeled versus 3.4 m^3/s observed). The 2011 ROS event started with a mixed precipitation event on 1/13/11 that produced 4-6

mm of snow in the LDP and higher elevation pixels and 4 mm of rain at the TL pixel. This was modeled successfully by both model runs.

The second and larger precipitation event that started on 1/15/11 produced 18-23 mm of rain on a ~75 cm snowpack. The melt from the rain and increase in temperature was much less than what was observed at the TL (snow depth decrease was 73% less than observed decrease, see Figure 24) and LDP (snow depth decrease was 65% less than the observed snow depth decrease, see Figure 25) pixels. The higher elevation pixels saw very minimal changes in snow depth (4 cm decrease in snow depth), leading to their very small contribution of melt water (<10 mm) to the stream channel, while the BOG site saw a 23 cm decrease in its snow depth, see Figure 26.

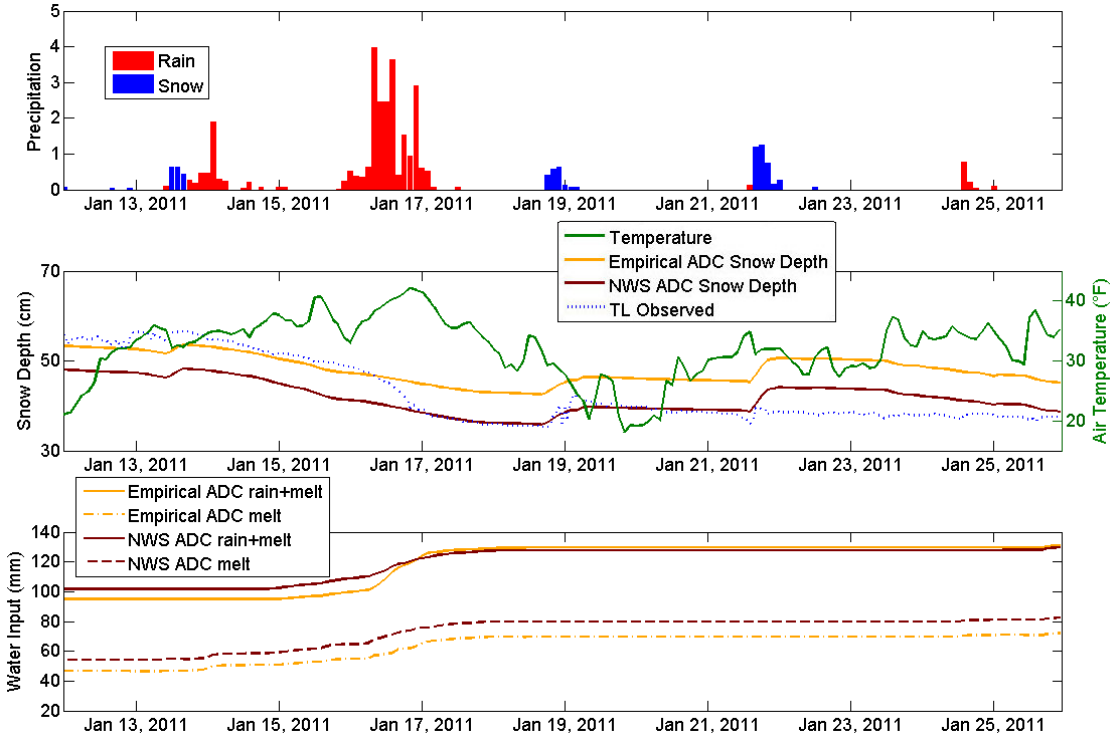

Figure 24. Snow Depth and Water Input Comparison at TL for ROS Event #6. Top Plot is Precipitation, Middle Plot is Temperature and Snow Depth, and Bottom Plot is Cumulative Water Input to the Subsurface.

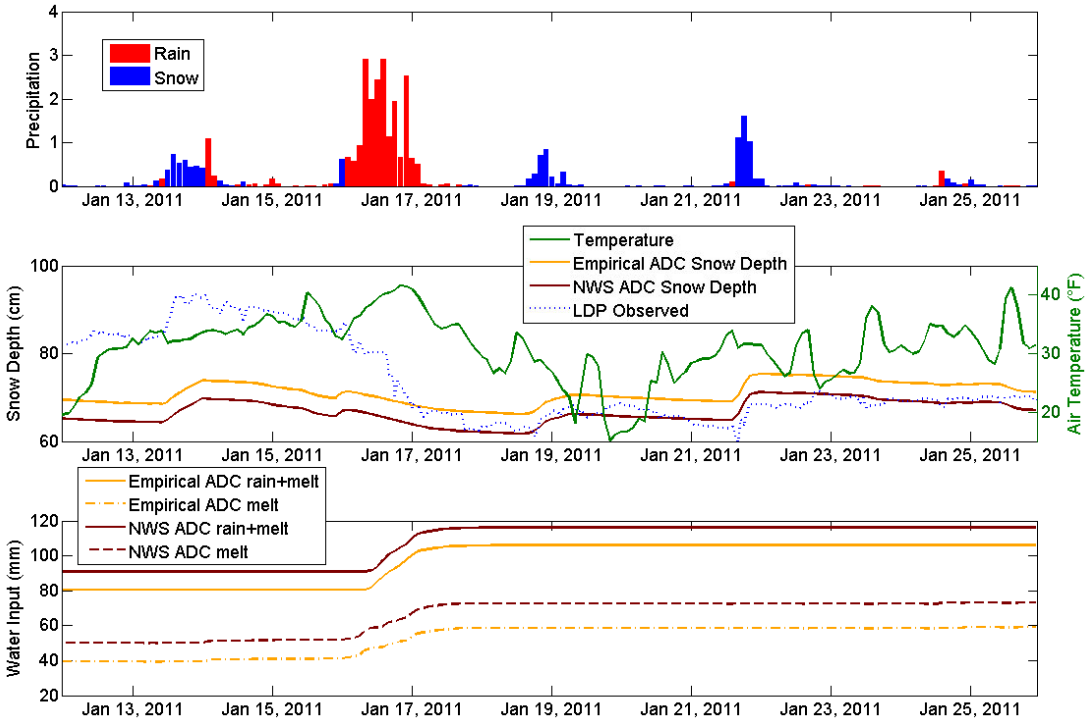

Figure 25. Snow Depth and Water Input Comparison at LDP for ROS Event #6. Top Plot is Precipitation, Middle Plot is Temperature and Snow Depth, and Bottom Plot is Cumulative Water Input to the Subsurface.

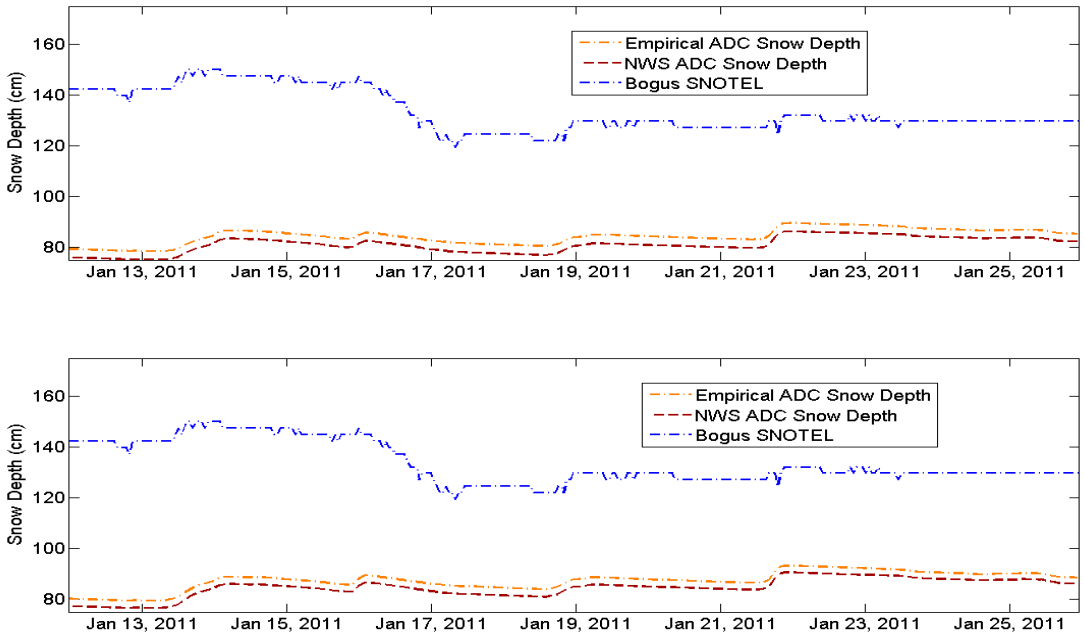

Figure 26. Snow Depth Comparison for ROS Event #6. Top Plot is Pixel 23 (Second Highest Elevation Pixel) Snow Depth and Bottom Plot is Pixel 24 (Highest Elevation Pixel) Snow Depth.

The same statistics were calculated for discharge, TL and LDP snow depths for this ROS event. Since both models performed equally poorly in representing the movement of water in the watershed, it is unnecessary to discuss the statistical results during this ROS event.

Spatial Scale Comparison – 1 HRAP versus ¼ HRAP Resolution (with the Empirical ADC)

The model was run at 1 HRAP resolution (16 km^2 pixels) with the same set of calibrated parameters to demonstrate the validity of running the model at a fine spatial resolution (¼ HRAP, 1 km^2 model pixels). The scaling factors used at ¼ HRAP had to be slightly adjusted to achieve the same parameter values at 1 HRAP resolution. The empirical ADC was used for this comparison between 1 HRAP and ¼ HRAP resolution model runs.

In general, the 1 HRAP resolution run did a satisfactory job of modeling the Dry Creek discharge observed at the LG (+4.9% to -45% annual bias, 0.47-0.77 annual NSE, and <0.2 m^3/s annual RMSE for WY2004 – WY2011). The 1 HRAP model run only had a positive annual bias, where the modeled discharge is larger than the observed discharge or an overestimation of discharge, in WY2004 and WY2011, with +3.2% and +4.9% annual bias, respectively. In contrast, the ¼ HRAP resolution run typically overestimates discharge, i.e., has positive bias (5% - 22% annual bias) and only two years with negative annual bias (underestimation of discharge), during WY2006 (-4.8%) and WY2008 (-4.1%). On a monthly basis, the 1 HRAP run does as good and sometimes better job of modeling the discharge early in the calendar year through the rising limb of the annual

hydrograph. The ¼ HRAP run typically hits the peak flow with higher accuracy and follows the receding limb of the annual hydrograph more closely.

In years with higher peak discharge (> 1.5 m^3/s), the 1 HRAP model run grossly underestimated the peak flow (WY2004, 2006, and 2010). In years with low peak discharges, the 1 HRAP model run typically modeled the observed discharge over time better than the ¼ HRAP model run (WY2005 and 2007) as the finer resolution model run significantly overestimated the peak flow both years. Years with moderate peak discharge (1-1.5 m^3/s) the ¼ HRAP model run did a much better job of modeling the annual streamflow by hitting the peak flow more closely and following the receding limb trend as the snow gradually melts (WY2008, 2009, and main peak in 2011).

Most years the 1 HRAP model run completely misses late season rises in discharge while the ¼ HRAP model run better predicts these late season events (WY2006, 2008, 2009, and 2011). This is due directly to the fact that the coarse model resolution melts the snow very quickly compared to what is actually occurring in the highest elevation pixels and what the finer resolution is predicting. This is very evident by inspection of the hydrograph (see Figure 27), snow depth trends (see Figure 28), as well as the monthly statistics for May and June.

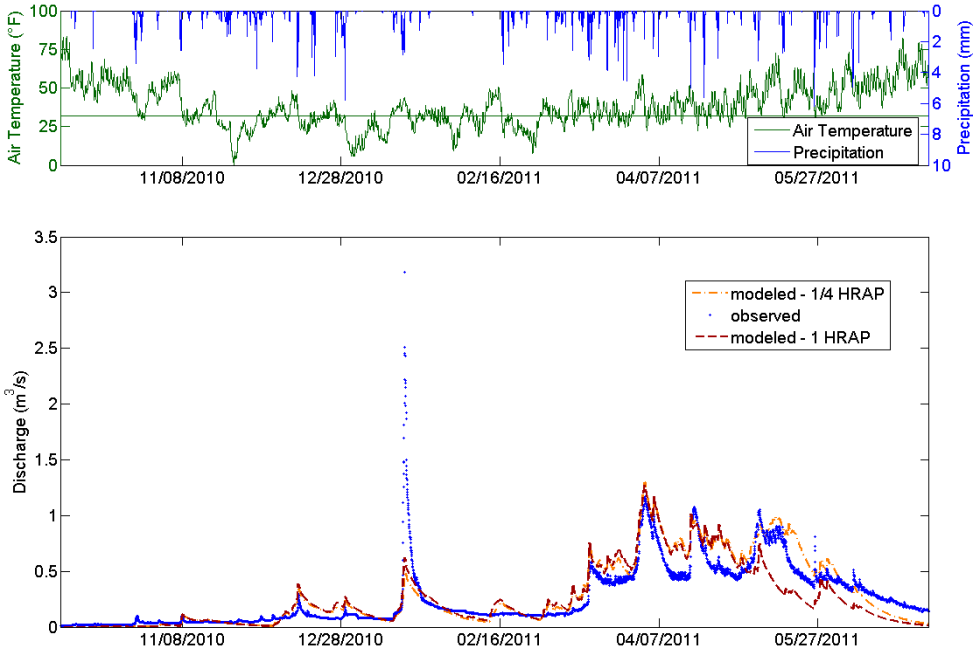

Figure 27. Spatial Resolution Hydrograph Comparison for WY2011.

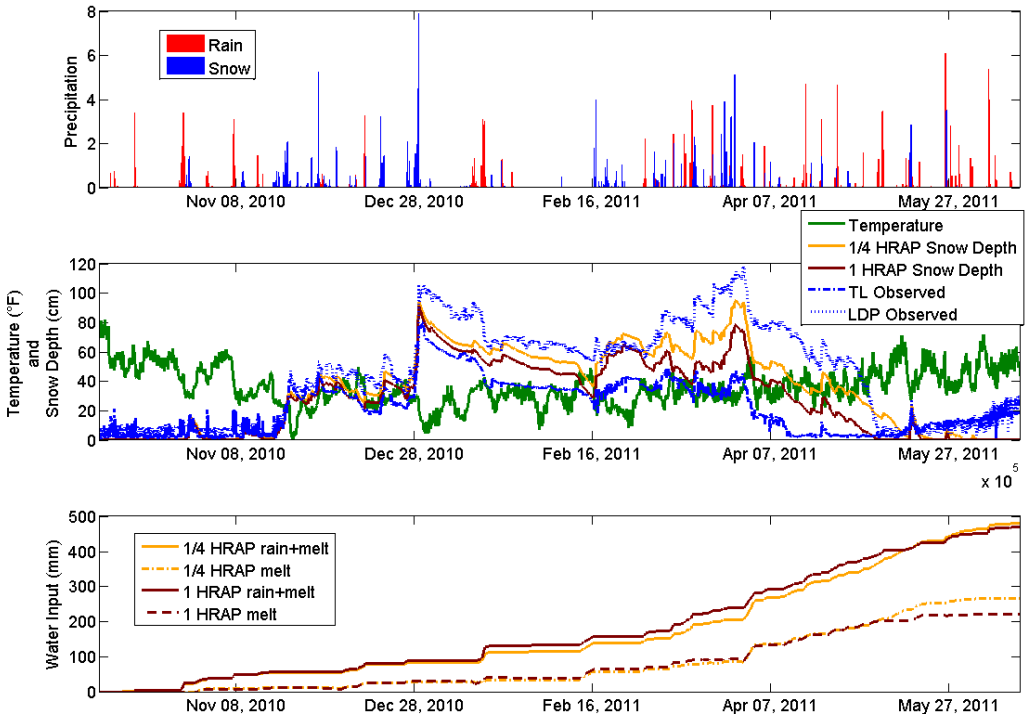

Figure 28. Snow Depth and Water Input Comparison at Highest Elevation Pixel for WY2011. The Fine Resolution Pixel Values Contained Inside the Larger Coarse Resolution Pixel were Averaged for these Plots. Top Plot is Precipitation, Middle Plot is Temperature and Snow Depth, and Bottom Plot is Cumulative Water Input to the Subsurface.

DISCUSSION

Based on the model results for WY2004-2011, both the empirical and NWS ADC model runs predict the streamflow accurately with certain times of the year being better than others. Annually, the empirical ADC has higher NSE and lower RMSE values while the percent bias between the two model runs is comparable across all years. The percent bias statistic is sensitive to low flow values such as those that occur in the winter and summer months in a semi-arid mountainous watersheds. The models tend to show small spikes in the hydrograph that are not observed during low flow times, therefore causing large biases. The monthly values, averaged across all years, are closer to zero for percent bias, higher NSE and lower RMSE for the empirical ADC, compared to the NWS ADC. The true value of a site derived ADC is seen with getting the melt dynamics correct during and at the end of the snowmelt season. More often than not, the empirical ADC predicted the melt dynamics of the snowpack more accurately than the NWS ADC and subsequently predicted the streamflow more accurately during these times.

Amount of Snow per Pixel Accuracy

There is a notable difference in observed snow depth and SWE data between the two interior DCEW locations, the TL and LDP sites. This elevation range is considered a rain to snow transition region where during any given winter/spring storm, these pixels can receive rain or snow or a combination of the two. Getting this difference in snow depths between elevations to show up in the model results is extremely important to

accurately predicting streamflow from a snow dominated catchment such as DCEW. It was seen on multiple occasions that when the snow depth trend was closely followed at TL and LDP pixels, the model more accurately predicted streamflow leaving the watershed during those times. The TL and LDP pixels are in a rain-to-snow transition region with the TL site being 240 m lower in elevation than the LDP site, and therefore more sensitive to the rain snow elevation.

It is evident from the model results that getting the amount of snow correct in each pixel is important to accurately predicting streamflow that is driven by snowmelt. This is more important in the pixels that receive a mixture of rain and snow on a regular basis as they will accumulate and melt snow throughout the winter season, contributing to streamflow for many months. When the melt regimes or snow depth decreases match between observed and modeled at the TL and LDP pixels, the discharge at LG also more closely matches. Each time there is a larger decrease in snow depth modeled than was seen in the observed data, there is a jump in modeled streamflow that also was not observed. The empirical ADC typically predicts the trends in snow depth with higher accuracy than the NWS ADC, which leads to more accurate discharge prediction during these time frames. However, when the NWS ADC predicts the snow depth trends at TL and LDP more accurately than the empirical ADC, it also predicts discharge more accurately during these times. In contrast, the NWS ADC better matches the interior hydrograph during several points in the modeled time frame but does not match the LG hydrograph as well as the empirical ADC during those times.

The empirical ADC snow depth also shows much better performance statistically in matching the snow depth at the TL and LDP pixels. For the events discussed above,

the ADC comparison and ROS events, the empirical ADC percent bias was closer to 0%, NSE was closer to 1, and RMSE was closer to zero for the majority of the events.

The advantage of a site-derived parameter to determine snowmelt on an areal basis, the empirical ADC, is seen by its ability to better predict the snowmelt trends in the high elevation pixels. The calculated statistics on the snow depth also support the fact that when there is a significant difference in discharge between the two model runs, the site derived ADC model run performs better most of the time. The amount of snow per area in the watershed and the timing of its melt are the two most important aspects to determining stream discharge from a snow-dominated watershed. This site derived parameter can theoretically be easily calculated using remote sensing data of fSCA (from MODIS) and SWE (from passive microwave remotely sensed data). The ability and availability of these remotely sensed data have become better over the last decade and should continue to improve into the future. Future studies should utilize these resources in order to create a site derived ADC for comparison purposes with a calibrated ADC.

The rain-to-snow transition elevation range is an important aspect of the snowmelt regime in a topographically complex watershed. In nearby Reynold's Creek Experimental Watershed, the elevation at which precipitation is predominately snow has steadily decreased in the last 35 years (Nayak et al., 2010). The empirical ADC was better at getting the amount of snow in these rain-to-snow transition pixels correct and better at predicting streamflow during those times, which demonstrates that this region of a watershed is extremely important to accurately represent. With more regions likely to be included in this rain-to-snow transition region in the future, if temperatures continue to

rise, the capability to predict the snowmelt regimes in these locations is that much more important for river forecasting.

Gridded Snow Parameter Importance

When the model inaccurately predicted the form of precipitation, the model discharge increased while the observed decreased or vice versa. This scenario further contributes to decreased accuracy of snow depth and SWE in each model pixel, which leads to inaccurate discharge predictions. The range of air temperatures at which precipitation is rain or snow or a mixture of rain and snow is larger in DCEW than what is parameterized in the model framework. The model only assigns one temperature value for the determination of precipitation as snow or rain and does not account for precipitation that falls as a mixture. SNOW-17 offers other options for the rain-to-snow transition such as providing a time series of rain-snow elevations or a time series of the fraction of precipitation that is snow (NWS, 2009; NWS, 2011). Both of these methods are likely more difficult to obtain an accurate time series and are not feasible for operational purposes.

Calibration of SACSMA/SNOW-17 plays a large role on the accuracy of the streamflow prediction. During the calibration process, it was difficult to get the amount of snow correct in both pixels where we have a time series of snow depth data. There is a significant difference in the observed depth of snow between these two locations (TL and LDP) because of differential accumulation and melt, and was not being captured by the model during early calibration stages. The elevation range between TL (1610 m) and LDP (1850 m) is in a sensitive rain to snow transition region and getting the amount of

snow correct in these pixels is extremely important to the accuracy of the modeled stream discharge.

Modifying the parameter values that affect snowmelt and snow accumulation was found to have a significant effect on modeling the snow depth and SWE separation that is observed at these interior watershed locations. The inability to get the snow depth difference correct between TL and LDP was resolved by incorporating a spatial grid of values for three of the snow parameters during the calibration stage, where their values differ as the pixel elevation changes. These parameters each have a single value across the watershed *apriori* and are extremely important in a rain-to-snow transition region. They include the air temperature at which precipitation is considered snow (PXTMP parameter, 0°C *apriori*), the temperature at which snowmelt occurs (MBASE parameter, 0°C *apriori*), and how the amount of snow can vary with phenomena such as sublimation, wind affects, and catch efficiency at the precipitation gage, and redistribution of snow by wind (SCF parameter, 1 *apriori*).

The spatial distribution of these parameters across the watershed is shown in Figure 11 and Figure 12**.** These distributions were determined by utilizing some topographic relationships between the known precipitation and snow regime patterns as well as trial and error during the calibration stage. SCF, which affects snow accumulation, should be higher around the edges of the watershed because of the wind effects present along the ridge lines. There is also a lot of variability in the aspect inside each pixel, which greatly affects both melt and accumulation.

Setting these three parameters to differ spatially in the watershed allows the model to vary these dominant melt and accumulation parameters in an elevation range

that is most susceptible to changes in the rain/snow transition elevation. With the changing climate, to a warmer climate (Hamlet and Lettenmaier, 2007; Hamlet et al., 2007; Mote et al., 2005; Nayak et al., 2010), that has been occurring and is expected to continue over the next several decades, this transition to more rain and less snow (Knowles et al., 2006; Regonda et al., 2005) is an extremely important phenomenon to be able to capture in hydrologic models. Not only is the temperature at which precipitation falls as rain or snow important but the temperature at which snow will begin to melt or begin to melt more quickly is just as important, if not more important, to be able to capture in these models.

Melting of snow is a spatially variable process that is dependent on the spatial distribution of snow prior to melt as well as hillslope characteristics such as aspect, slope, vegetation, and land surface cover (Anderton et al., 2002). Conceptual models such as SNOW-17 simplify the snowmelt processes for efficiency and larger scale application in the RFC's. This conceptual nature of snowmelt assumes that snowmelt is uniform across each model pixel and that it is only dependent on a few calibrated parameters. Proper values of these parameters are difficult to achieve because of the annual variation in the snow that is present at hillslope, pixel, and watershed scale. While the gridded nature of three SNOW-17 parameters was found to provide a more accurate representation of the hydrology occurring in DCEW, specifically at the higher elevations, it was still seen that these values were not accurate for all years of simulation. Varying parameter values across different years is not a feasible option for operational hydrologic models but has been considered by others as a topic of future studies (Franz et al., 2008).

A suggestion to eliminate these variances is to incorporate differential accumulation (SCF parameter) and melt temperatures (MBASE parameter) at different times of the season or based on recent meteorologic or climatic factors such as a rolling average temperature from the previous several days or week. These recent factors will affect the antecedent conditions of the snowpack and therefore the melt dynamics that are likely to occur. The early season accumulation is more correct with higher SCF values while late season accumulation does not need the higher SCF. Melt dynamics also change throughout the season, varying with the amount of snow on the ground, the amount of melt that has already occurred from the snowpack, the antecedent air temperature, and hillslope characteristics, among other things.

Air Temperature Sensitivity

Temperatures in the western United States have been on the rise (Hamlet and Lettenmaier, 2007; Hamlet et al., 2007; Mote et al., 2005; Nayak et al., 2010) and have caused shifts in form of precipitation to more rain, seasonal snowpack to be less abundant, and timing of spring runoff to be earlier. Air temperature is the main driver in melting snow within a temperature-index model so understanding how sensitive the model is to temperature changes is an important aspect of modeling with a conceptual hydrologic model of this nature. When the temperature is above freezing and there is no precipitation, SNOW-17 linearly relates air temperature to snowmelt using a seasonal snowmelt factor. The melt factor varies in a sinusoidal nature to estimate the affect of solar radiation on the magnitude of snowmelt. This melt factor is multiplied by the difference in the air temperature and the snowmelt temperature (MBASE parameter), so on any given day, there is a linear relationship with the degrees Celcius above freezing.

Snowmelt or decreases in snow depth have been observed to not occur in such a simple fashion.

The SACSMA/SNOW-17 model is extremely sensitive to air temperature changes, usually melting more snow during the high temperature times than what is observed. There were several events discussed above where there was a large increase in temperature, which was modeled as a large decrease in snow depth that was not observed at the same magnitude. During Event #4, for example, there was an overestimation of melt water leaving the LDP pixel, as shown in Figure 18, and likely an overestimation of melt water leaving the two highest elevation pixels, which were modeled by a decrease in snow depth of similar but slightly greater magnitude than the observed LDP pixel snow depth but theoretically should have a lower magnitude of snow depth decrease. However, the nature of a temperature index snowmelt model is to vary snowmelt incrementally by degrees of air temperature difference.

The model appears to be releasing water from the snowpack as it is melted, immediately after the temperatures rise above freezing, whereas this does not occur in the observed data. Based on the observed snow depth data and the interior hydrographs, water does not make it into the stream channel until several days after the temperature has been above freezing. This is especially true when the temperatures were below freezing for several days before the above freezing temperatures. Even when there are rises in the observed discharge, the magnitude of the rise is always less than the magnitude of the rise in modeled discharge.

There is a SNOW-17 model parameter that affects the antecedent temperature the model is using to calculate the heat deficit. This parameter, TIPM, which weights the

previous time step air temperature by a factor, would theoretically help speed up or slow down the rate of heat deficit changes, which directly affects the amount of melt once the heat deficit is diminished. However, model discharge was not found to be sensitive to changes in the TIPM parameter.

Another parameter that appears to be related to the air temperature sensitivity issue seen is the liquid water holding capacity, PLWHC parameter. Some of the differences in discharge are because there was a larger decrease in modeled snow depth than was observed and this extra water is being routed directly to the stream channel. If the snow pack was holding more water, as the observed data is suggesting, then the decrease in snow depth would be less and less water would be in the stream channel. However, changes to this parameter were also not translating to significant changes in model discharge.

The non-rain melt is calculated by multiplying the seasonally variable melt factor and the temperature difference between the air temperature and the snowmelt temperature (MBASE), the true definition of a temperature index snowmelt model. This inherently results in a large quantity of snowmelt during times when the temperature significantly rises above freezing. Any heat deficit that was present is almost immediately reduced to zero and melt begins to occur. This is not what actually happens in the field though. Eiriksson (2012) has shown that snowmelt at the TL site in DCEW occurs minimally after extended above freezing temperatures, e.g., for the melt event 2/12/11 – 2/17/11, there was <20 mm of snowmelt observed while the empirical ADC melted 29 mm and the NWS ADC melted 41 mm.

Rain on Snow Events

Rain on snow events have become more common in the last couple of decades because of warming temperatures around the globe (Knowles et al., 2006; Leung et al., 2004; Marks et al., 1998; Marks et al., 2001; McCabe et al., 2007). The timing of peak streamflow as well as snowmelt regimes has been shifting over this time period (Dyer and Mote, 2007; Fritze et al., 2011; Knowles et al., 2006; Mauget, 2003; Maurer et al., 2007; Nayak et al., 2010; Regonda et al., 2005; Stewart et al., 2005) because of the shift in air temperature over the snow accumulation and ablation season. There has also been an increase in ROS events during this shift as many snow dominated watersheds are seeing a larger percentage of their winter precipitation in a mixed or rain only form instead of mostly snow. These events can be minimal and cause little to no change in streamflow but can also cause large flooding and diminish the snowpack significantly. The antecedent conditions of the snowpack play a significant role in how severe the ROS event will be to the discharge. Singh et al. (1997) demonstrated that only the second of two subsequent ROS events (of the same intensity) produced runoff from two experimental plots. The first ROS event served to saturate the snowpack and store the water that was rained on it while the second ROS event moved the rainwater through the snowpack quickly because the snowpack was already saturated.

The model does not respond to ROS events in the same fashion every time as shown by the example ROS events discussed above. The models underestimate the magnitude of streamflow following a ROS event the majority of the time and the modeled streamflow rise is usually delayed. ROS events are always accompanied by an increase in air temperature above the melting temperature (MBASE) during the time

frame surrounding the actual ROS event. This phenomena convolutes the streamflow response but it is generally seen that the model overpredicts the rise in streamflow from an above MBASE air temperature and underpredicts the rise from the ROS event itself, regardless of the ADC in use. The overprediction from the above freezing temperature melt is usually much greater than the underprediction of the ROS event and thus the streamflow is usually overpredicted overall. The model framework calculates snowmelt using only one method during each time step, depending on whether it is raining or not.

In this study, both model runs did not perform well in predicting the discharge when there was a large increase in streamflow from an onslaught of water, such as that moved by the January 2011 ROS event. However, during minor ROS events, where the discharge does not increase significantly, the models do fairly well at predicting the increase in streamflow, but both typically underestimate the rise in discharge. ROS events are typically accompanied by an increase in temperature prior to the event that alters the streamflow response. The subsequent rise in discharge has two sources, one from snow melting solely because of the increase in temperature and the other from the ROS induced melt and the rain water moving through the snowpack. As seen in the example ROS events above, this combination affect is usually but not always the case and the model tended to more accurately predict the rise in discharge from an ROS event when there is not a rise in air temperature prior to the event. This varying response of the model to ROS events raises concern for the accuracy of the model during future ROS events.

A snowpack can act as a low permeability conduit for rain water to move through it during a ROS event (Eiriksson, 2012) and not much snow is actually melting during

these types of events. The permeability of snow can range from 6 x 10^{-10} m^2 for small grained snow to 524 x 10^{-10} m^2 for a depth hoar (Jordan et al., 1999). During the large ROS event in January 2011, Eiriksson's (2012) paired lysimeter experimental plot at TL saw ~170 mm of snowmelt while the models recorded 16 mm of snowmelt at the TL pixel during the same time frame. It is obvious that the model could not properly handle the movement of water through the snowpack properly during this heavy rain event. The ROS event in late 2005 and early 2006 had a less but similar magnitude of rainfall but onto a much shallower snowpack. There was also an early rise predicted in discharge that was initiated by an increase in temperature prior to the rainfall event. The first portion of this ROS event could have served to saturate the snowpack.

Visual inspection of all hydrologic variables, as compared to observed values, demonstrate that a more sophisticated process representation is necessary to model large ROS events such as the one on January 17, 2011. One solution to alleviate this problem with extreme ROS events is to incorporate another snowmelt equation based on the amount of rain and depth of snow during a given storm. Currently, there is a ROS melt equation for times when there is more than 0.25 mm/hr of rainfall and a melt equation for non-rain or less than 0.25 mm/hr of rainfall. The ROS melt equation does not vary seasonally as does the non-rain melt equation and the user's manual even states that this is not the case in nature but only says that the wind speed would vary seasonally, therefore varying the melt. However, the wind speed representation in the model, UADJ parameter, is not sensitive to stream discharge. Large changes to the UADJ parameter produce very minimal changes in snow depth, which therefore lead to very minimal changes in water leaving the snowpack and water in the stream. This is a possible

indication that wind is not the dominating factor in ROS melt. After analysis of the ROS event behavior, a differential ROS melt equation that incorporates both seasonal melt in addition to rainfall intensity differences in melt could lead to more consistent model behavior during these events. When there is heavier rainfall, more of the rain is likely to completely migrate through the snowpack, and as the storm continues, larger macropores and preferential flow paths will develop leading to more runoff leaving the base of the snowpack.

Impact of Scale

Computational speed and efficiency are two important aspects to running an operational hydrologic model. The temporal and spatial resolution at which a hydrologic model is run at plays a large role in the computation time required to simulate water movement in a watershed. The NWS runs the coupled SACSMA/SNOW-17 model at 1 HRAP spatial resolution for normal day-to-day operations, which has been shown to work well for the large scale RFC model domain that they work within. This study was ran at ¼ HRAP resolution initially, to be able to capture the heterogeneous nature of snow processes that occur in our model domain, and subsequently at the coarser 1 HRAP resolution to compare model results against.

There have been very few successful model simulations using SACSMA/SNOW-17 at a finer spatial resolution than the standard 1 HRAP resolution, especially in complex mountainous terrain. Model simulations using a downscaled version of SACSMA have typically been run in Arkansas and Oklahoma i.e. (Reed et al., 2007). The NWS has interest in determining if the finer spatial resolution provides any benefit to forecasting ability of the SACSMA/SNOW-17 model. The greatest impact that finer

spatial resolution had on model results in DCEW was seen in the receding limb of the annual hydrograph, after peak discharge, which is directly related to the presence of snow in the highest elevations of the watershed. The snow signature in these high elevation pixels was masked by the coarser resolution because of the location of the 1 HRAP model pixels versus the ¼ HRAP model pixels.

The coarse resolution missed late season events because of the location of the larger pixels in relation to the highest elevations of DCEW. The 1 HRAP resolution only has portions of 4 model pixels that cover DCEW with pixel elevations ranging from 1232 meters to 1667 meters. The ¼ HRAP resolution has 24 model pixels, which range in elevation from 1133 meters to 1844 meters, with 7 model pixels being higher in elevation than the highest 1 HRAP resolution model pixel. The elevation range of DCEW is 1000 meters to 2100 meters.

At 1 HRAP resolution, the model underestimated the amount of snow in the watershed, especially in the two most northern pixels (highest elevation) because of the effect of averaging over such a large area in a topographically complex region. These higher elevation pixels cross the rain-to-snow transition region, which is affected by snow in highly different ways. The amount of accumulated snow as well as the timing of its melt are important factors in determining the amount of runoff that is produced from this water input. It is clear in a small watershed like DCEW that the coarse spatial resolution does a poor job of simulating the important snow processes.

The coarse spatial resolution does surprisingly well prior to the peak discharge, despite the inability to even slightly capture the late season snowmelt events. The hydrologic statistics make one believe that this model simulation is better overall than the

finer spatial resolution when this in fact is not the case. The 1 HRAP model run grossly underestimates the peak discharge during years when the peak streamflow is greater than 0.5 m^3/s. The timing of the peak flow is accurate but the magnitude is never reached, again because of the lack of snow in the higher elevations, which dominate the peak discharge in DCEW.

It would be useful to implement the finer spatial resolution SACSMA/SNOW-17 in a larger watershed to determine if the elevation averaging effect is only site-specific to DCEW. It would also be a useful experiment to test the effect of ½ HRAP resolution in comparison to both 1 HRAP and ¼ HRAP resolution to determine if the same results can be achieved. A final recommendation for the use of this more accurate fine spatial resolution would be to test if incorporating only SNOW-17 at the finer resolution would produce similar results. Since the snow processes of melt and accumulation are the main factors in the poor performance of the 1 HRAP model run and movement of this water through the subsurface (SACSMA) is less of an issue, running the model at dual resolutions might be beneficial.

CONCLUSIONS

The SACSMA/SNOW-17 model was run in DCEW at ¼ HRAP resolution to determine the importance of a site derived areal depletion curve (ADC). Through the analysis performed, some watershed processes that the model framework does not represent accurately were found and potential solutions were presented. The model was also run at the standard 1 HRAP resolution to determine the effect of spatial scale in a topographically complex, snow dominated watershed.

The site derived empirical ADC model more closely matches the snow depth accumulation and ablation trends more often during the modeled time frame than the calibrated NWS ADC model run. During the times that either ADC model run's snow data matches the observed snow data, that model's discharge leaving DCEW also closely matches. Overall, the empirical ADC performed better than the NWS ADC in predicting streamflow leaving the watershed in addition to the snowmelt regime.

Modeling a topographically complex mountainous watershed required downscaling from the standard 1 HRAP spatial resolution to ¼ HRAP resolution. It was determined in the calibration stage that several of the dominant SNOW-17 parameters produced better model output when they were allowed to vary spatially across the watershed. Allowing the melt temperature (MBASE), rain/snow temperature (PXTMP), and snow correction factor (SCF) to change as elevation changed produced a more accurate difference in observed snow depth in the higher elevation pixels.

ROS events are simulated accurately during small events with minimal rainfall inputs. When there are significantly large rainfall amounts on a snowpack during short periods of time, such as with the January 2011 ROS event, the model framework does not have the capability to handle these events. SNOW-17, by design, is very sensitive to large changes in air temperature, typically melting much more snow than is seen in the observed record. Model simulations compared with snow depth records in DCEW indicate that snowmelt does not increase linearly with increases in temperature, as SNOW-17 calculates the snowmelt.

Finer spatial resolution also provided much more accurate discharge simulation results, particularly after the peak discharge was observed. The average elevation of the model pixels between 1 HRAP and ¼ HRAP spatial resolution was the primary cause of this improvement. The elevations in the coarser resolution were much lower overall than those in the finer resolution, which resulted in less snow accumulating and therefore less snow left on the ground to melt later in the spring season.

REFERENCES

Abbott, M.B., Bathurst, J.C., Cunge, J.A., O'Connell, P.E., Rasmussen, J., 1986. An introduction to the European Hydrological System — Systeme Hydrologique Europeen, "SHE", 1: History and philosophy of a physically-based, distributed modelling system. Journal of Hydrology, 87(1–2): 45-59.

Anderson, B., 2011. Spatial distribution and evolution of a seasonal snowpack in complex terrain: An evaluation of the SNODAS modeling framework, Boise State University.

Anderson, E.A., 1973. National Weather Service River Forecast System - Snow accumulation and ablation model. NOAA Technical Memorandum. NWS Hydro-17., pp. 217.

Anderson, R.M., Koren, V.I., Reed, S.M., 2006. Using SSURGO data to improve Sacramento Model a priori parameter estimates. Journal of Hydrology, 320(1-2): 103-116.

Anderton, S.P., White, S.M., Alvera, B., 2002. Micro-scale spatial variability and the timing of snow melt runoff in a high mountain catchment. Journal of Hydrology, 268(1-4): 158-176.

Bae, D.H., Georgakakos, K.P., 1994. Climatic Variability of Soil Water in the American Midwest: Part 1. Hydrologic Modeling. Journal of Hydrology, 162(3-4): 355-377.

Bales, R.C., Dressler, K.A., Imam, B., Fassnacht, S.R., Lampkin, D., 2008. Fractional snow cover in the Colorado and Rio Grande basins, 1995-2002. Water Resources Research, 44(1).

Boyle, D.P. et al., 2001. Toward improved streamflow forecasts: Value of semidistributed modeling. Water Resources Research, 37(11): 2749-2759.

Brath, A., Montanari, A., 2000. The effects of the spatial variability of soil infiltration capacity in distributed flood modelling. Hydrological Processes, 14(15): 2779-2794.

Burnash, R.J.C., 1995. The NWS river forecast system - catchment modeling. In: Singh, V.P.a.F., Donald K. (Ed.), Computer Models of Watershed Hydrology. Water Resources Publications, Littleton, CO, pp. 311-366.

Chu, W., Gao, X., Sorooshian, S., 2010. Improving the shuffled complex evolution scheme for optimization of complex nonlinear hydrological systems: Application to the calibration of the Sacramento soil-moisture accounting model. Water Resources Research [Water Resour. Res.]. Vol., 46(09).

Dai, Y.J. et al., 2003. The Common Land Model. Bulletin of the American Meteorological Society, 84(8): 1013-+.

Daly, S.F., Davis, R., Ochs, E., Pangburn, T., 2000. An approach to spatially distributed snow modelling of the Sacramento and San Joaquin basins, California. Hydrological Processes, 14(18): 3257-3271.

Dery, S.J., Salomonson, V.V., Stieglitz, M., Hall, D.K., Appel, I., 2005. An approach to using snow areal depletion curves inferred from MODIS and its application to land surface modelling in Alaska. Hydrological Processes, 19(14): 2755-2774.

Dingman, S.L., 2002. Physical Hydrology. Waveland Press, Inc., Long Grove, IL.

Downer, C.W., Ogden, F.L., 2004. GSSHA: Model to simulate diverse stream flow producing processes. Journal of Hydrologic Engineering, 9(3): 161-174.

Downer, C.W., Ogden, F.L., Martin, W.D., Harmon, R.S., 2002. Theory, development, and applicability of the surface water hydrologic model CASC2D. Hydrological Processes, 16(2): 255-275.

Dunne, T., Leopold, L.B., 1978. Water in environmental planning. W.H. Freeman and Company, San Francisco.

Dyer, J.L., Mote, T.L., 2007. Trends in snow ablation over North America. International Journal of Climatology, 27(6): 739-748.

Eiriksson, D., 2012. The Hydrologic Significance of Lateral Water Flow in Snow, Boise State University.

Franz, K.J., Hogue, T.S., Sorooshian, S., 2008. Operational snow modeling: Addressing the challenges of an energy balance model for National Weather Service forecasts. Journal of Hydrology, 360(1-4): 48-66.

Fritze, H., Stewart, I.T., Pebesma, E., 2011. Shifts in Western North American Snowmelt Runoff Regimes for the Recent Warm Decades. Journal of Hydrometeorology, 12(5): 989-1006.

Hamlet, A.F., Lettenmaier, D.P., 2007. Effects of 20th century warming and climate variability on flood risk in the western U.S. Water Resources Research, 43(6).

Hamlet, A.F., Mote, P.W., Clark, M.P., Lettenmaier, D.P., 2007. Twentieth-century trends in runoff, evapotranspiration, and soil moisture in the western United States. Journal of Climate, 20(8): 1468-1486.

Hogue, T.S., Gupta, H., Sorooshian, S., 2006. A 'User-Friendly' approach to parameter estimation in hydrologic models. Journal of Hydrology, 320(1-2): 202-217.

Homan, J., 2008. The Development and Evaluation of Ground, Model and Satellite-Based Snowmelt Depletion Curves, Boise State University.

Horne, F.E., Kavvas, M.L., 1997. Physics of the spatially averaged snowmelt process. Journal of Hydrology, 191(1-4): 179-207.

Ivanov, V.Y., Vivoni, E.R., Bras, R.L., Entekhabi, D., 2004. Preserving high-resolution surface and rainfall data in operational-scale basin hydrology: a fully-distributed physically-based approach. Journal of Hydrology, 298(1–4): 80-111.

Jordan, R.E., Hardy, J.P., Perron, F.E., Fisk, D.J., 1999. Air permeability and capillary rise as measures of the pore structure of snow: an experimental and theoretical study. Hydrological Processes, 13(12-13): 1733-1753.

Khakbaz, B., Imam, B., Hsu, K., Sorooshian, S., From lumped to distributed via semi-distributed: Calibration strategies for semi-distributed hydrologic models. Journal of Hydrology, In Press, Corrected Proof.

Kling, H., Gupta, H., 2009. On the development of regionalization relationships for lumped watershed models: The impact of ignoring sub-basin scale variability. Journal of Hydrology, 373(3-4): 337-351.

Knowles, N., Dettinger, M.D., Cayan, D.R., 2006. Trends in snowfall versus rainfall in the Western United States. Journal of Climate, 19(18): 4545-4559.

Kumar, M., Duffy, C.J., Salvage, K.M., 2009. A Second-Order Accurate, Finite Volume-Based, Integrated Hydrologic Modeling (FIHM) Framework for Simulation of Surface and Subsurface Flow. Vadose Zone Journal, 8(4): 873-890.

Leung, L.R. et al., 2004. Mid-century ensemble regional climate change scenarios for the western United States. Climatic Change, 62(1-3): 75-113.

Liston, G.E., 1999. Interrelationships among Snow Distribution, Snowmelt, and Snow Cover Depletion: Implications for Atmospheric, Hydrologic, and Ecologic Modeling. Journal of Applied Meteorology [J. Appl. Meteorol.]. Vol. 38(10): 1474-1487.

Luce, C.H., Tarboton, D.G., 2004. The application of depletion curves for parameterization of subgrid variability of snow. Hydrological Processes [Hydrol. Process.]. Vol. 18(8): 1409-1422.

Luce, C.H., Tarboton, D.G., Cooley, K.R., 1999. Sub-grid parameterization of snow distribution for an energy and mass balance snow cover model. Hydrological Processes, 13(12-13): 1921-1933.

Marks, D., Kimball, J., Tingey, D., Link, T., 1998. The sensitivity of snowmelt processes to climate conditions and forest cover during rain-on-snow: a case study of the 1996 Pacific Northwest flood. Hydrological Processes, 12(10-11): 1569-1587.

Marks, D., Link, T., Winstral, A., Garen, D., 2001. Simulating snowmelt processes during rain-on-snow over a semi-arid mountain basin. Annals of Glaciology, Vol 32, 2001, 32: 195-202.

Martin, K., 2002. NWSRFS calibration parameter selection and geologic reasoning: Pacific Northwest cases. Journal of the American Water Resources Association, 38(5): 1349-1362.

Martinec, J., 1985. SNOWMELT RUNOFF MODELS FOR OPERATIONAL FORECASTS. Nordic Hydrology, 16(3): 129-136.

Martinec, J., Rango, A., Roberts, R., 2008. Snowmelt Runoff Model (SRM) User's Manual, Updated Edition 2008, WinSRM Version 1.11.

Mauget, S.A., 2003. Multidecadal regime shifts in US streamflow, precipitation, and temperature at the end of the twentieth century. Journal of Climate, 16(23): 3905-3916.

Maurer, E.P., Stewart, I.T., Bonfils, C., Duffy, P.B., Cayan, D., 2007. Detection, attribution, and sensitivity of trends toward earlier streamflow in the Sierra Nevada. Journal of Geophysical Research-Atmospheres, 112(D11).

McCabe, G.J., Clark, M.P., Hay, L.E., 2007. Rain-on-snow events in the western United States. Bulletin of the American Meteorological Society, 88(3): 319-+.

Mote, P.W., Hamlet, A.F., Clark, M.P., Lettenmaier, D.P., 2005. Declining mountain snowpack in western north America. Bulletin of the American Meteorological Society, 86(1): 39-+.

Nayak, A., Marks, D., Chandler, D.G., Seyfried, M., 2010. Long-term snow, climate, and streamflow trends at the Reynolds Creek Experimental Watershed, Owyhee Mountains, Idaho, United States. Water Resources Research [Water Resour. Res.]. Vol., 46(06).

NWS, 2009. NWS Calibration Workshop, LMRFC, Powerpoint slides.

NWS, 2011. The National Weather Service River Forecast System User's Manual.

Procsal, M., 2005. Development of an areal snow depletion curve in the Dry Creek Experimental Watershed using MODIS satellite imagery and the Utah Energy Balance snow accumulation and melt model, Boise State University.

Qu, Y.Z., Duffy, C.J., 2007. A semidiscrete finite volume formulation for multiprocess watershed simulation. Water Resources Research, 43(8).

Reba, M.L., Marks, D., Winstral, A., Link, T.E., Kumar, M., 2011. Sensitivity of the snowcover energetics in a mountain basin to variations in climate. Hydrological Processes, 25(21): 3312-3321.

Reed, S. et al., 2004. Overall distributed model intercomparison project results. Journal of Hydrology, 298(1-4): 27-60.

Reed, S., Schaake, J., Zhang, Z., 2007. A distributed hydrologic model and threshold frequency-based method for flash flood forecasting at ungauged locations. Journal of Hydrology, 337(3–4): 402-420.

Reed, S.M., 2003. Deriving flow directions for coarse-resolution (1-4 km) gridded hydrologic modeling. Water Resources Research, 39(9).

Regonda, S.K., Rajagopalan, B., Clark, M., Pitlick, J., 2005. Seasonal cycle shifts in hydroclimatology over the western United States. Journal of Climate, 18(2): 372-384.

Rice, R., Bales, R.C., Painter, T.H., Dozier, J., 2011. Snow water equivalent along elevation gradients in the Merced and Tuolumne River basins of the Sierra Nevada. Water Resources Research, 47.

Rothwell, E., 2005. The influence of hyporheic flow on stream temperature., Boise State University.

Salomonson, V.V., Appel, I., 2004. Estimating fractional snow cover from MODIS using the normalized difference snow index. Remote Sensing of Environment, 89(3): 351-360.

Shallcross, A., 2011. LIDAR investigations of snow distribution in mountainous terrain, Boise State University.

Shamir, E., Carpenter, T.M., Fickenscher, P., Georgakakos, K.P., 2006. Evaluation of the National Weather Service operational hydrologic model and forecasts for the American River basin. Journal of Hydrologic Engineering, 11(5): 392-407.

Shamir, E., Georgakakos, K.P., 2007. Estimating snow depletion curves for American River basins using distributed snow modeling. Journal of Hydrology, 334(1-2): 162-173.

Shamir, E., Imam, B., Gupta, H.V., Sorooshian, S., 2005. Application of temporal streamflow descriptors in hydrologic model parameter estimation. Water Resources Research, 41(6).

Singh, P., Spitzbart, G., Hubl, H., Weinmeister, H.W., 1997. Hydrological response of snowpack under rain-on-snow events: a field study. Journal of Hydrology, 202(1-4): 1-20.

Smith, T.J., 2010. Using Soil Moisture Trends Across Topographic Gradients to Examine Controls on Semi-Arid Ecosystem Dynamics., Boise State University.

Stewart, I.T., Cayan, D.R., Dettinger, M.D., 2004. Changes in snowmelt runoff timing in western North America under a 'business as usual' climate change scenario. Climatic Change, 62(1-3): 217-232.

Stewart, I.T., Cayan, D.R., Dettinger, M.D., 2005. Changes toward earlier streamflow timing across western North America. Journal of Climate, 18(8): 1136-1155.

Tesfa, T.K., Tarboton, D.G., Chandler, D.G., McNamara, J.P., 2009. Modeling soil depth from topographic and land cover attributes. Water Resources Research, 45.

USDA, 1974. Soil-Hydrologic Reconnaissance Survey. Forest Service, Boise, Idaho.

Vrugt, J.A. et al., 2006. Application of stochastic parameter optimization to the Sacramento Soil Moisture Accounting Model. Journal of Hydrology, 325(1-4): 288-307.

Williams, C.J., 2005. Characterization of the spatial and temperal controls on soil moisture and streamflow generation in a semi-arid headwater catchment., Boise State University.

Yatheendradas, S. et al., in review. Does the distributed assimilation of fractional snow extent improve simulated streamflow 1 in mountainous, densely forested basins? Journal of Hydrology.

Zhang, Y., Zhang, Z.Y., Reed, S., Koren, V., 2011. An enhanced and automated approach for deriving a priori SAC-SMA parameters from the soil survey geographic database. Computers & Geosciences, 37(2): 219-231.

Zhang, Z.Y., Koren, V., Smith, M., Reed, S., Wang, D., 2004. Use of next generation weather radar data and basin disaggregation to improve continuous hydrograph simulations. Journal of Hydrologic Engineering, 9(2): 103-115.

APPENDIX A

Hydrograph Comparisons for Empirical ADC versus NWS ADC

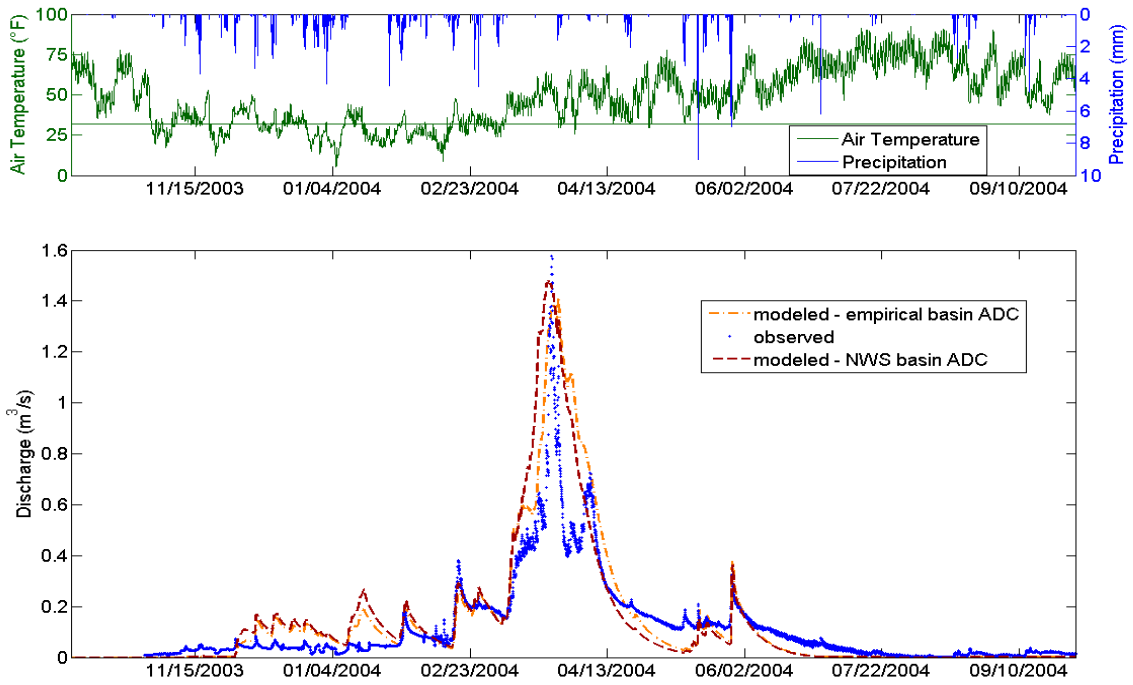

Figure A.1 ADC Hydrograph Comparison for WY2004 at LG.

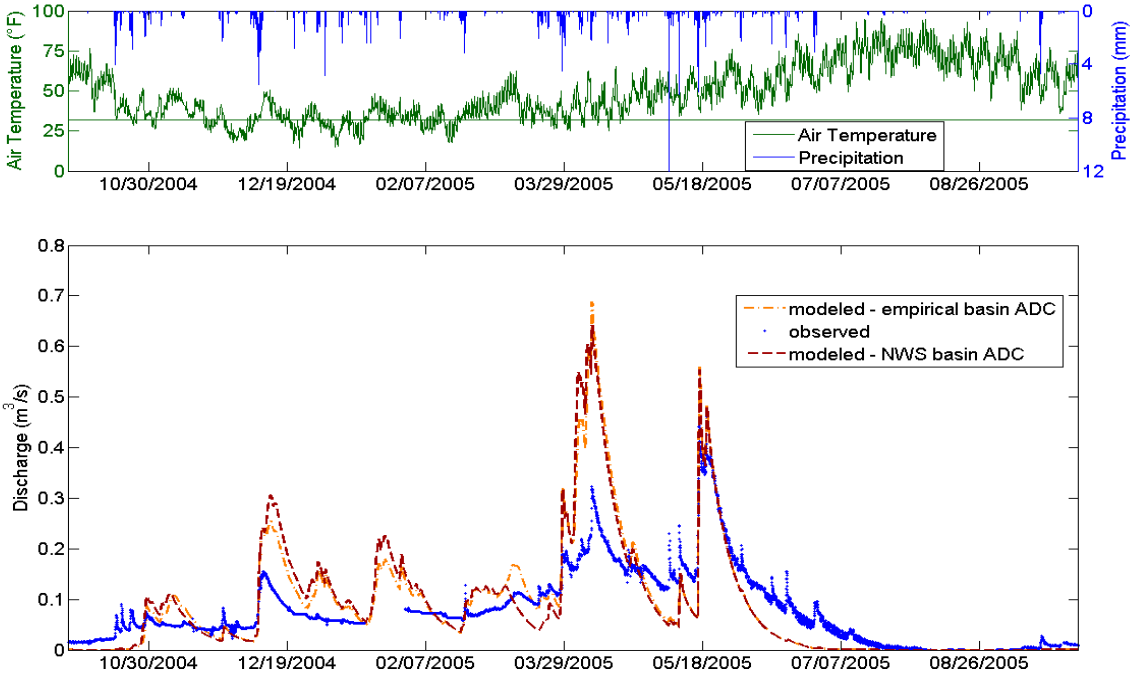

Figure A.2 ADC Hydrograph Comparison for WY2005 at LG.

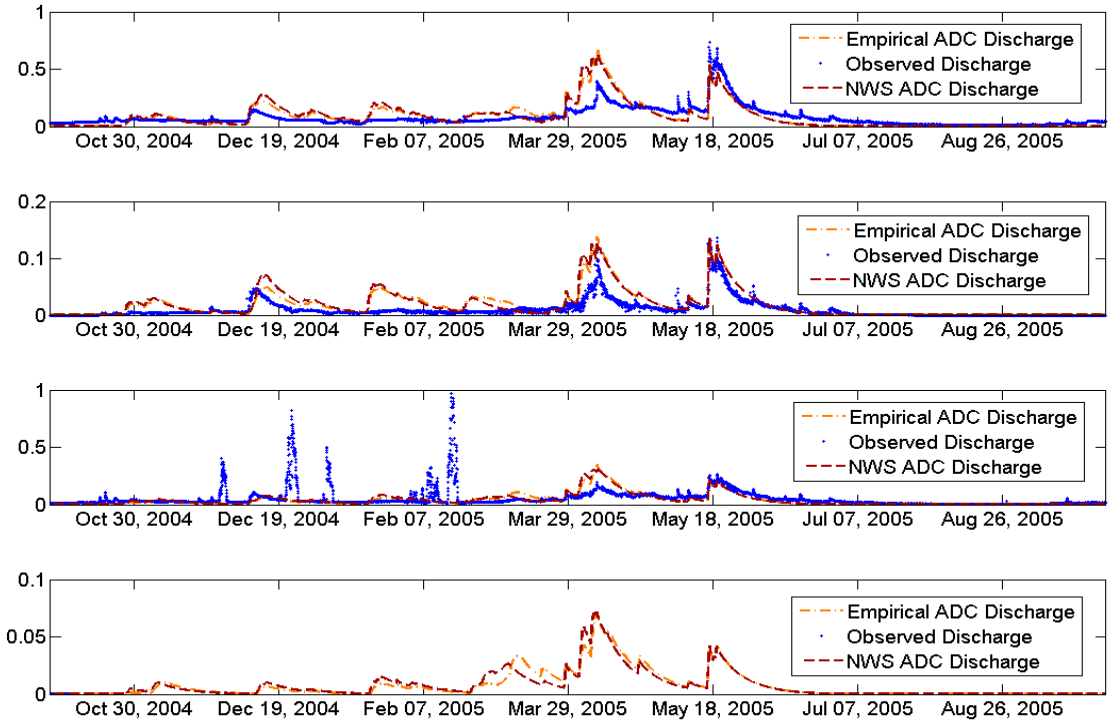

Figure A.3 Interior Hydrograph Comparison for WY2005. Subplots are C2M, C1W, C1E, and BG from Top to Bottom.

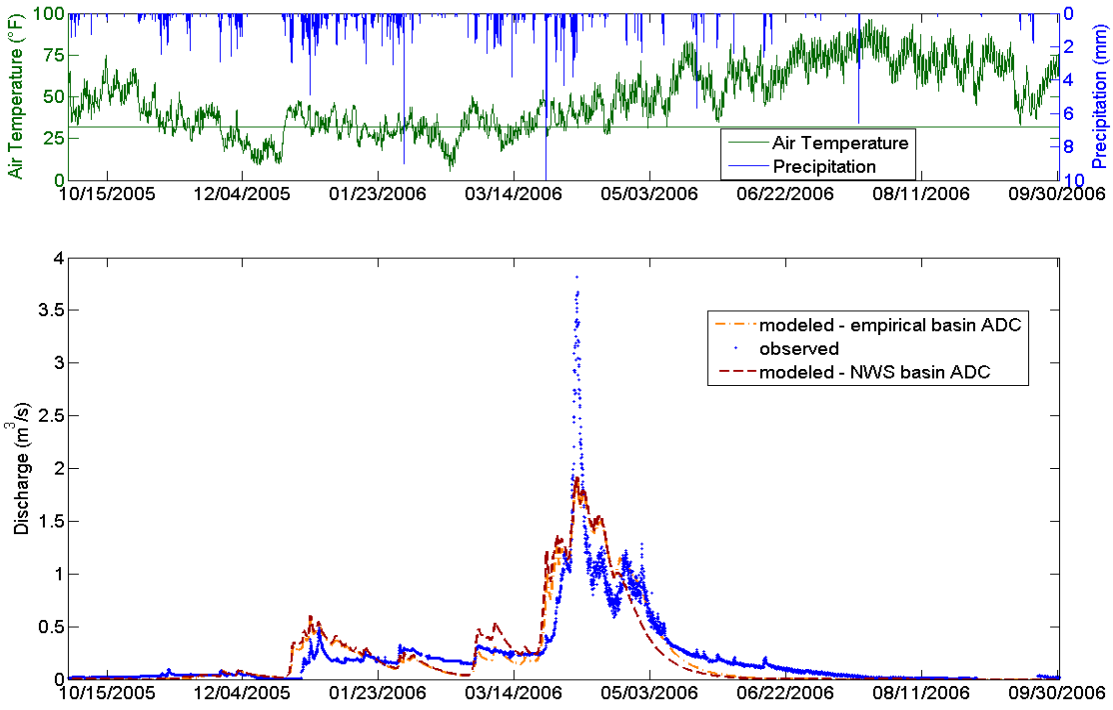

Figure A.4 ADC Hydrograph Comparison for WY2006 at LG.

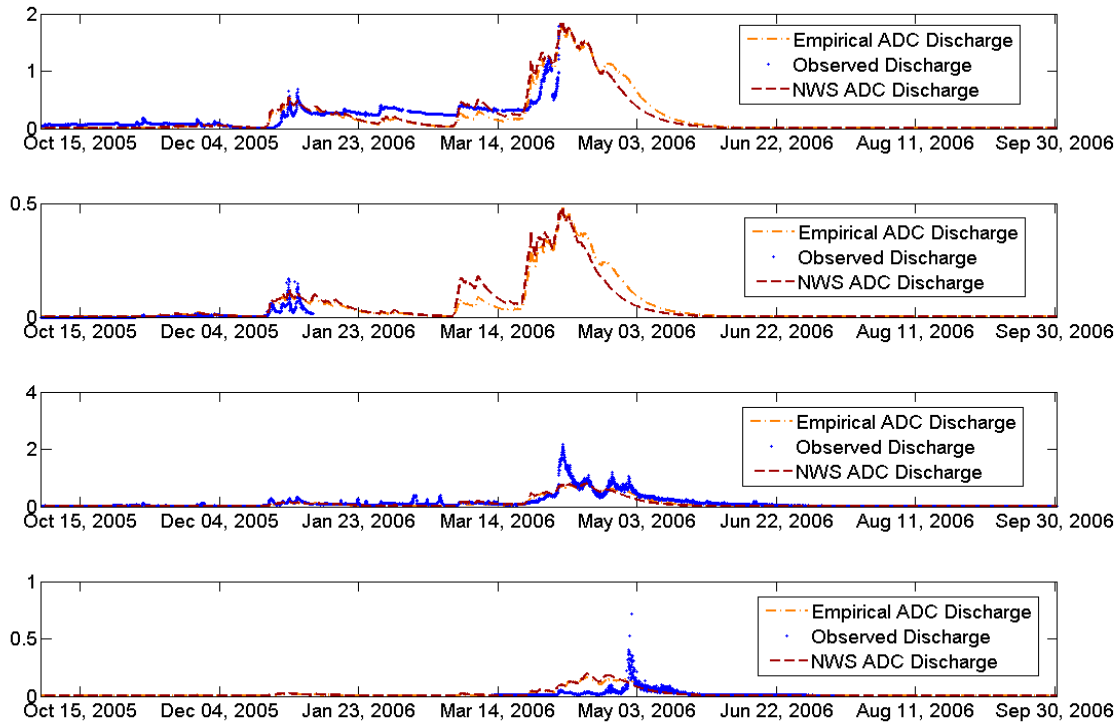

Figure A.5 Interior Hydrograph Comparison for WY2006. Subplots are C2M, C1W, C1E, and BG from Top to Bottom.

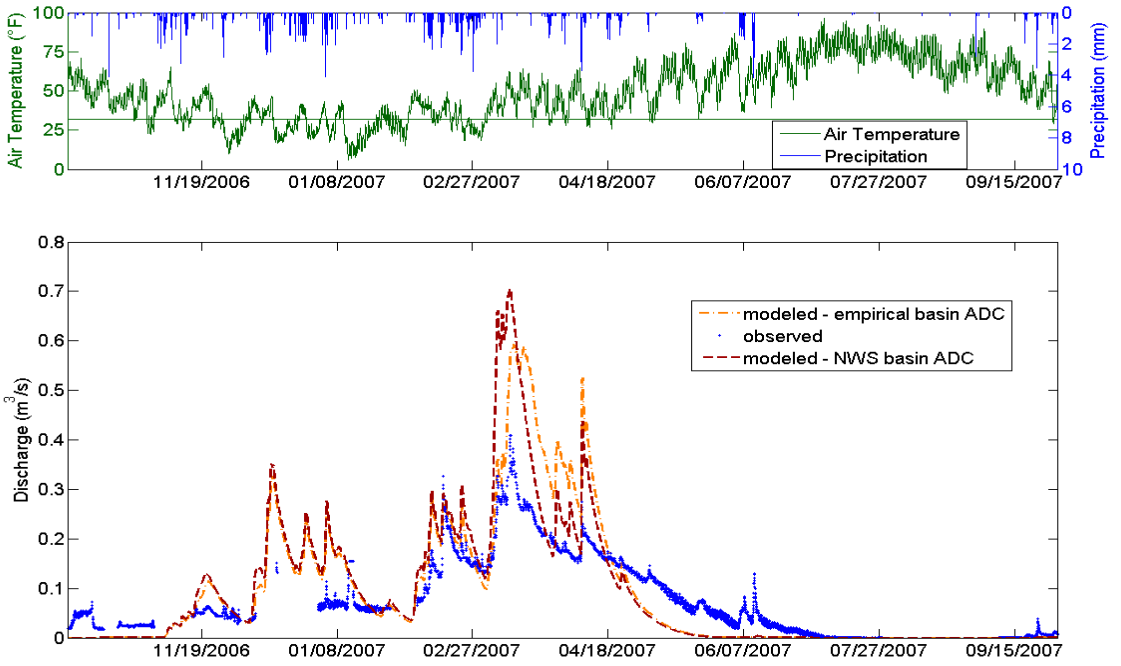

Figure A.6 ADC Hydrograph Comparison for WY2007 at LG.

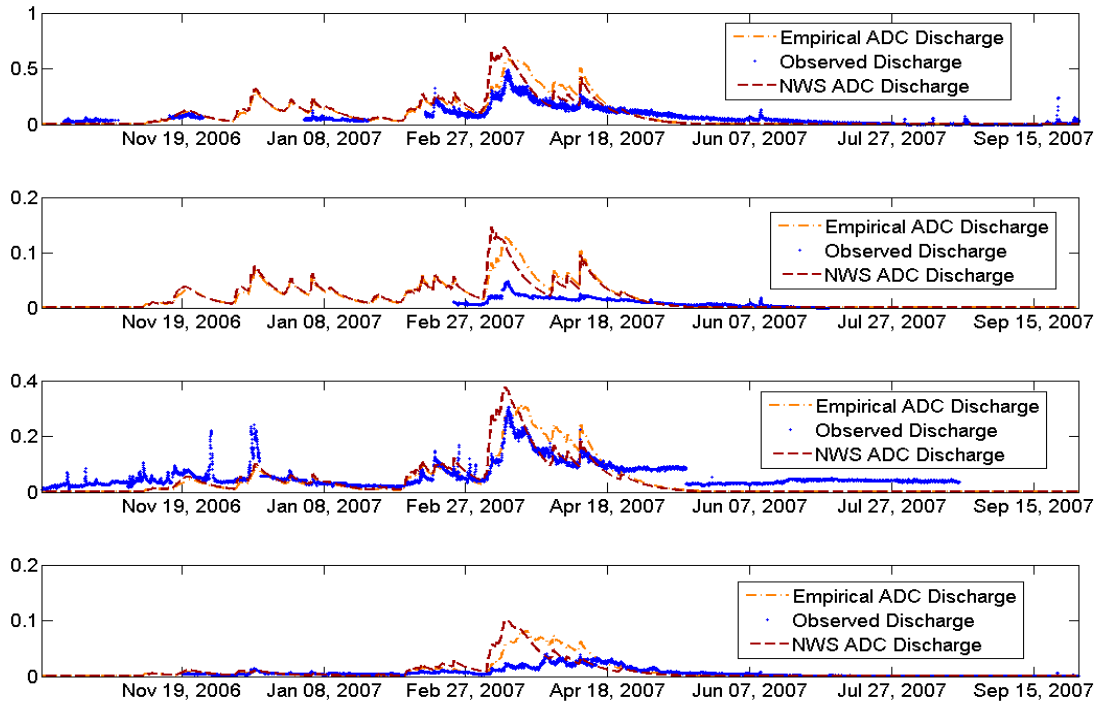

Figure A.7 Interior Hydrograph Comparison for WY2007. Subplots are C2M, C1W, C1E, and BG from Top to Bottom.

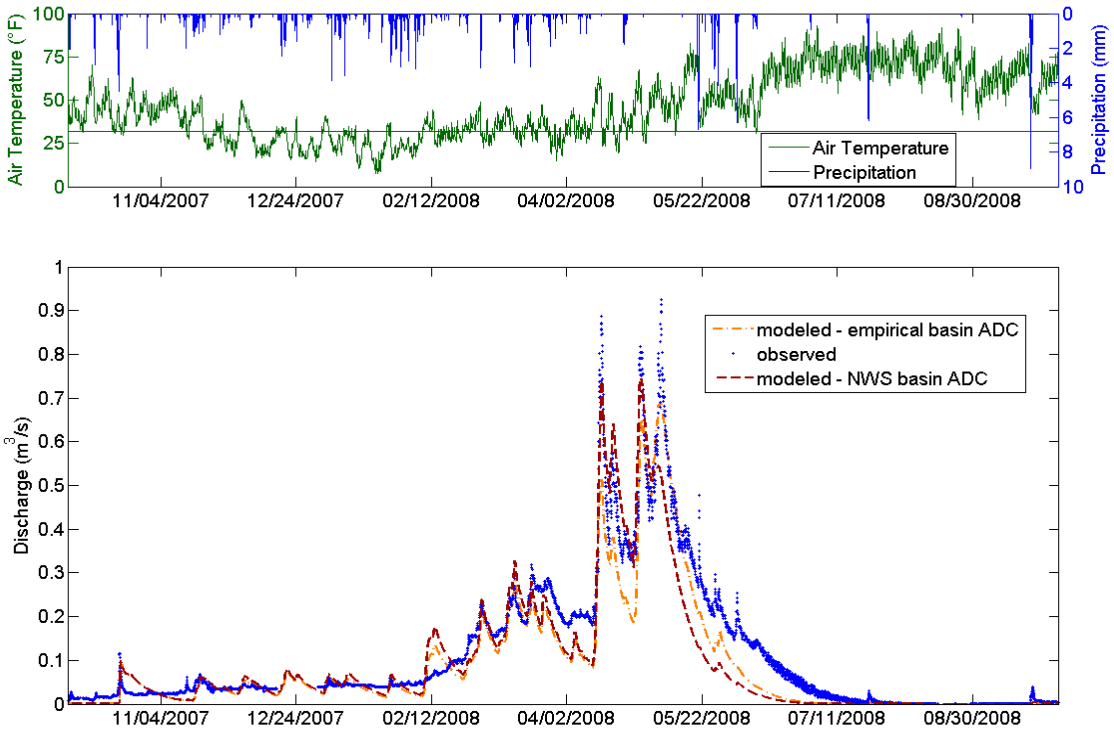

Figure A.8 ADC Hydrograph Comparison for WY2008 at LG.

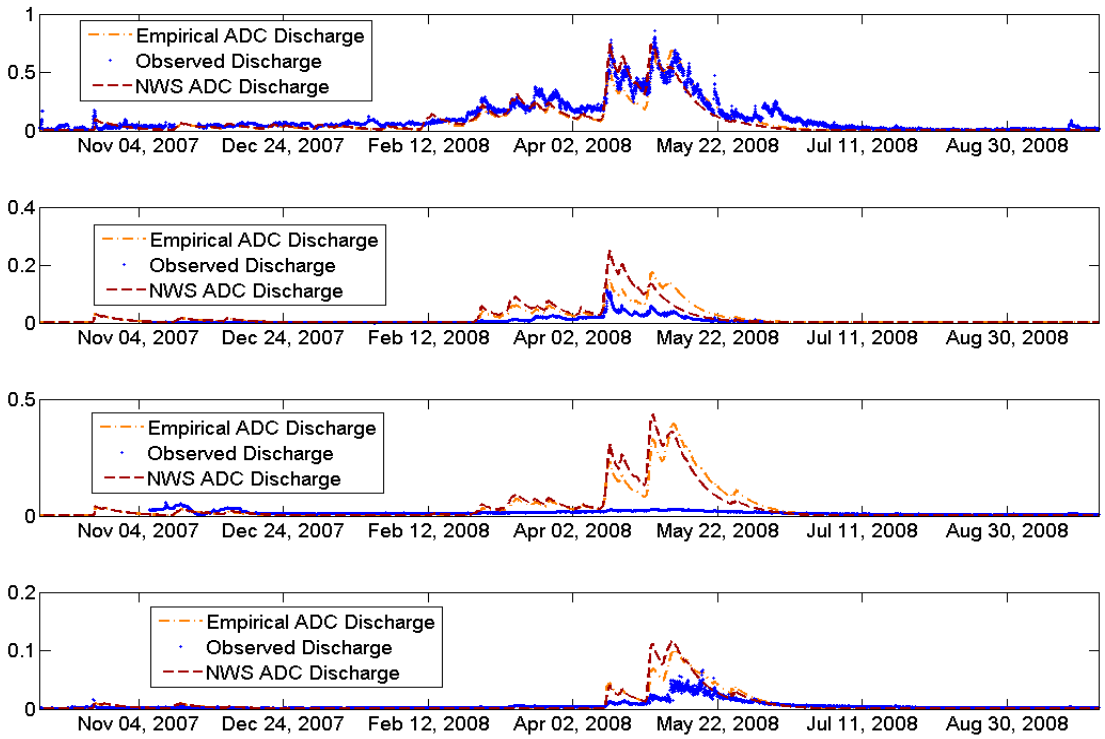

Figure A.9 Interior Hydrograph Comparison for WY2008. Subplots are C2M, C1W, C1E, and BG from Top to Bottom.

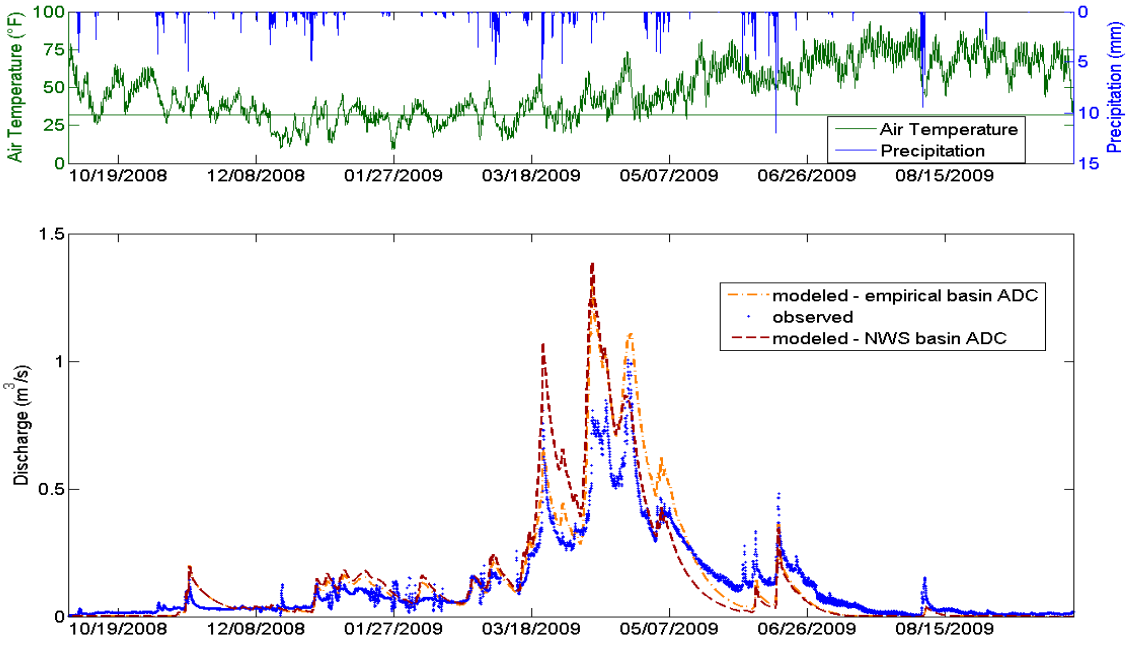

Figure A.10 ADC Hydrograph Comparison for WY2009 at LG.

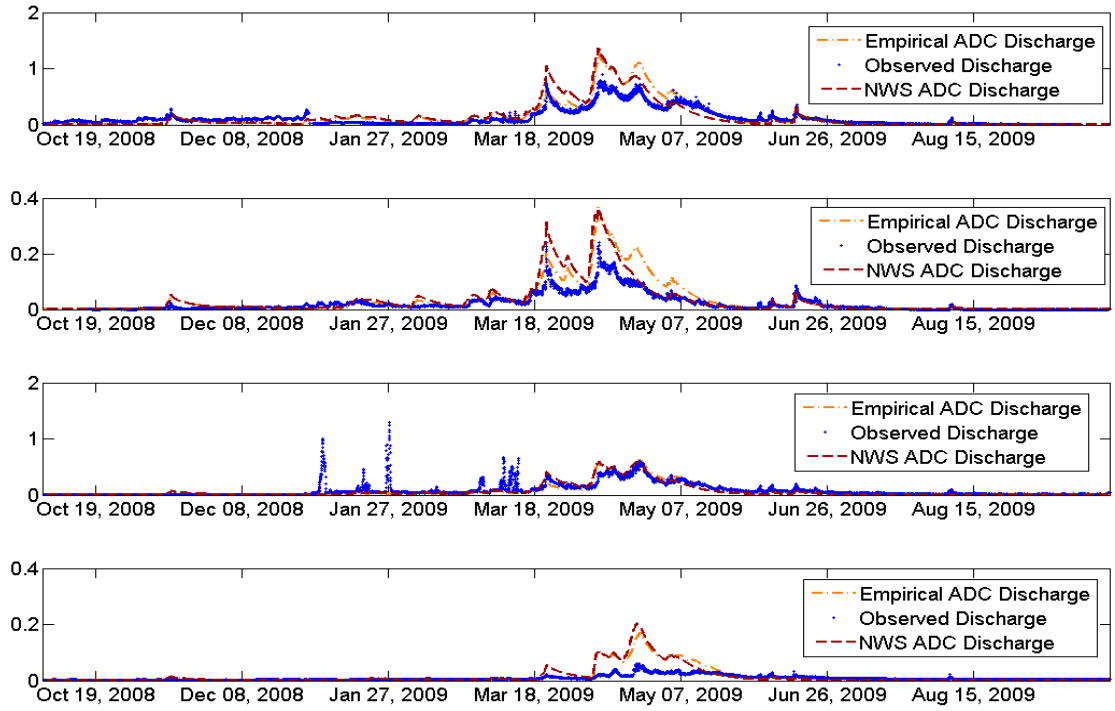

Figure A.11 Interior Hydrograph Comparison for WY2009. Subplots are C2M, C1W, C1E, and BG from Top to Bottom.

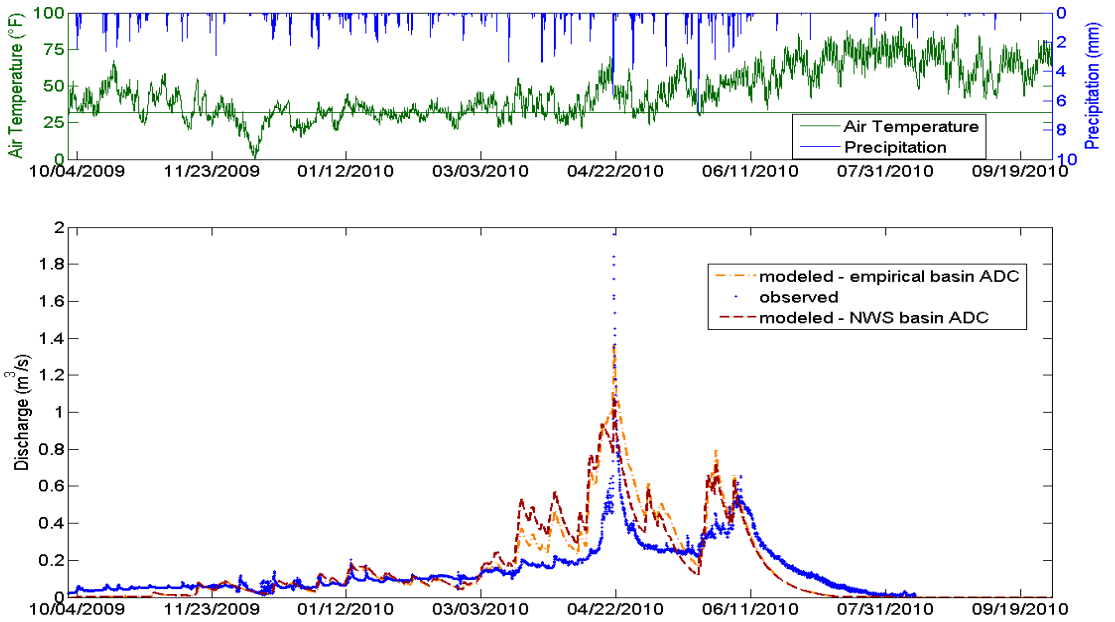

Figure A.12 ADC Hydrograph Comparison for WY2010 at LG.

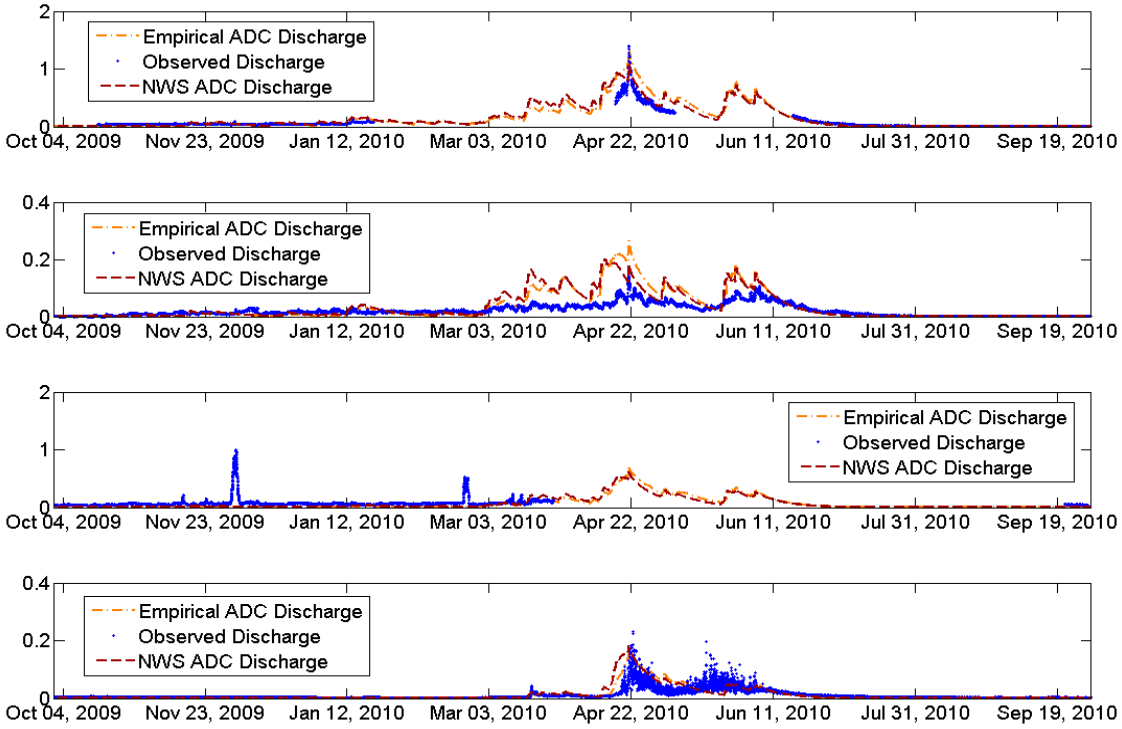

Figure A.13 Interior Hydrograph Comparison for WY2010. Subplots are C2M, C1W, C1E, and BG from Top to Bottom.

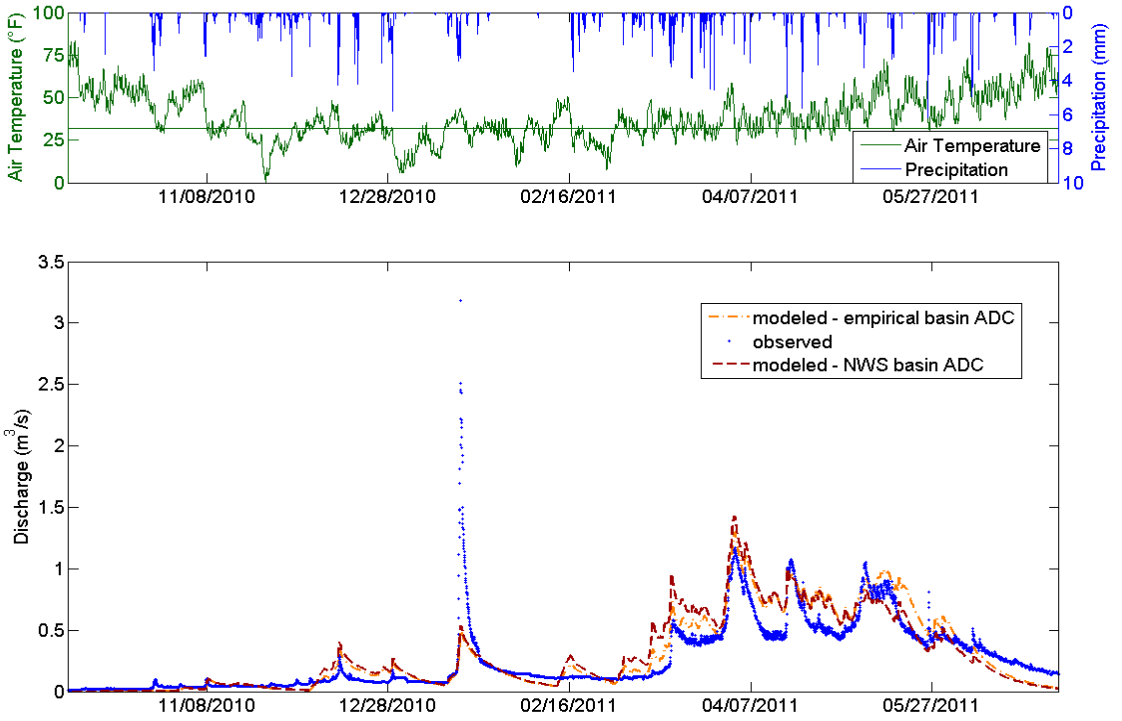

Figure A.14 ADC Hydrograph Comparison for WY2011 at LG.

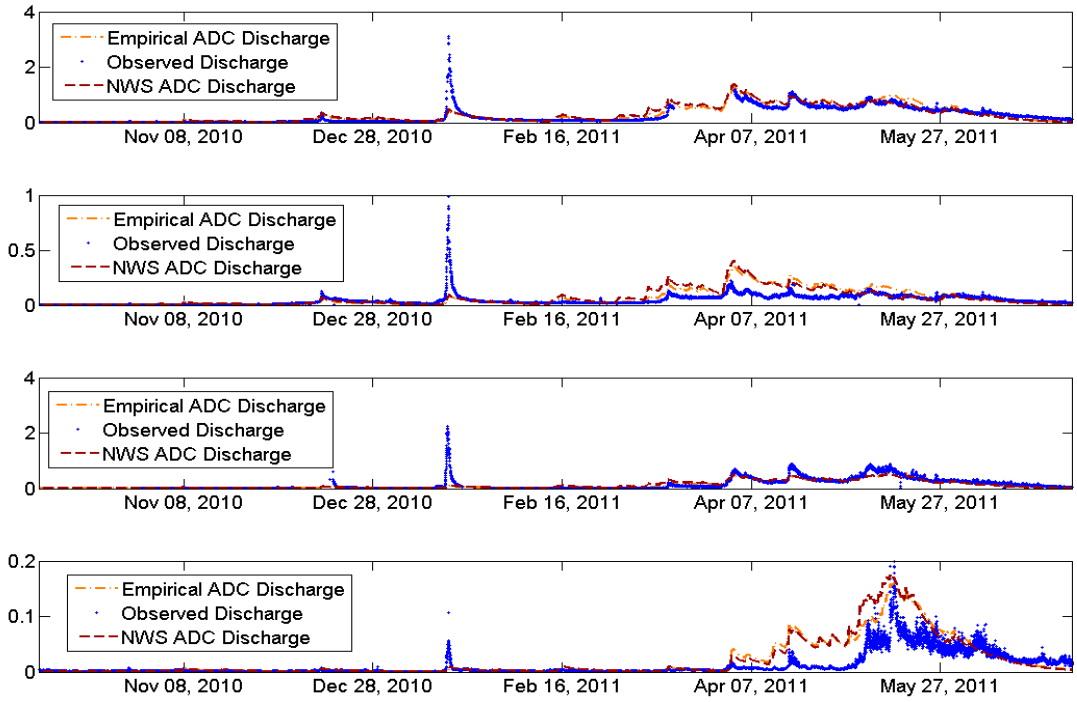

Figure A.15 Interior Hydrograph Comparison for WY2011. Subplots are C2M, C1W, C1E, and BG from Top to Bottom.

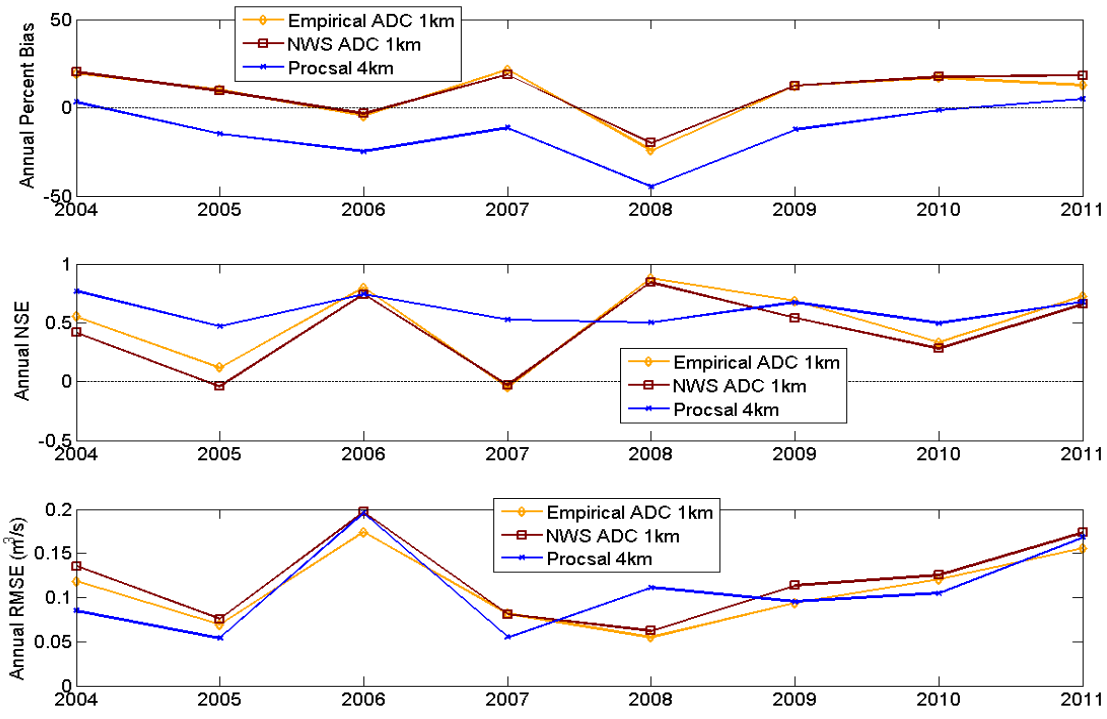

Figure A.16 Annual Statistics Averaged over WY2004-2011. Subplots are Percent Bias, NSE, and RMSE from Top to Bottom.

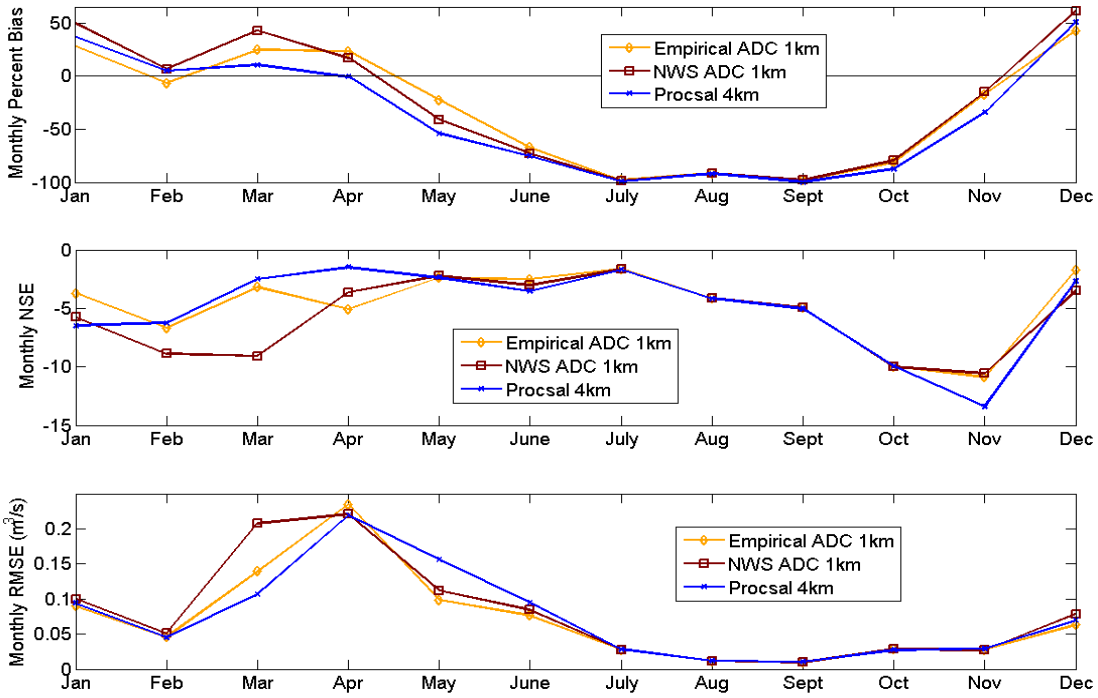

Figure A.17 Monthly Statistics Averaged over WY2004-2011. Subplots are Percent Bias, NSE, and RMSE from Top to Bottom.

APPENDIX B

Other Event Hydrograph Comparison, Snow Depth Comparison, and Statistics

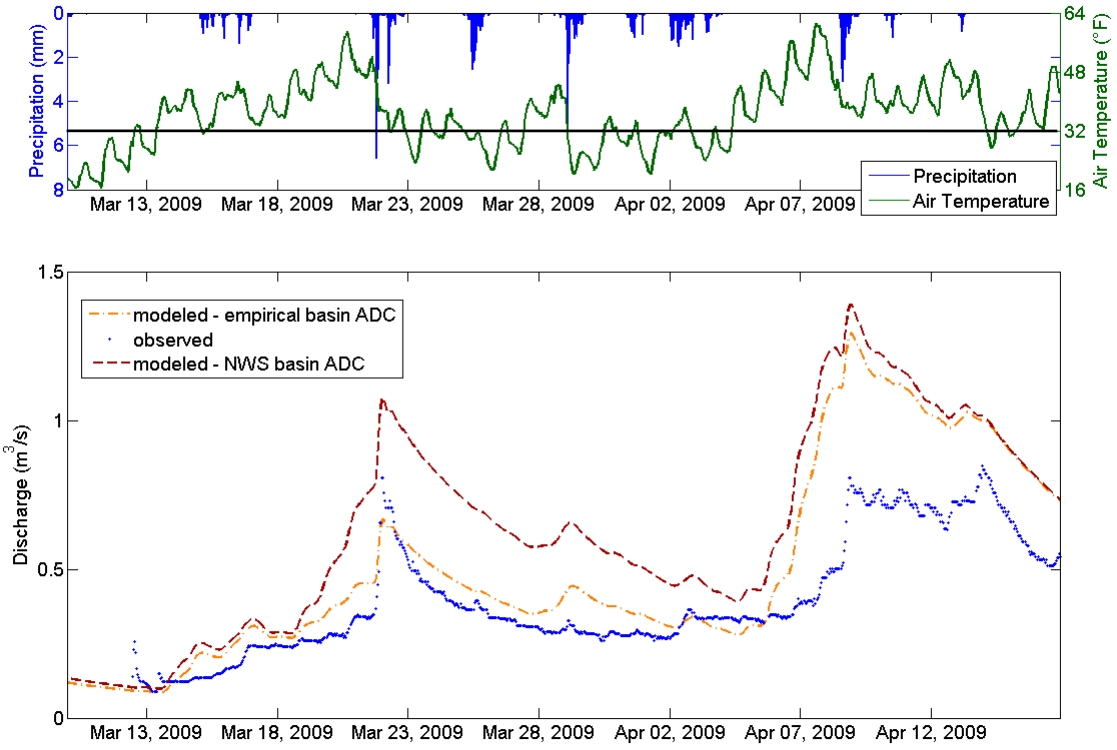

Figure B.1 Hydrograph Comparison for Event #1.

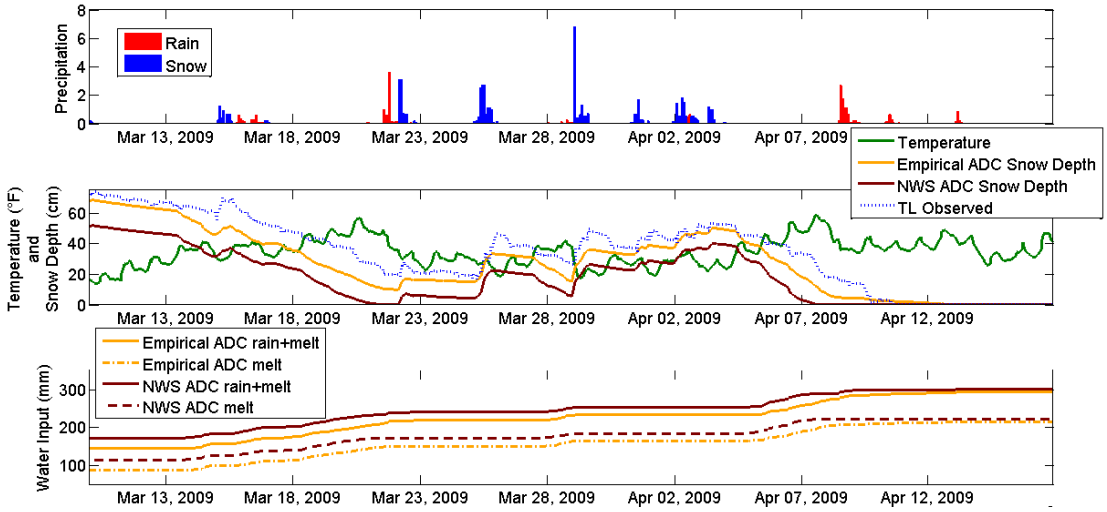

Figure B.2 Snow Depth and Water Input Comparison at TL for Event #1. Top Plot is Precipitation, Middle Plot is Temperature and Snow Depth, and Bottom Plot is Cumulative Water Input to the Subsurface.

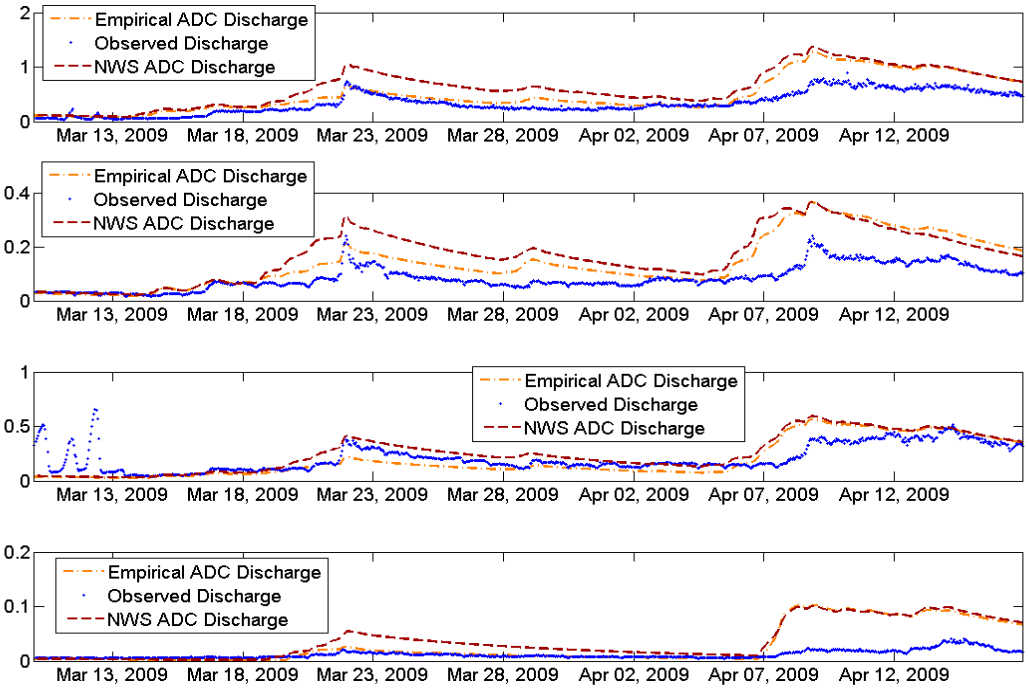

Figure B.3 Interior Hydrograph Comparison for Event #1. Subplots are C2M, C1W, C1E, and BG from Top to Bottom.

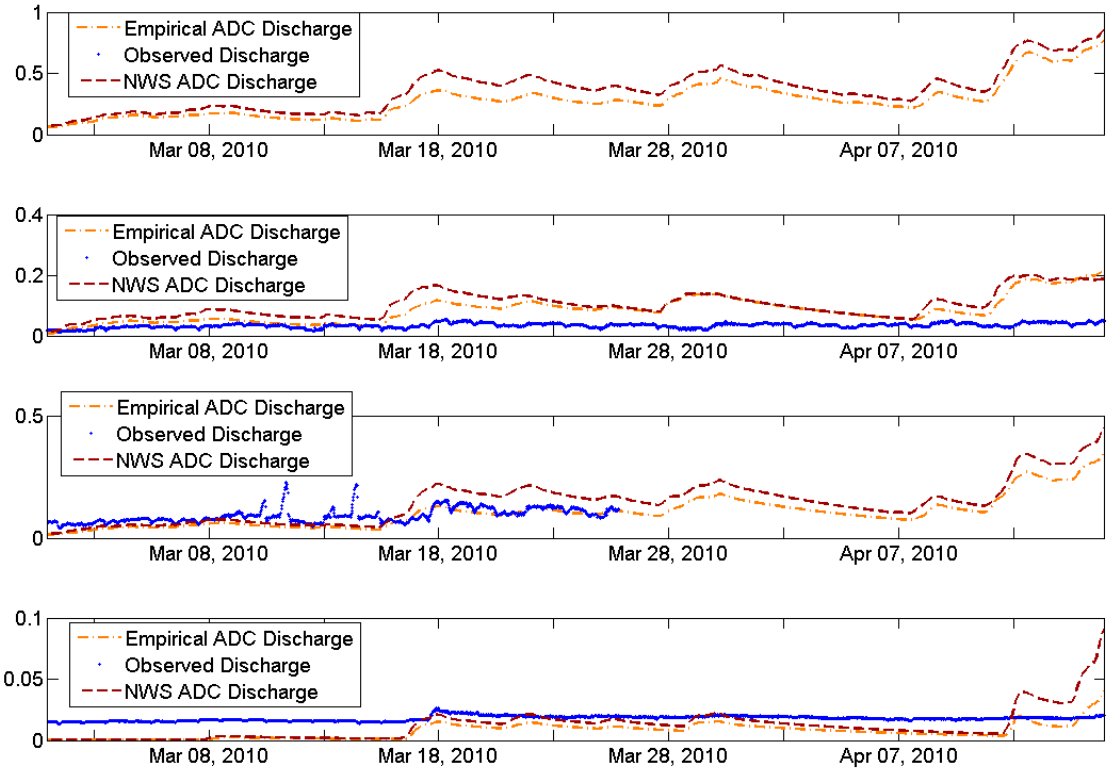

Figure B.4 Interior Hydrograph Comparison for Event #3. Subplots are C2M, C1W, C1E, and BG from Top to Bottom.

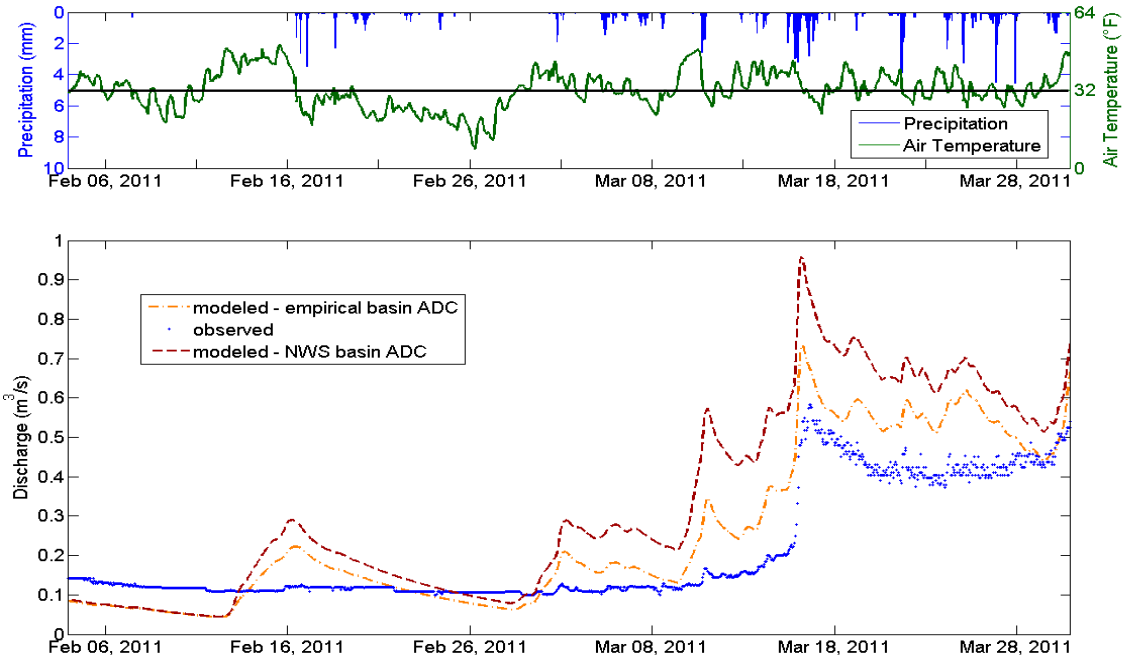

Figure B.5 Hydrograph Comparison for Event #5.

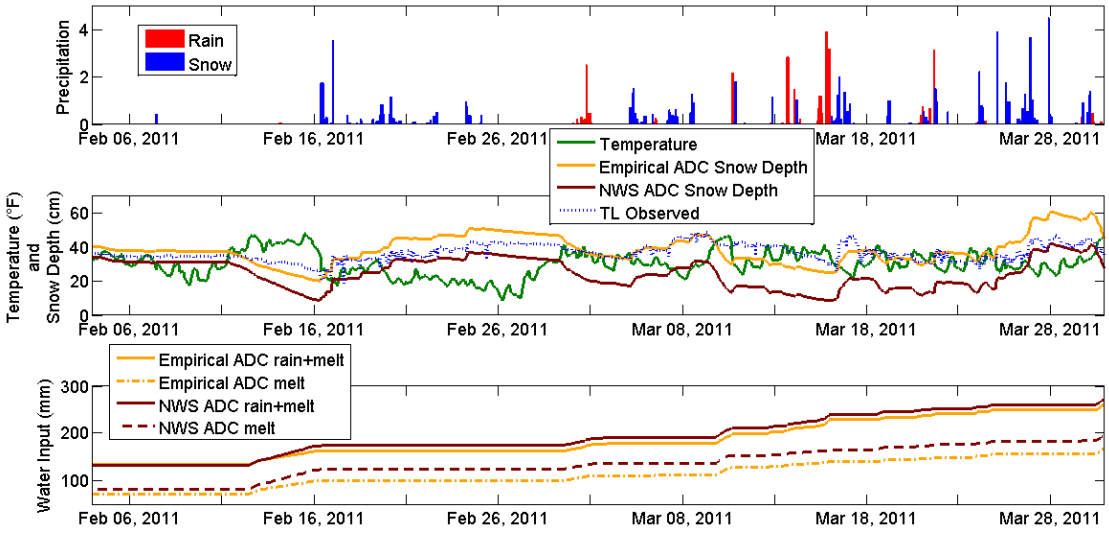

Figure B.6 Snow Depth and Water Input Comparison at TL for Event #5. Top Plot is Precipitation, Middle Plot is Temperature and Snow Depth, and Bottom Plot is Cumulative Water Input to the Subsurface.

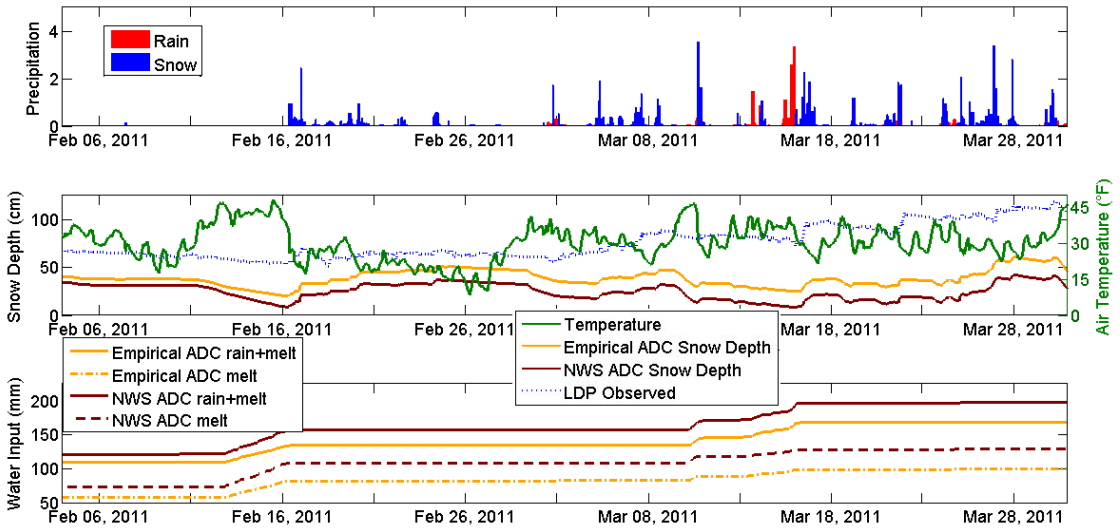

Figure B.7 Snow Depth and Water Input Comparison at LDP for Event #5. Top Plot is Precipitation, Middle Plot is Temperature and Snow Depth, and Bottom Plot is Cumulative Water Input to the Subsurface.

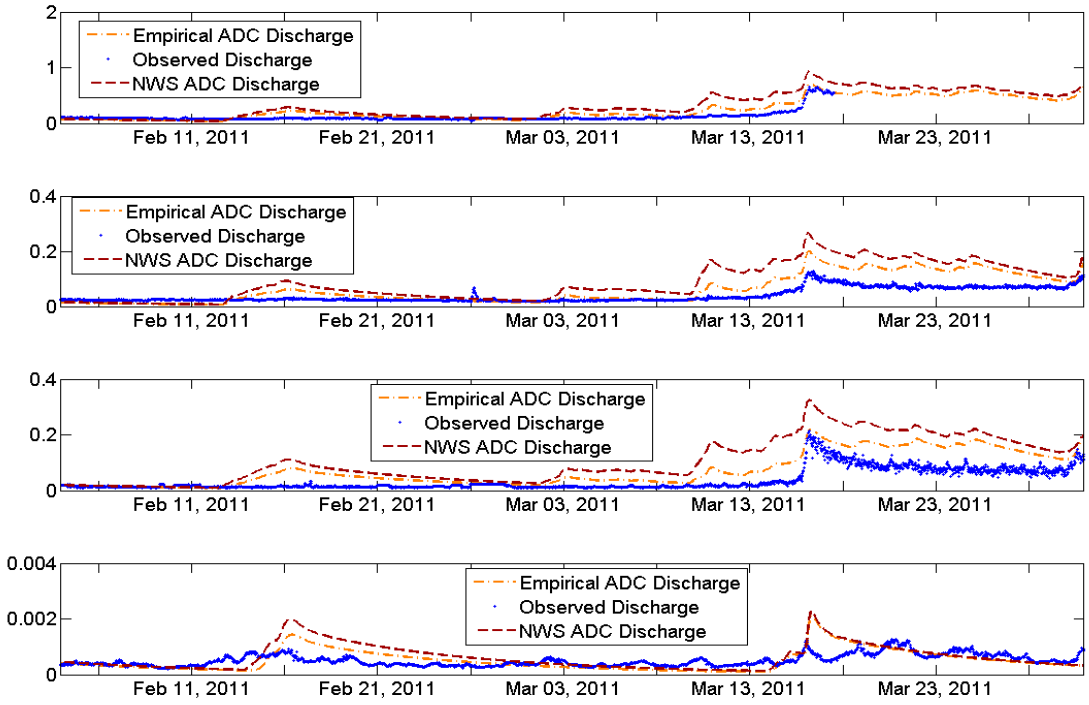

Figure B.8 Interior Hydrograph Comparison for Event #5. Subplots are C2M, C1W, C1E, and BG from Top to Bottom.

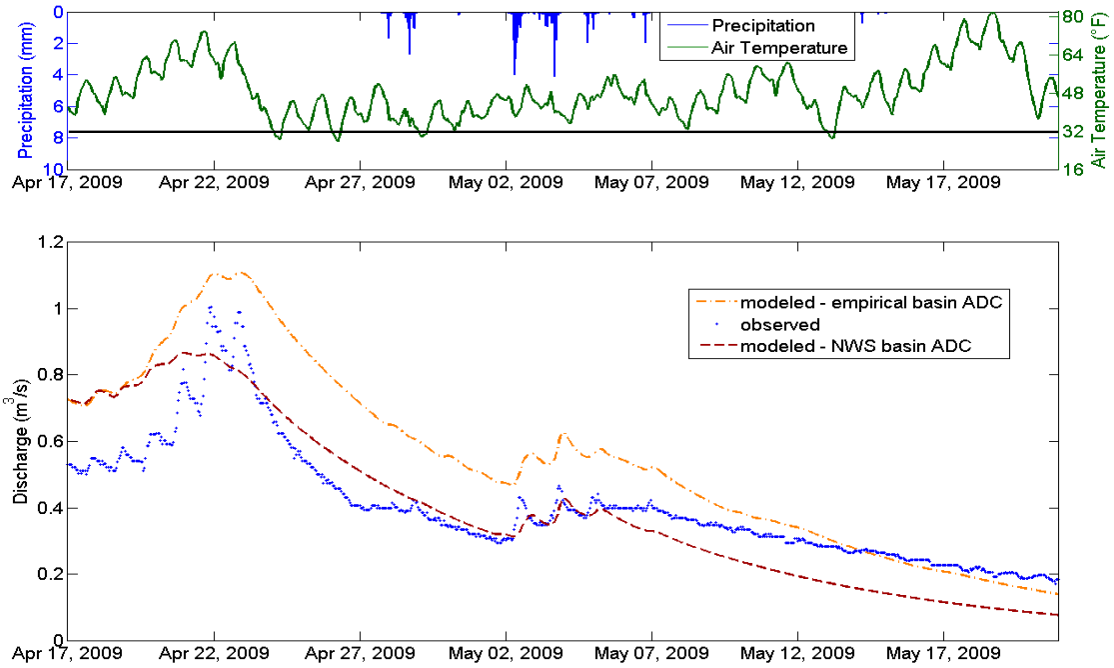

Figure B.9 Hydrograph Comparison for Event #2.

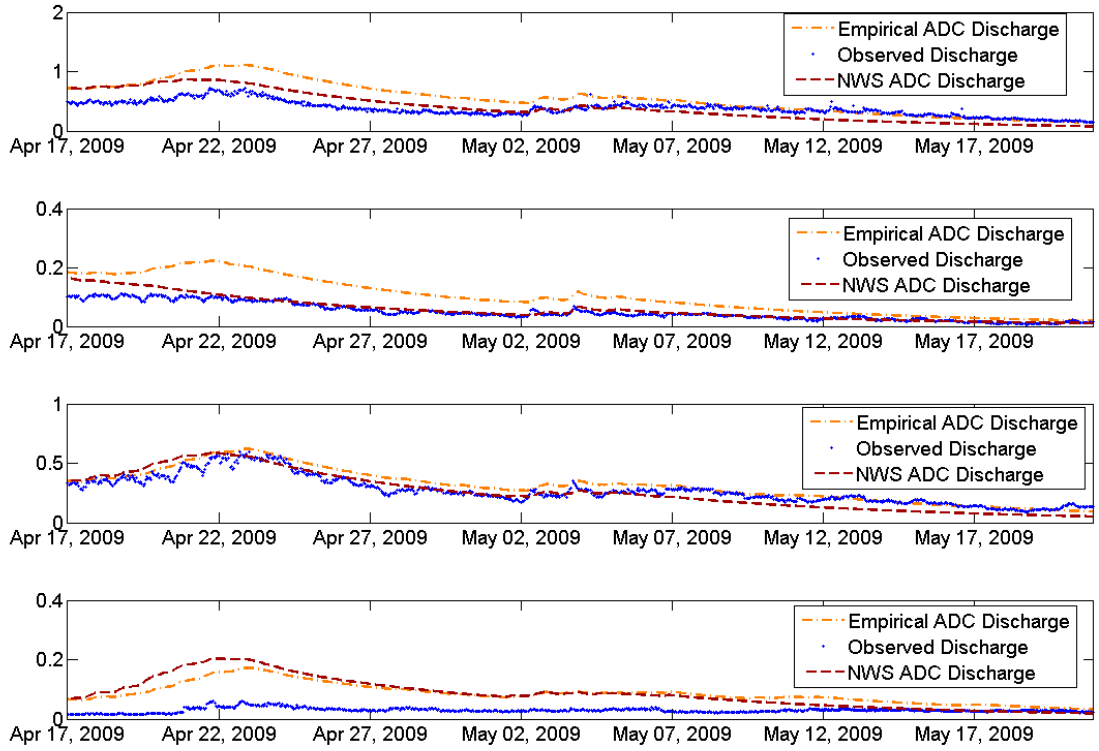

Figure B.10 Interior Hydrograph Comparison for Event #2. Subplots are C2M, C1W, C1E, and BG from Top to Bottom.

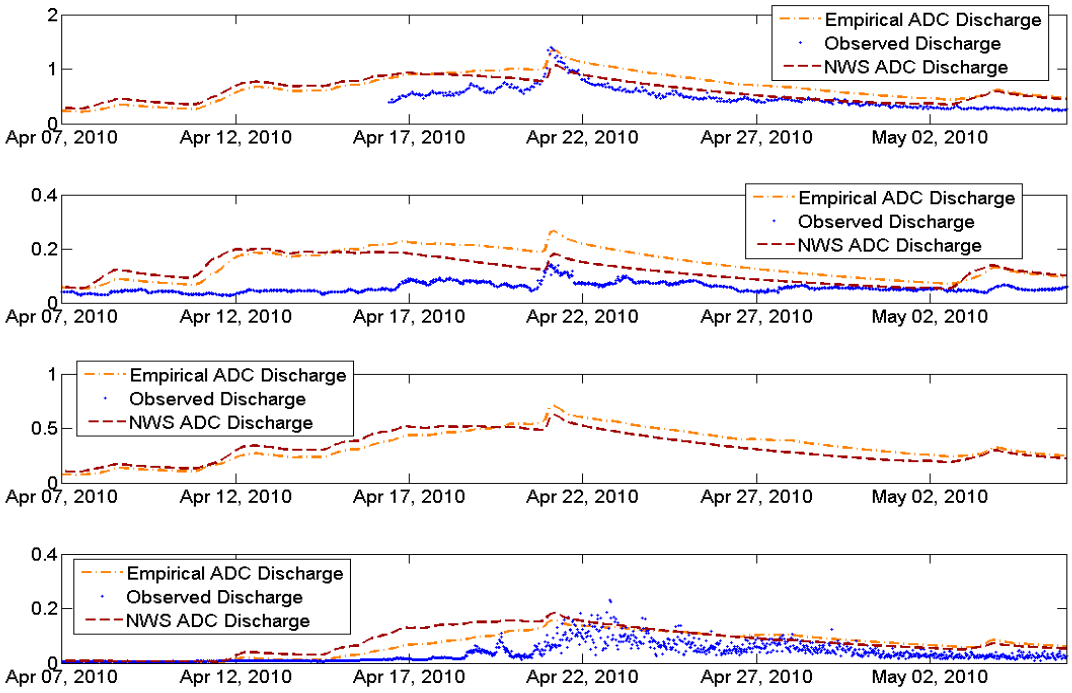

Figure B.11 Interior Hydrograph Comparison for Event #4. Subplots are C2M, C1W, C1E, and BG from Top to Bottom.

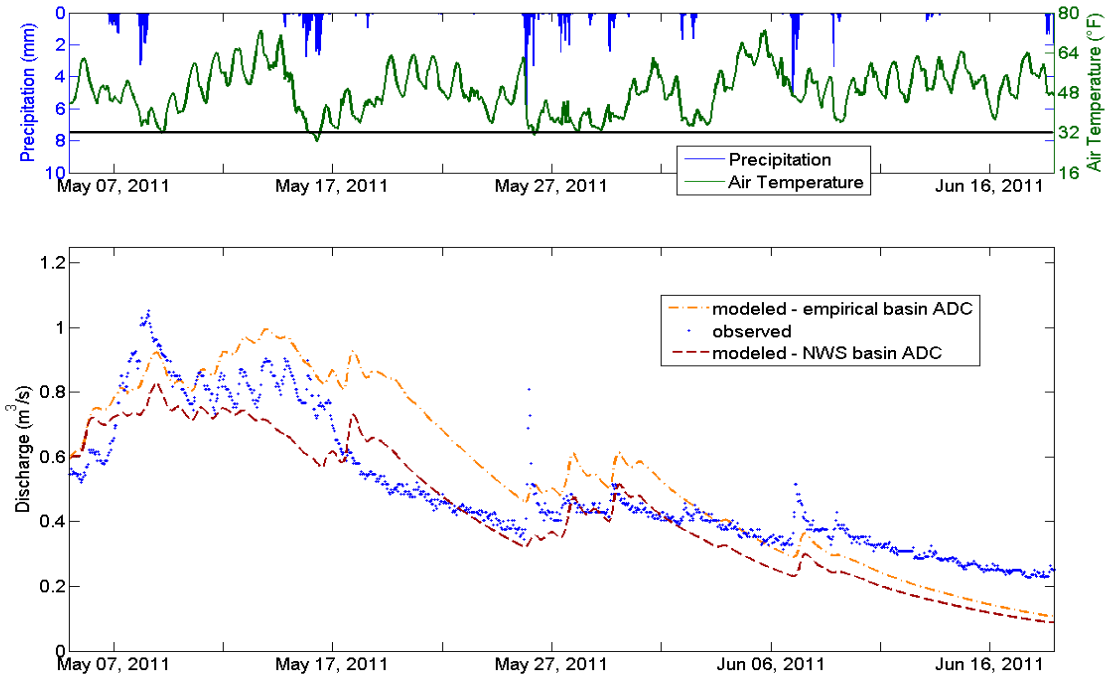

Figure B.12 Hydrograph Comparison for Event #6.

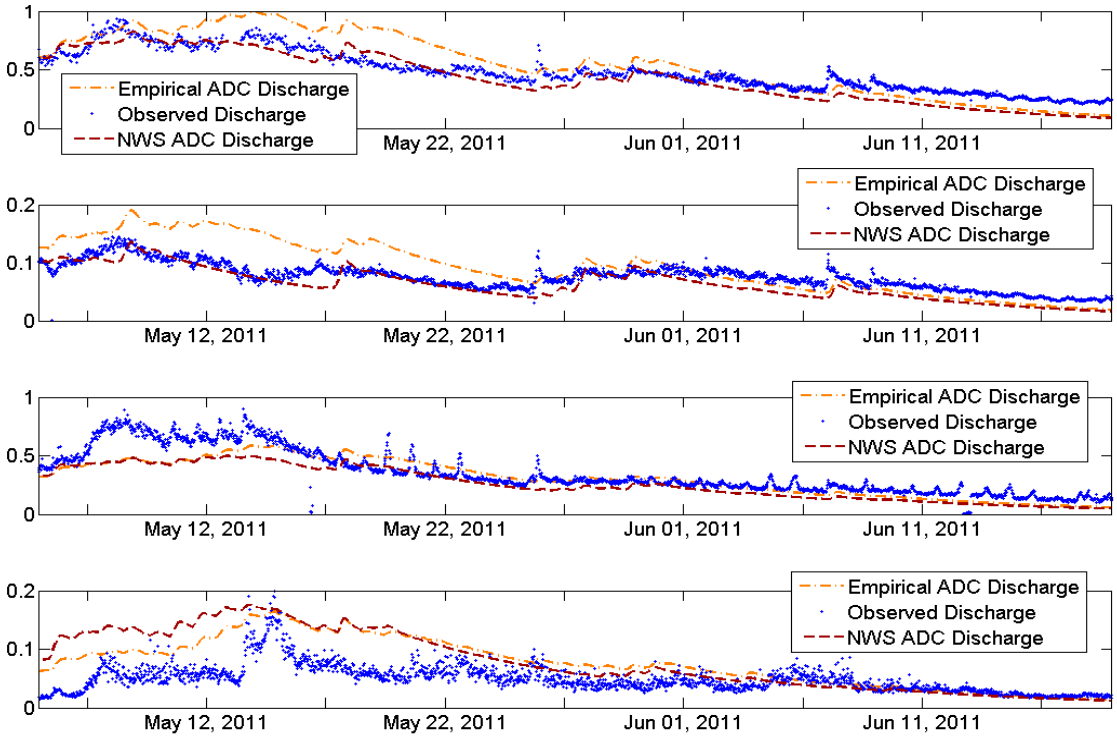

Figure B.13 Interior Hydrograph Comparison for Event #6. Subplots are C2M, C1W, C1E, and BG from Top to Bottom.

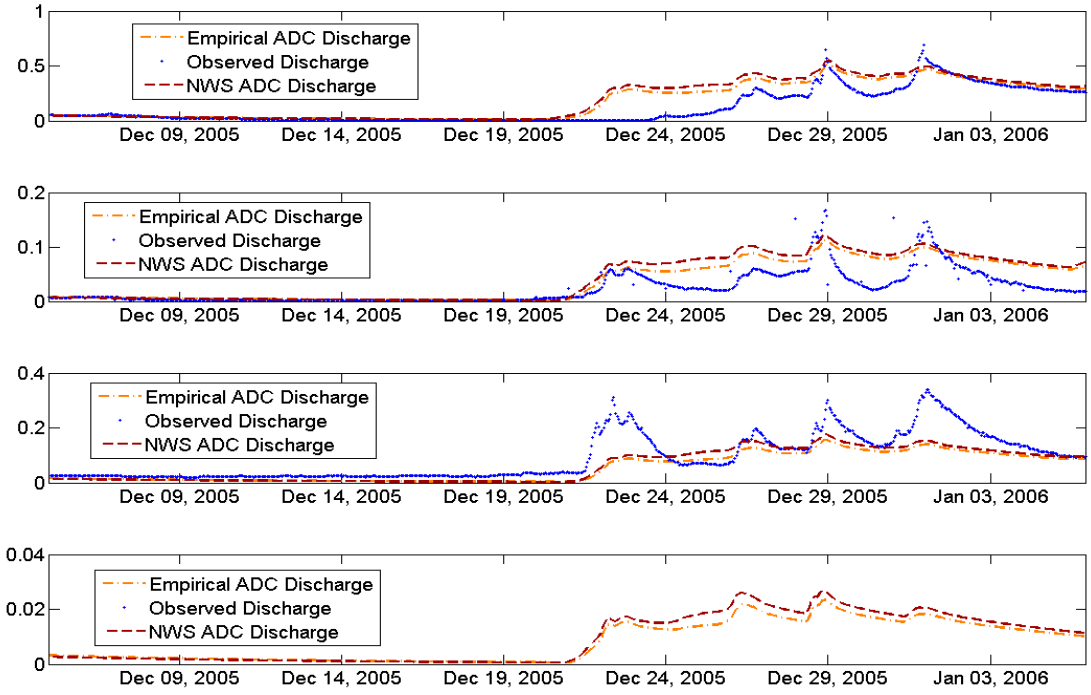

Figure B.14 Interior Hydrograph Comparison for ROS Event #1. Subplots are C2M, C1W, C1E, and BG from Top to Bottom.

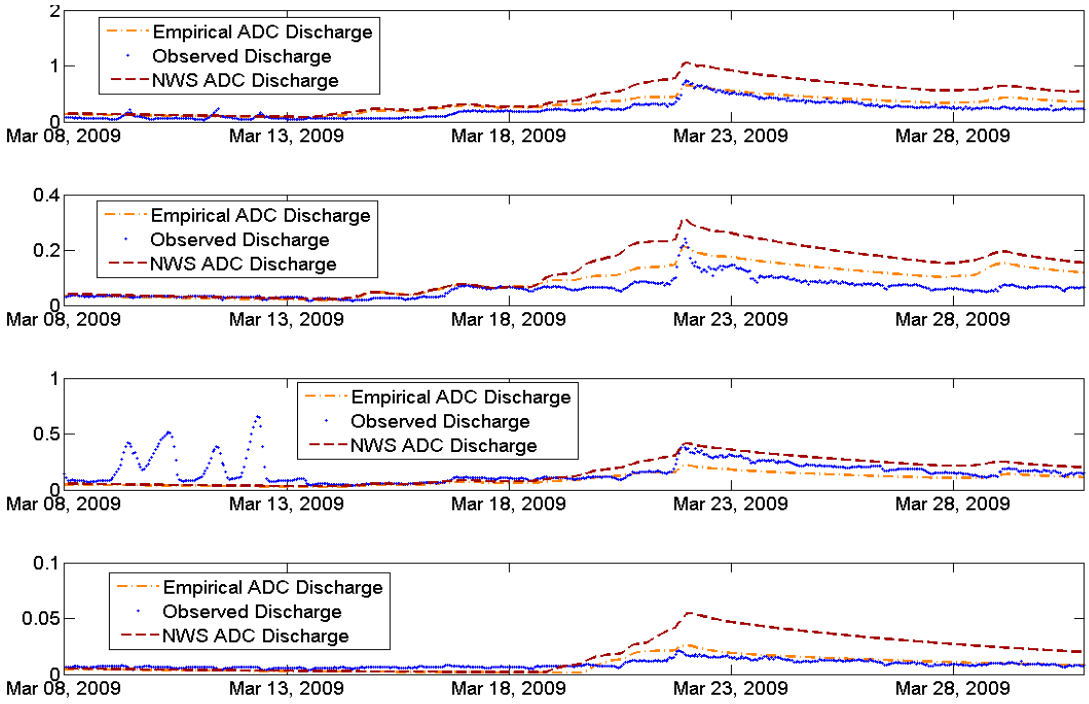

Figure B.15 Interior Hydrograph Comparison for ROS Event #2. Subplots are C2M, C1W, C1E, and BG from Top to Bottom.

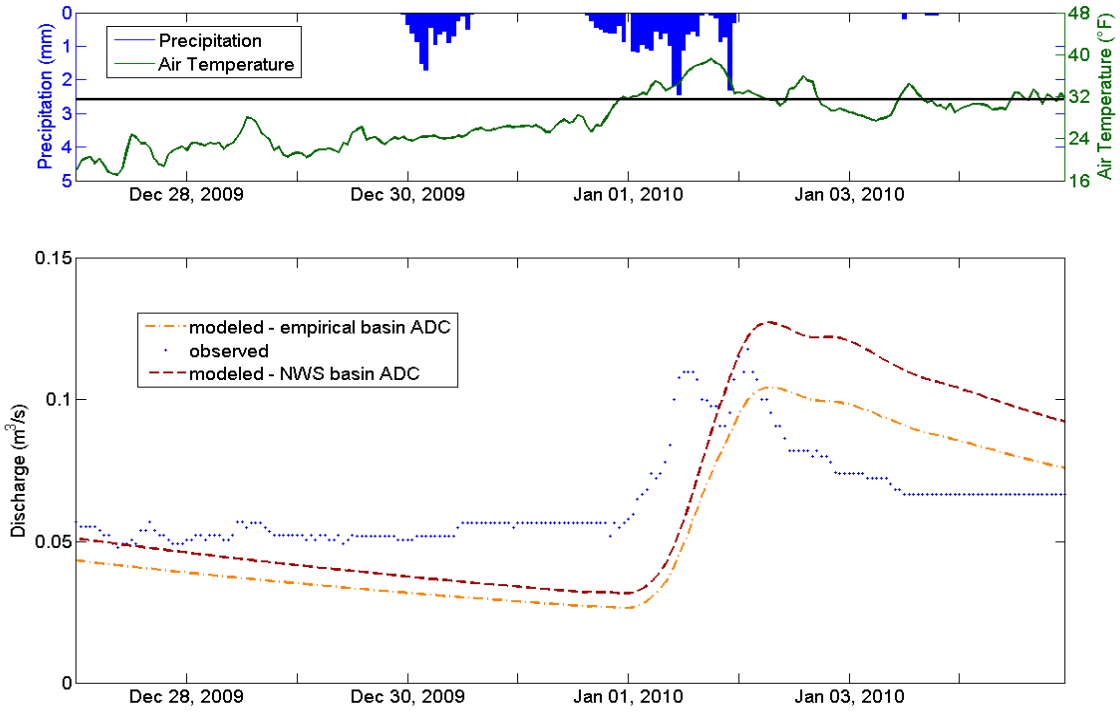

Figure B.16 Hydrograph Comparison for ROS Event #3.

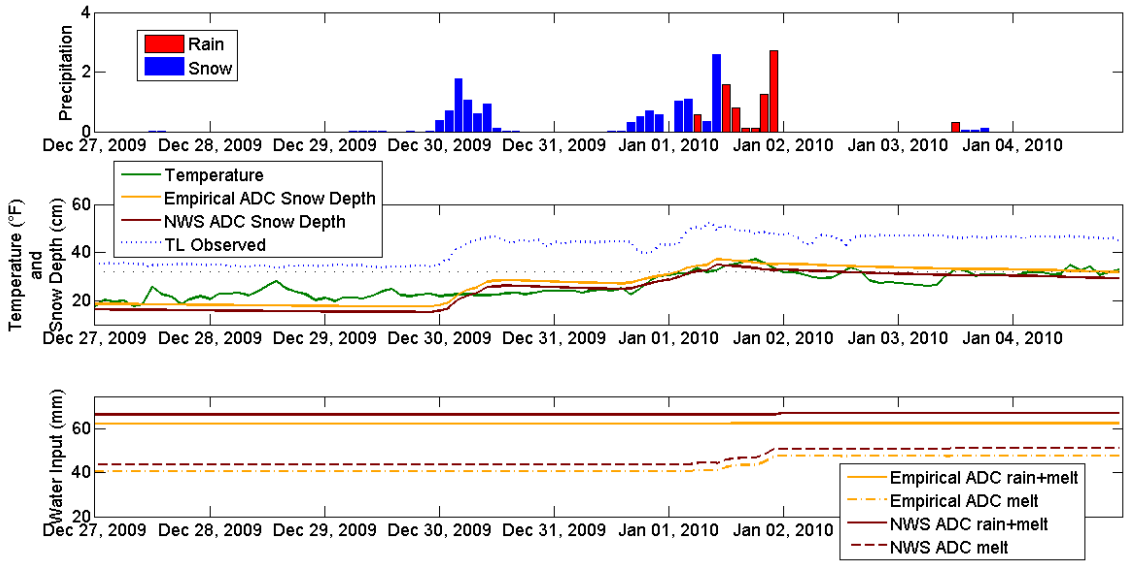

Figure B.17 Snow Depth and Water Input Comparison at TL for ROS Event #3. Top Plot is Precipitation, Middle Plot is Temperature and Snow Depth, and Bottom Plot is Cumulative Water Input to the Subsurface.

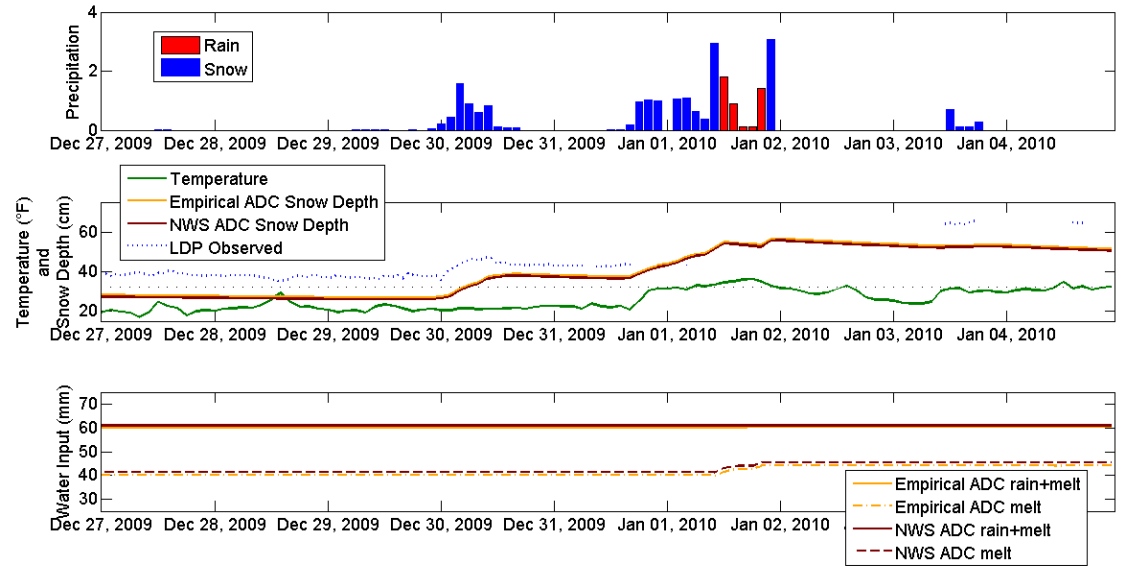

Figure B.18 Snow Depth and Water Input Comparison at TL for ROS Event #3. Top Plot is Precipitation, Middle Plot is Temperature and Snow Depth, and Bottom Plot is Cumulative Water Input to the Subsurface.

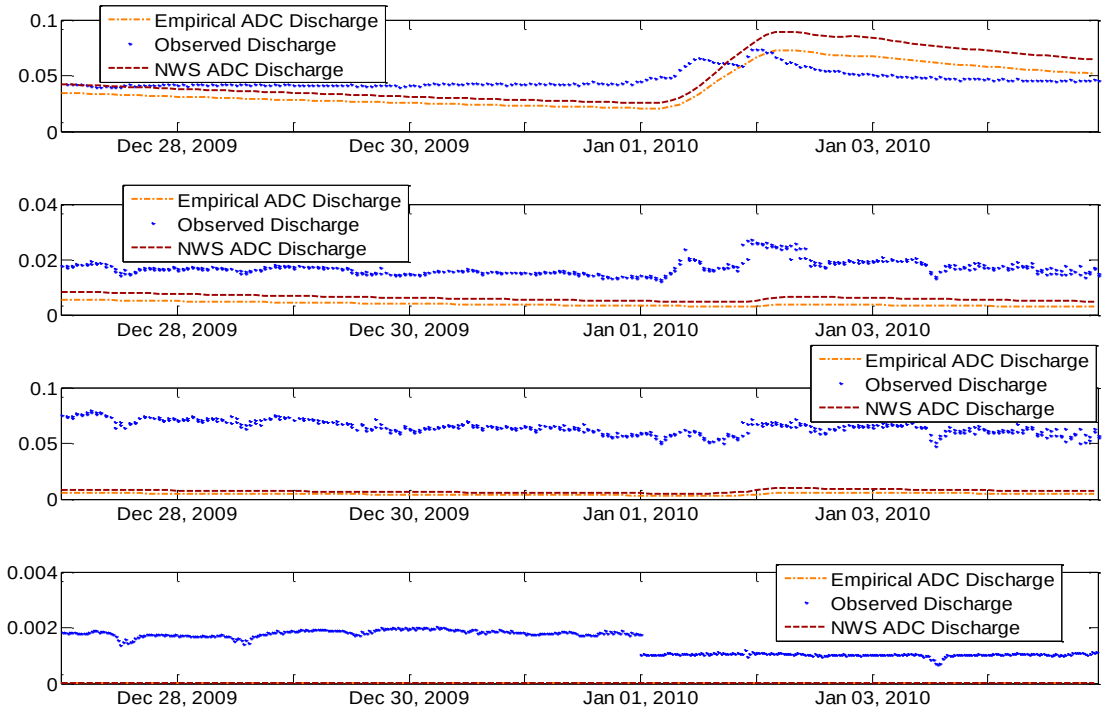

Figure B.19 Interior Hydrograph Comparison for ROS Event #3. Subplots are C2M, C1W, C1E, and BG from Top to Bottom.

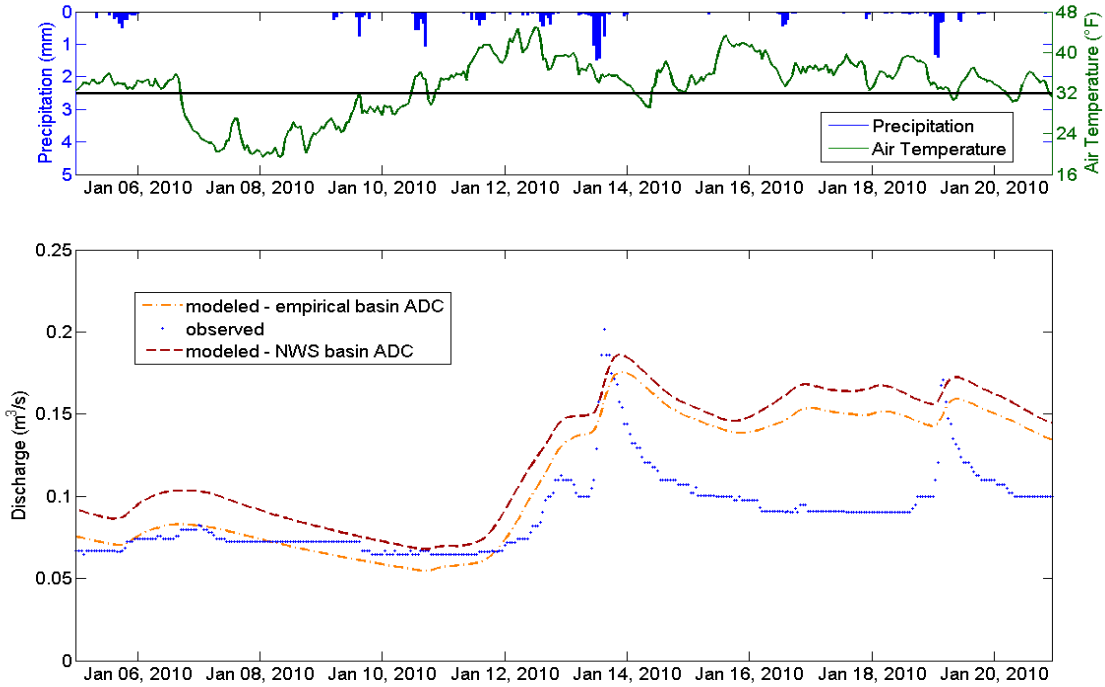

Figure B.20 Hydrograph Comparison for ROS Event #4.

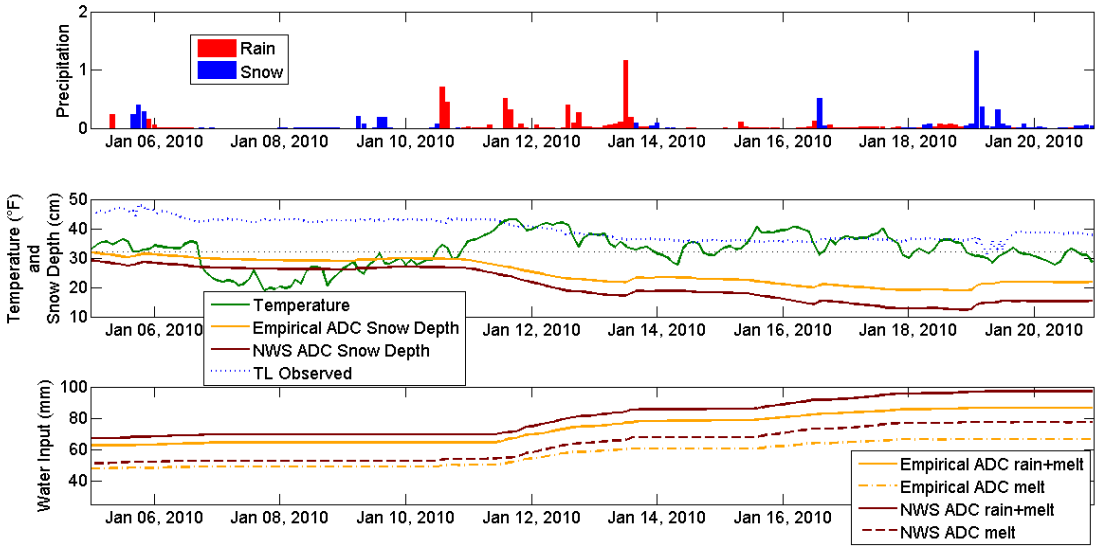

Figure B.21 Snow Depth and Water Input Comparison at TL for ROS Event #4. Top Plot is Precipitation, Middle Plot is Temperature and Snow Depth, and Bottom Plot is Cumulative Water Input to the Subsurface.

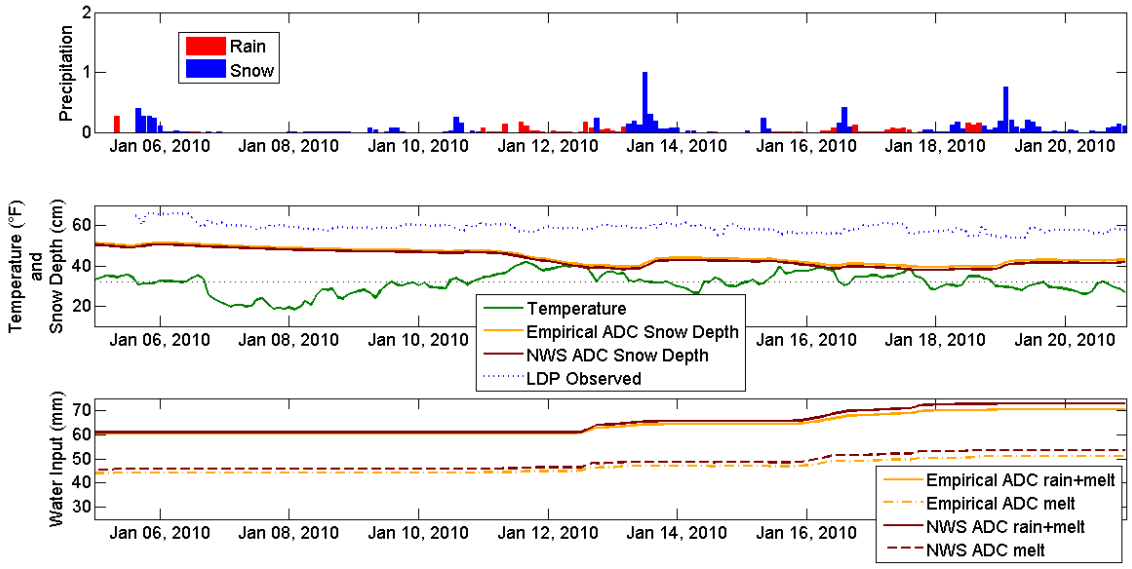

Figure B.22 Snow Depth and Water Input Comparison at LDP for ROS Event #4. Top Plot is Precipitation, Middle Plot is Temperature and Snow Depth, and Bottom Plot is Cumulative Water Input to the Subsurface.

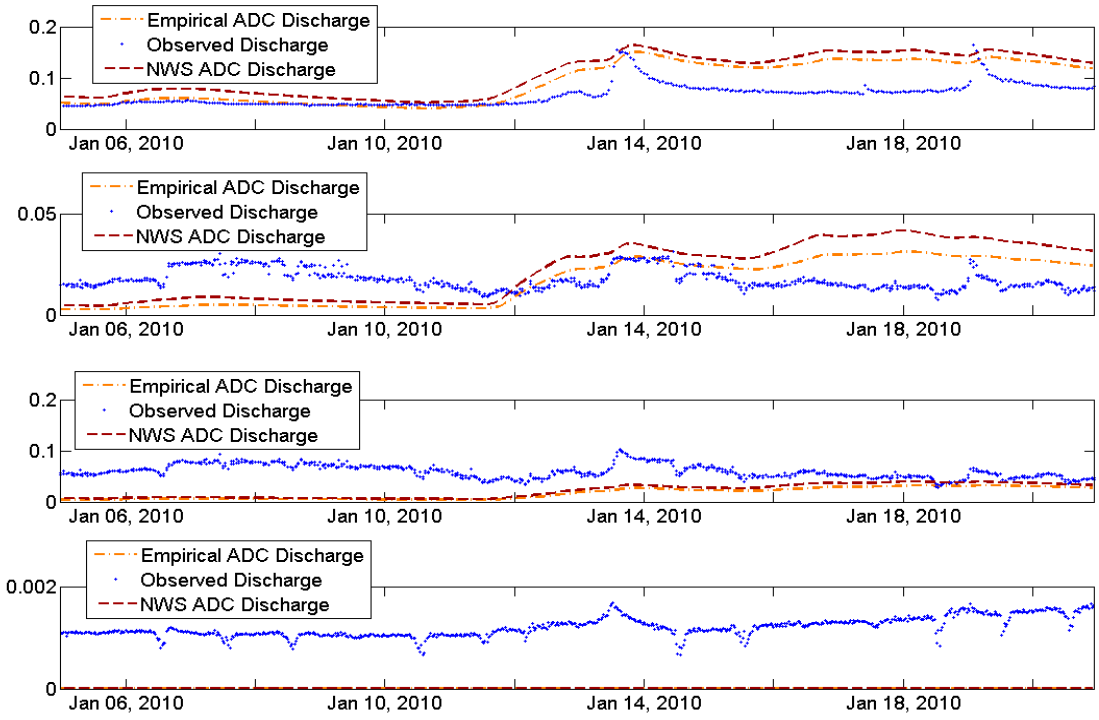

Figure B.23 Interior Hydrograph Comparison for ROS Event #4. Subplots are C2M, C1W, C1E, and BG from Top to Bottom.

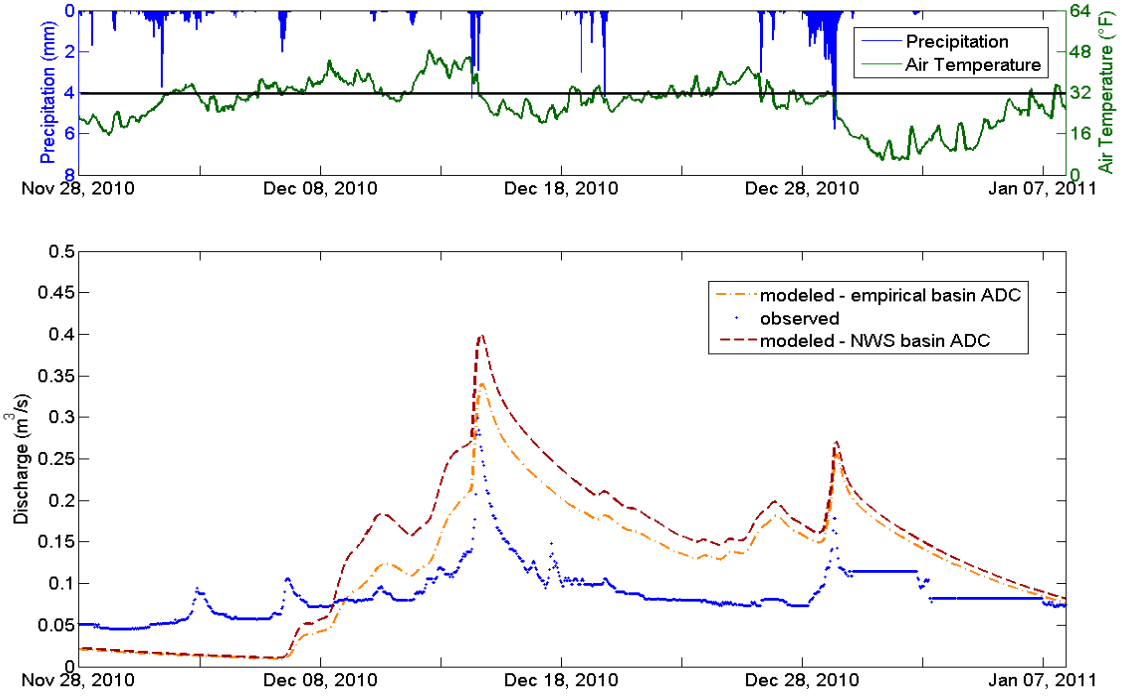

Figure B.24 Hydrograph Comparison for ROS Event #5.

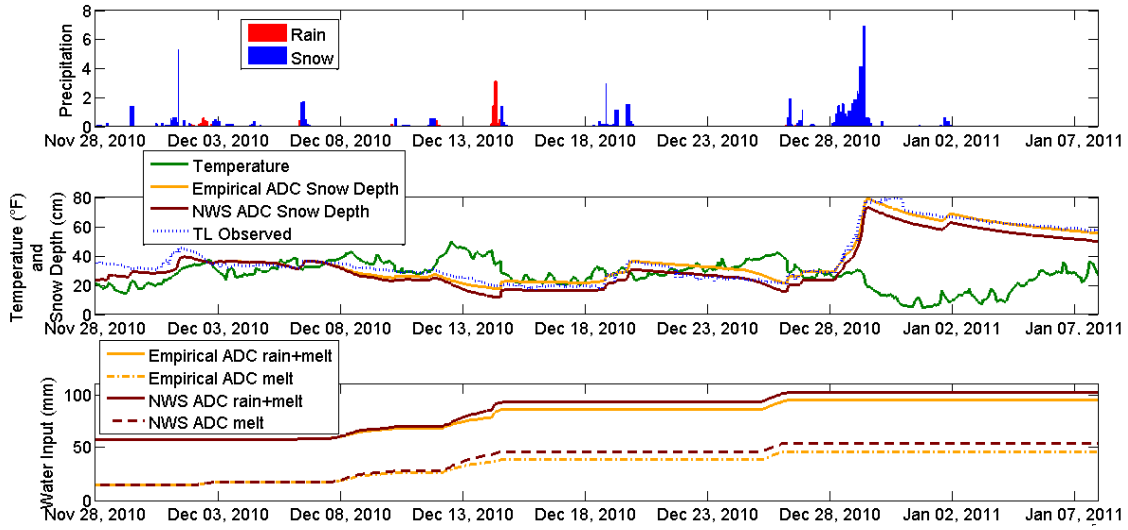

Figure B.25 Snow Depth and Water Input Comparison at TL for ROS Event #5. Top Plot is Precipitation, Middle Plot is Temperature and Snow Depth, and Bottom Plot is Cumulative Water Input to the Subsurface.

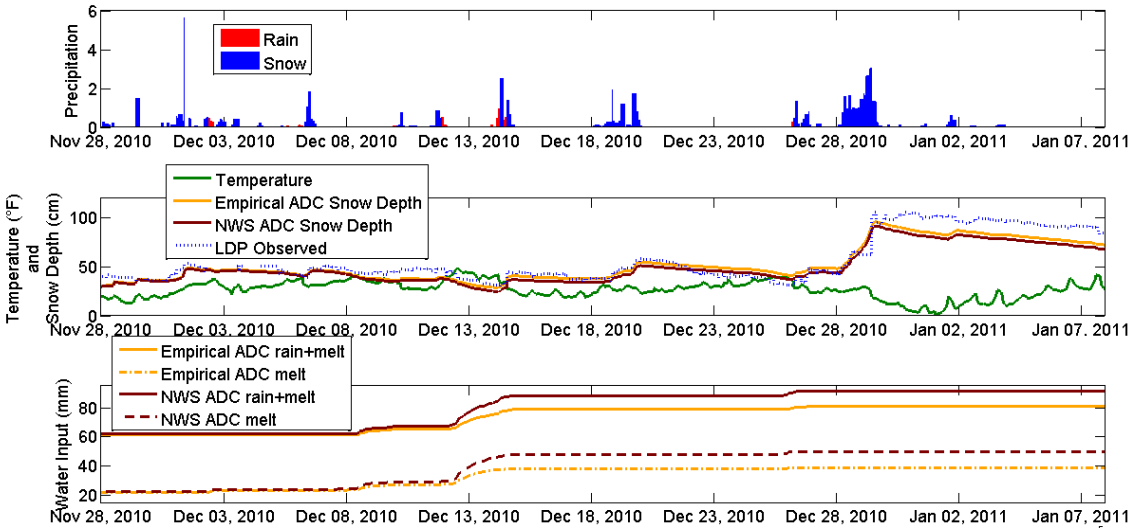

Figure B.26 Snow Depth and Water Input Comparison at LDP for ROS Event #5. Top Plot is Precipitation, Middle Plot is Temperature and Snow Depth, and Bottom Plot is Cumulative Water Input to the Subsurface.

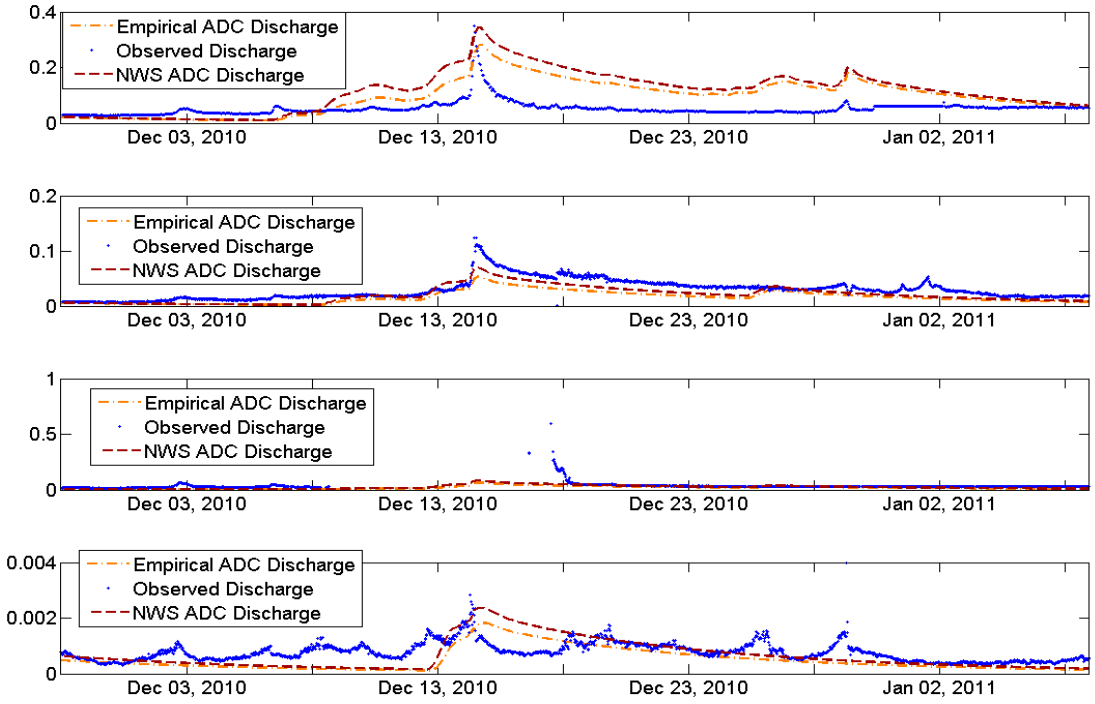

Figure B.27 Interior Hydrograph Comparison for ROS Event #5. Subplots are C2M, C1W, C1E, and BG from Top to Bottom.

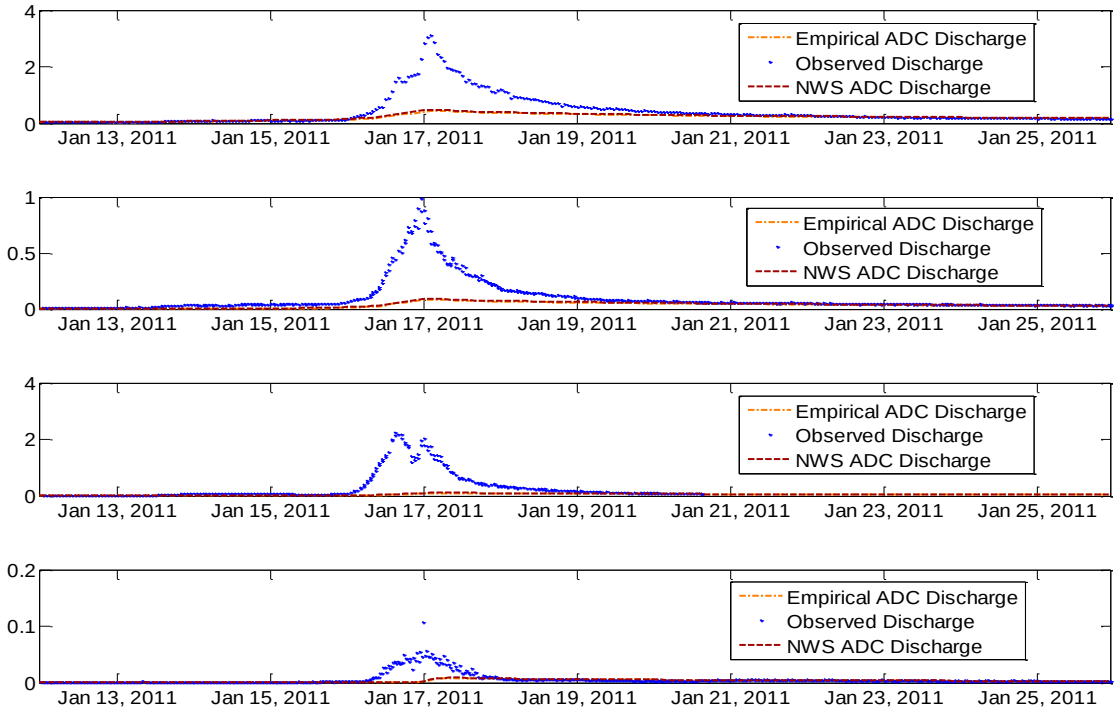

Figure B.28 Interior Hydrograph Comparison for ROS Event #6. Subplots are C2M, C1W, C1E, and BG from Top to Bottom.

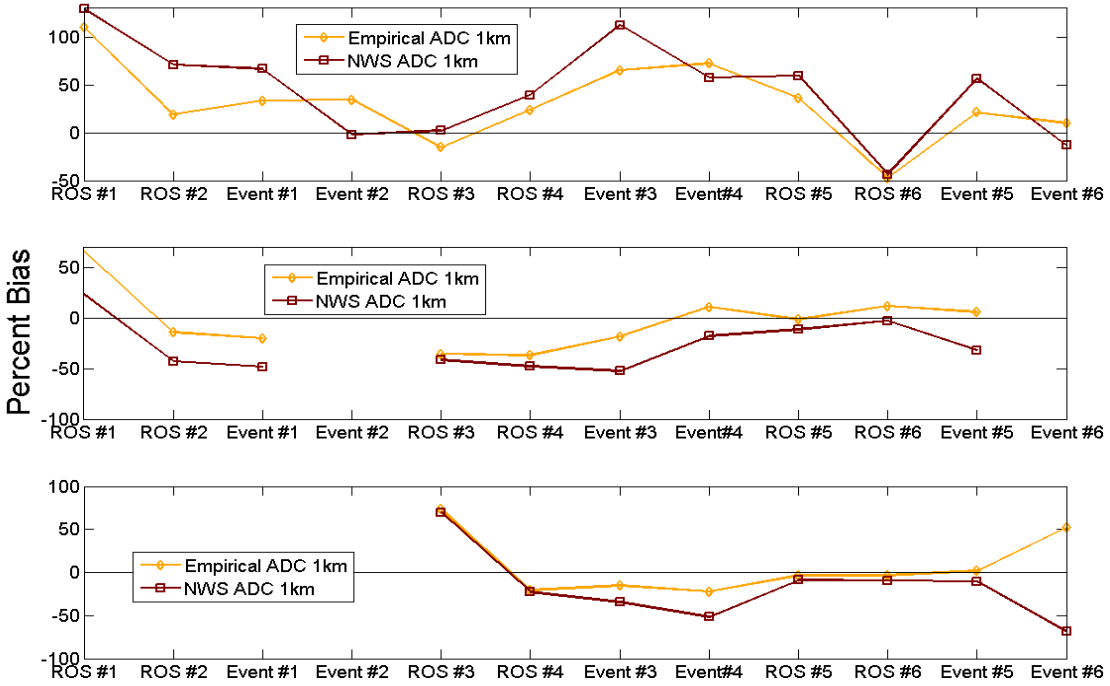

Figure B.29 Percent Bias Statistics for All Events. Subplots are LG Discharge, TL Snow Depth, and LDP Snow Depth from Top to Bottom.

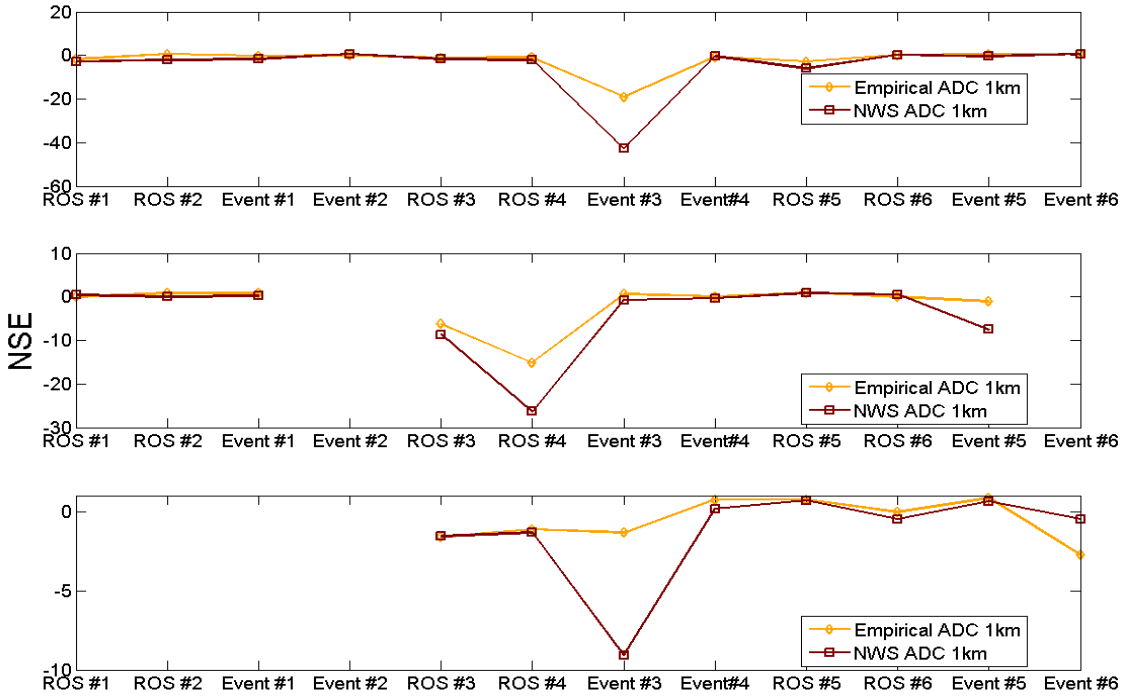

Figure B.30 Nash-Sutcliffe Efficiency Statistics for All Events. Subplots are LG Discharge, TL Snow Depth, and LDP Snow Depth from Top to Bottom.

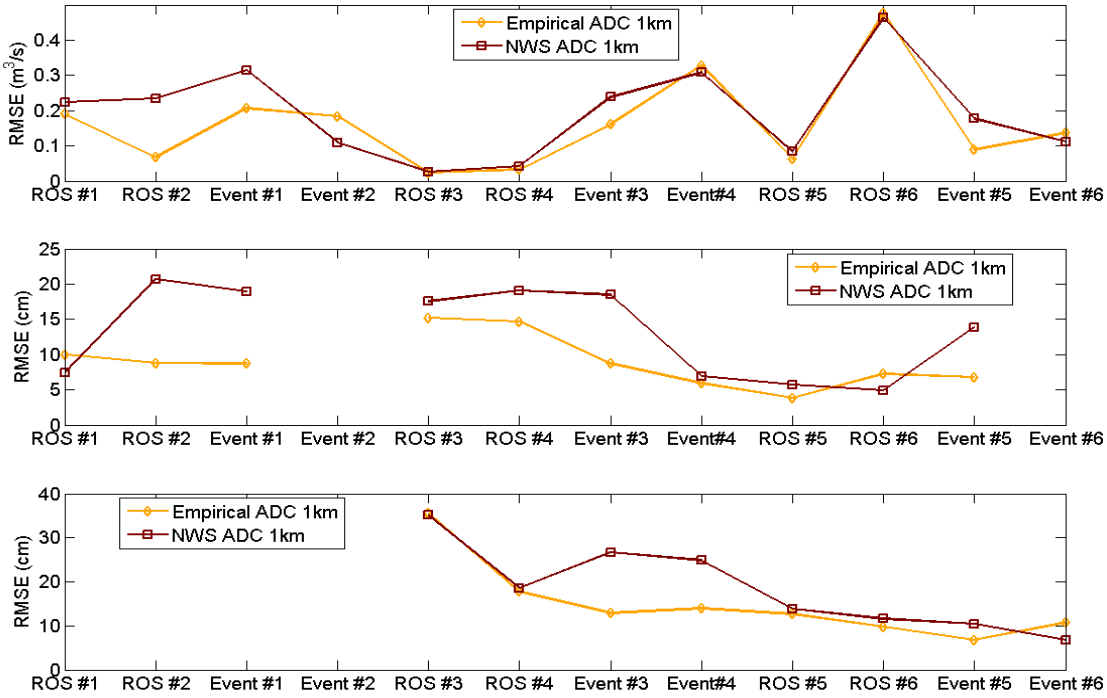

Figure B.31 Root Mean Square Error Statistics for All Events. Subplots are LG Discharge, TL Snow Depth, and LDP Snow Depth from Top to Bottom.

APPENDIX C

Hydrograph Comparisons for ¼ HRAP Versus 1 HRAP (with Empirical ADC)

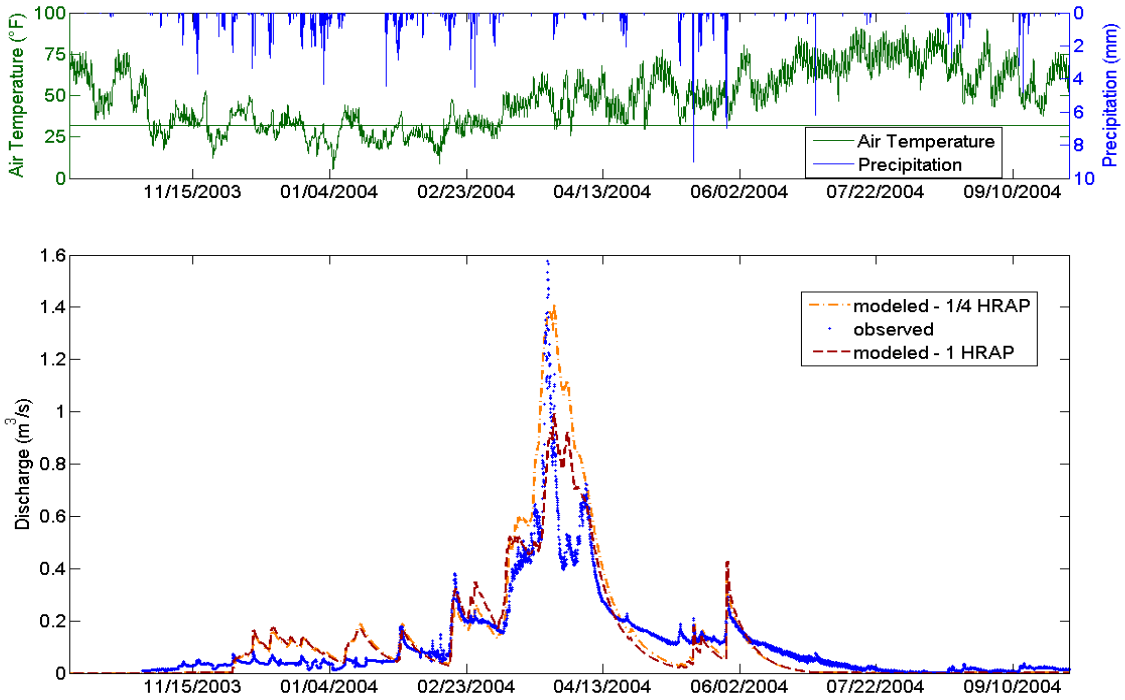

Figure C.1 Spatial Resolution Hydrograph Comparison for WY2004.

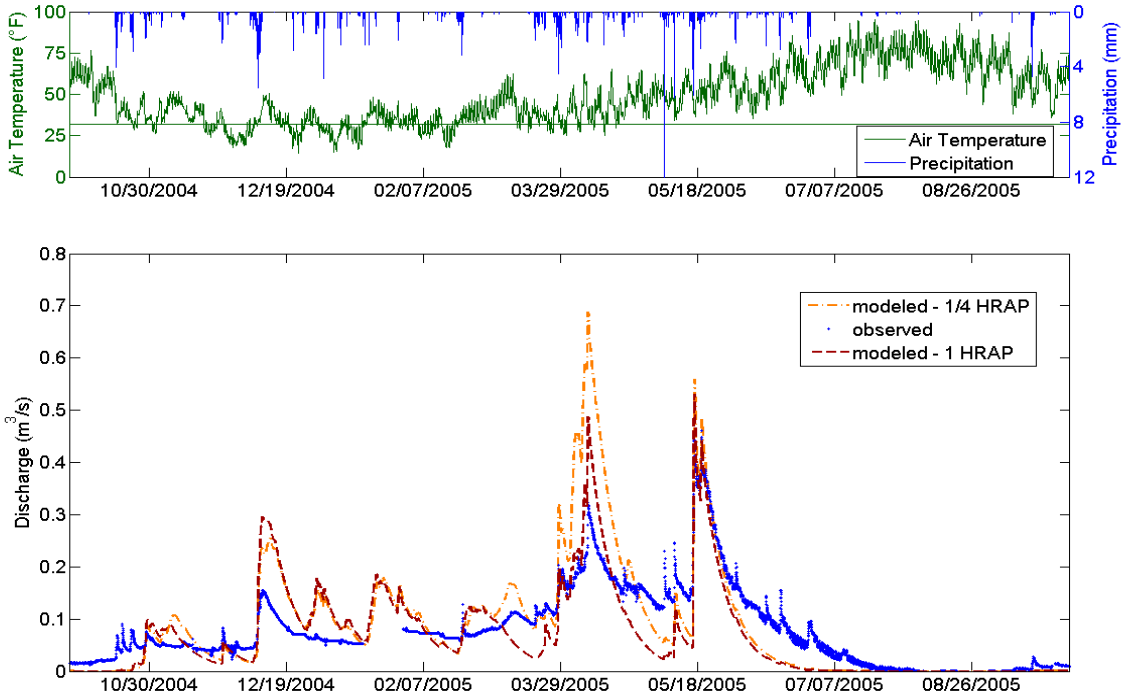

Figure C.2 Spatial Resolution Hydrograph Comparison for WY2005.

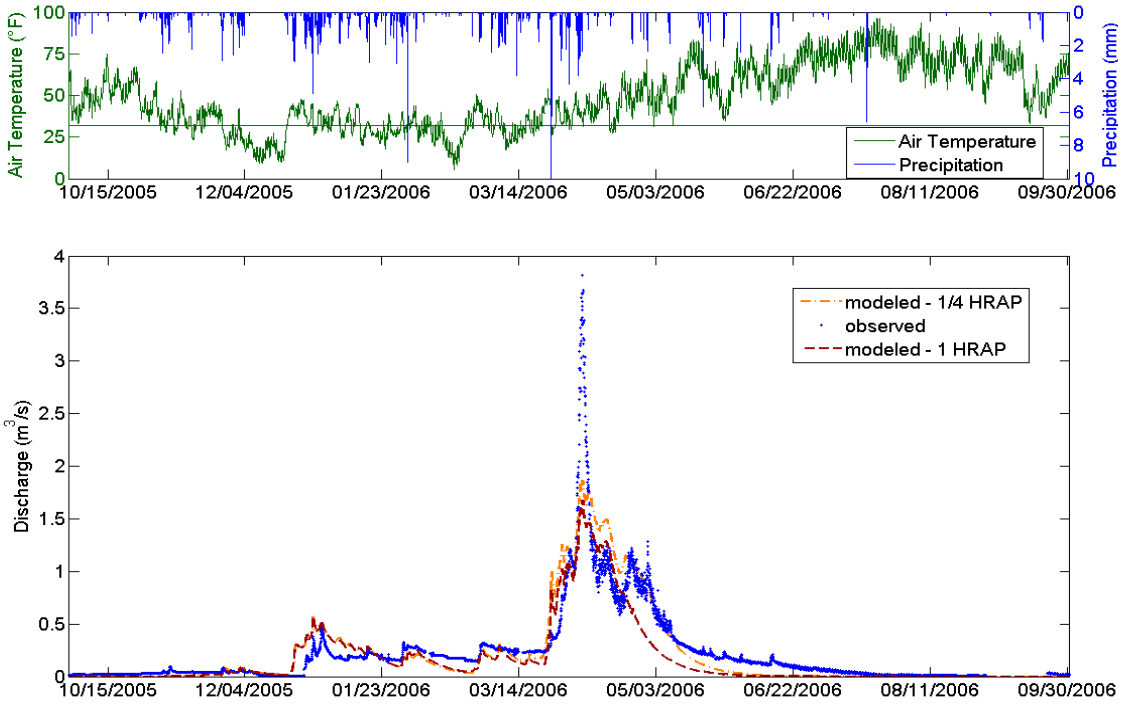

Figure C.3 Spatial Resolution Hydrograph Comparison for WY2006.

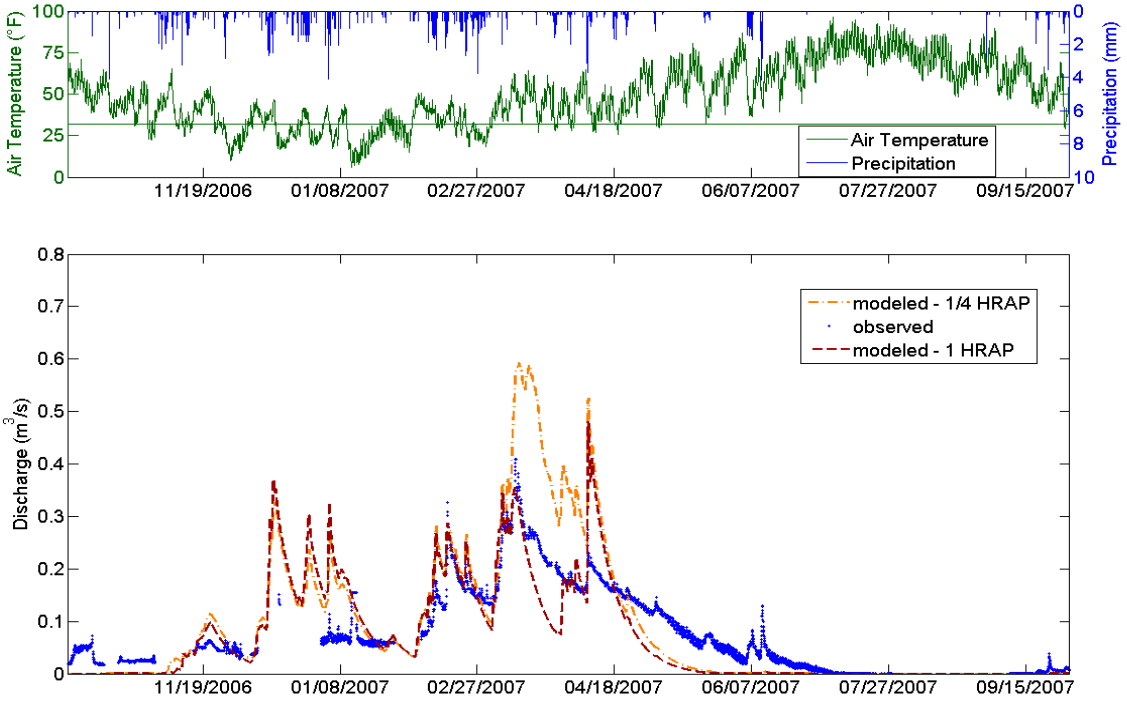

Figure C.4 Spatial Resolution Hydrograph Comparison for WY2007.

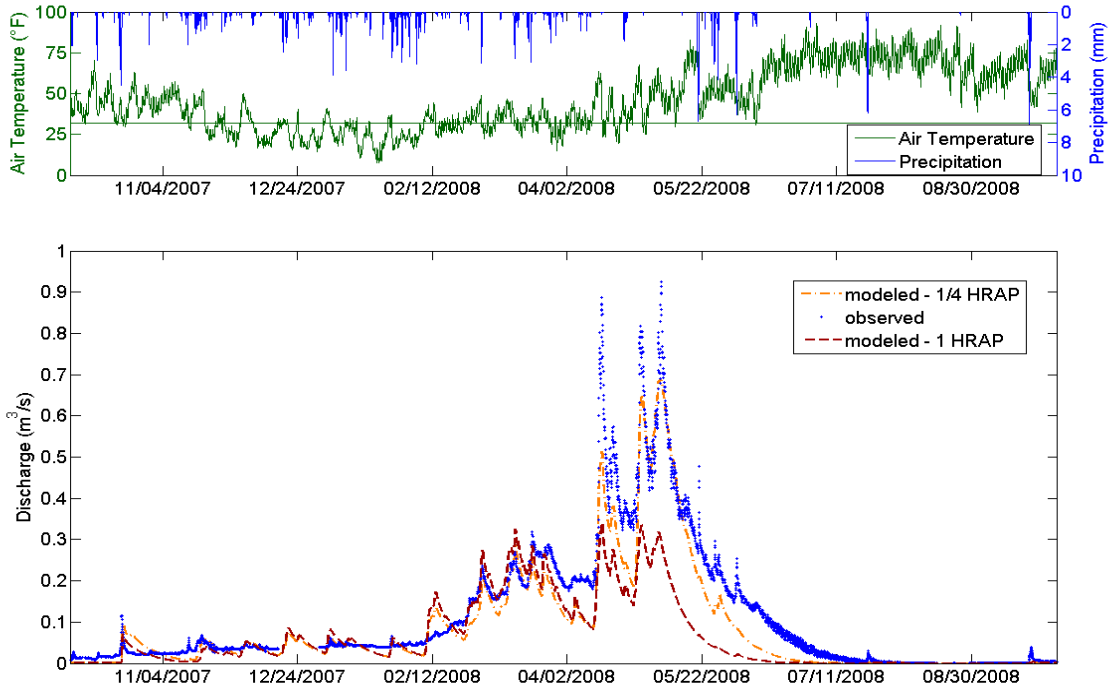

Figure C.5 Spatial Resolution Hydrograph Comparison for WY2008.

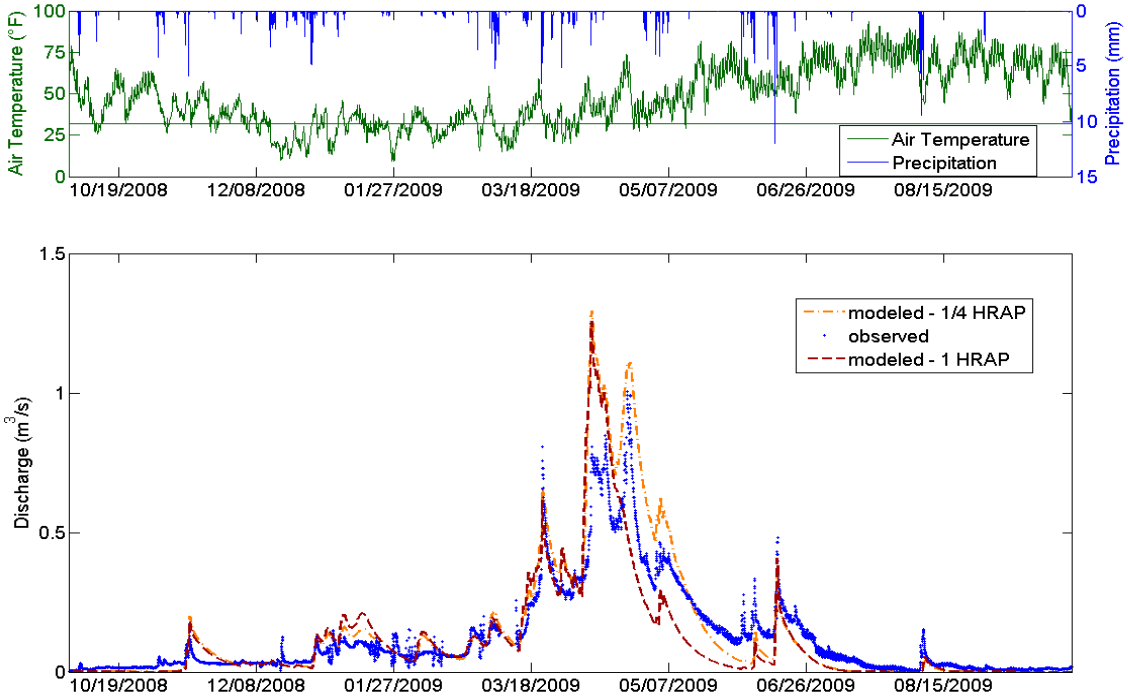

Figure C.6 Spatial Resolution Hydrograph Comparison for WY2009.

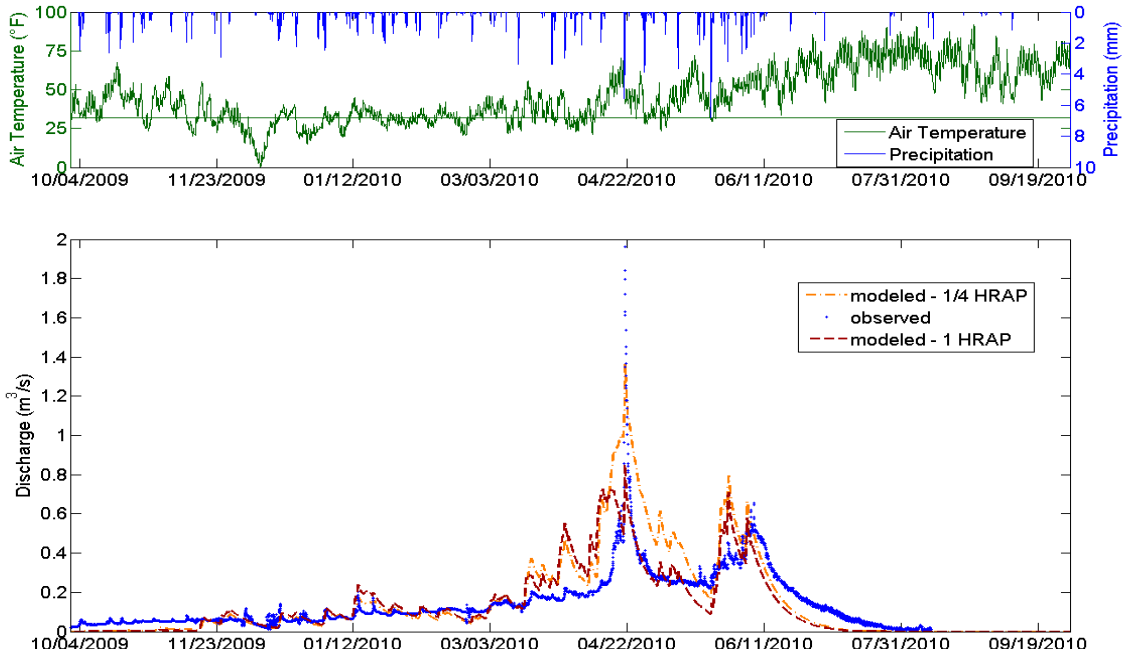

Figure C.7 Spatial Resolution Hydrograph Comparison for WY2010.

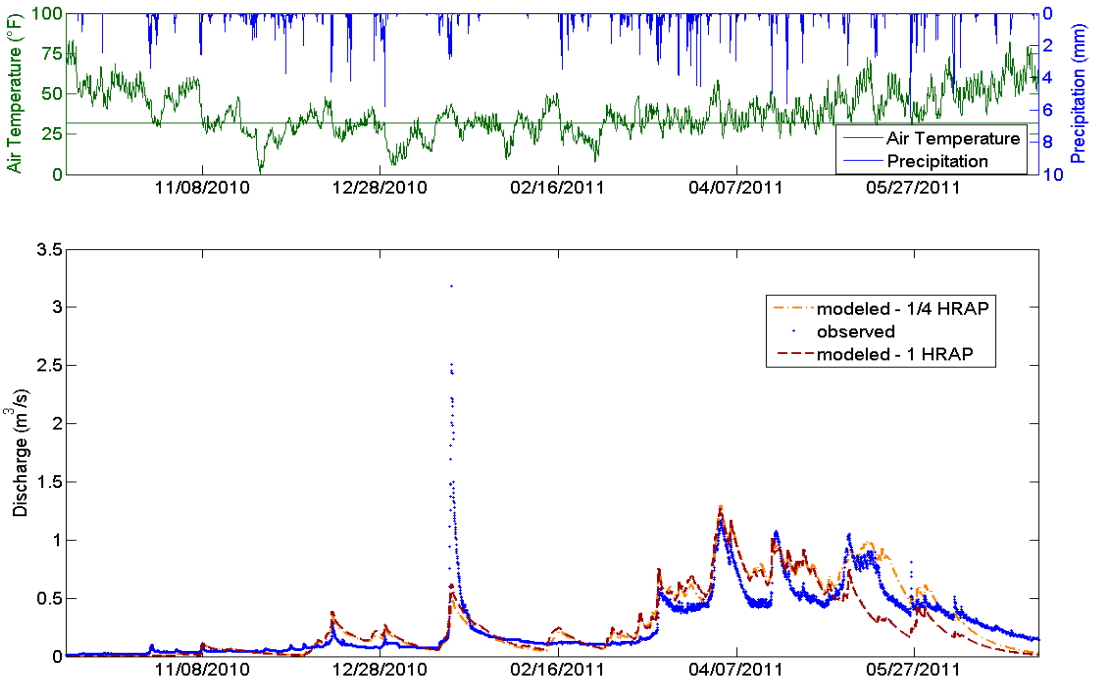

Figure C.8 Spatial Resolution Hydrograph Comparison for WY2011.